

University of Alberta

**Drug Resistance in Breast Cancer: Characterization of Rationally Designed
Paclitaxel Analogs in Model Systems**

By

Marc Christopher St.George

A thesis submitted to the Faculty of Graduate Studies and Research
in partial fulfillment of the requirements for the degree of

Master of Science

Medical Sciences – Laboratory Medicine and Pathology

©Marc Christopher St.George

Fall 2013

Edmonton, Alberta

Permission is hereby granted to the University of Alberta Libraries to reproduce single copies of this thesis and to lend or sell such copies for private, scholarly or scientific research purposes only. Where the thesis is converted to, or otherwise made available in digital form, the University of Alberta will advise potential users of the thesis of these terms.

The author reserves all other publication and other rights in association with the copyright in the thesis and, except as herein before provided, neither the thesis nor any substantial portion thereof may be printed or otherwise reproduced in any material form whatsoever without the author's prior written permission.

Abstract

Breast cancer is a leading cause of cancer related deaths among women in the developed world. Treatment options for breast cancer include taxanes, which mediate cytotoxic effects by inducing microtubule polymerization which impedes cell division. Taxane resistant breast cancer is a mounting clinical problem, and can in part be explained by differential expression of β -III tubulin and/or multidrug efflux pumps. I hypothesized that drugs traverse to the taxane active site through interactions at 275 and 278 residues (intermediate binding sites) within microtubule nanopores. I developed paclitaxel resistant SKBR-3 cell sub-lines, used synthesized paclitaxel analogs designed to interact with the suggested residues and attempted to dissect the progression of resistance by monitoring global microRNA profiles. Data did not favour interpretations on the hypothesized interactions with amino acid residues; evidence suggested that expression of β -III tubulin alone does not explain drug resistance and a combination of mechanisms likely mediates resistance.

Acknowledgements

First and foremost, I would like to thank my supervisors, Dr. Sambasivarao Damaraju and Dr. Jack Tuszynski, for their support and most importantly guidance in developing technical skills and contributed to my intellectual growth enabling the research contributions made to-date since the beginning of my journey approximately three years ago.

I would also like to thank the members of my supervisory committee; Drs. Carol E Cass and Ing Swie Goping for continued guidance, providing positive direction to make this undertaking a success.

I would like to thank members of the Damaraju laboratory: Dr. Yadav Sapkota, Mohsen Hajiloo, Preethi Krishnan and Ashok Narasimhan for being excellent colleagues, interactions at personal and professional levels, and I derived much benefit from their discussions during the lab meetings.

I also thank Jennifer Dufour, Diana Carandang, Lillian Cook, Gerry Baron, Mesfin Fanta, Delores Mowles, Marni Wilson, Michelle Kuzma, and Dr. Todd Mereniuk for training and technical assistance as I progressed through my program.

I thank my family: my parents, and my sister. Although at times their support came from across the oceans, it was there when needed. And, finally I would like to thank my fiancée Sandra, for her love and patience as I labored through this process and was the person I looked forward to going home to at the end of each day.

Table of Contents

1.	Introduction.....	1
1.1	Cancer.....	1
1.2	Breast Cancer.....	4
1.2.1	Hormone Receptor Status.....	5
1.2.1.1	Triple Negative Breast Cancer.....	6
1.2.1.2	Her2+ Breast Cancer.....	7
1.2.1.3	Luminal A Breast Cancer.....	8
1.2.1.4	Luminal B Breast Cancer.....	8
1.3	Microtubules.....	9
1.3.1	Microtubule Composition, Mechanisms and Functions.....	9
1.3.2	Tubulin.....	10
1.3.3	Targeting Microtubules with Anti-Cancer Therapeutic Agents.....	13
1.4	Taxanes.....	15
1.4.1	Origins of Paclitaxel.....	15
1.4.2	Mechanisms of Action.....	18
1.4.2.1	Protein Target of Taxane Drugs.....	18
1.4.2.2	Taxane Mediated Changes in Gene Expression.....	19
1.5	MicroRNAs.....	20
1.5.1	MiRNA Origins and Biosynthesis.....	20

1.5.2	MicroRNAs Deregulation in Breast Cancer	22
1.6	Mechanisms of Taxane Mediated Drug Resistance	24
1.6.1	Over-Expression of Drug Efflux Pumps	24
1.6.2	Variable Tubulin Isozyme Expression	25
1.6.2.1	β I Tubulin	26
1.6.2.2	β II Tubulin	27
1.6.2.3	β III Tubulin	27
1.6.2.4	β IV Tubulin	28
1.6.3	β Tubulin Mutations	29
1.7	<i>In Silico</i> Design of Paclitaxel Analogs and the Rationale	30
1.7.1	Nano Pore	30
1.7.2	Rationale for the Synthesis of Paclitaxel Analogs	33
2.	Materials and Methods	39
2.1	Cell Culture	39
2.2	Paclitaxel Resistant Derived Sub-Lines	39
2.3	Cell Imaging	41
2.4	Cytotoxicity Experiments	42
2.5	Cell Pellet Preparation from Wild Type Cell Lines	42
2.6	Cell Pellet Preparation from Resistant Sub-Lines	44
2.7	Sodium Dodecyl Sulphate (SDS) Polyacrylamide Gel Electrophoresis (PAGE) Analysis	46

2.8	Western Blot Analysis.....	47
2.9	Lowry Protein Assay	49
2.10	Recombinant Protein	50
2.11	Protein Purification.....	50
2.12	Tubulin Polymerization Assay	53
2.13	Small RNAome Profiling of Resistant Sub-Lines Using Next Generation Sequencing (NGS) Platform.....	54
2.14	Statistical Analysis.....	56
3.	Characterization of Paclitaxel Analogs and the Influences of β III Tubulin Expression on Resistance	57
3.1	Determining Cytotoxicity of Paclitaxel Analogs Against a Panel of Breast Cancer Cell Lines	57
3.2	Expression of β Tubulin Isoforms and Association with Observed Sensitivity of Cell Lines to Paclitaxel and Analogs.....	64
3.3	Substrate Specificity of Paclitaxel Analogs to Drug Efflux Pump P-glycoprotein	67
3.4	Additional Experimental Evidence in Support of the Cytotoxic Potential of Paclitaxel Analogs	68
3.5	The Contributions of β Tubulin Isoform Expression for the Observed Resistance within MESSA/DX5 Ovarian and K562/R7 CML Cell Lines	75
3.6	Combination Treatments Containing Verapamil and Paclitaxel Analogs Contribute to Enhanced Cell Kill	76

4.	Developing a Panel of Resistant Sub-Lines to Understand Mechanisms of Taxane Resistance	92
4.1	Development of Paclitaxel Resistant SKBR-3 Sub-Lines	92
4.2	Characterization of Derived Drug Resistance Sub-Lines for Phenotypic (Morphological) Changes	94
4.3	Determining Changes in β Tubulin Isozyme Expression from SKBR-3 Resistant Sub-Lines.....	97
4.4	Cytotoxicity Profiles from Paclitaxel and Analogs Correlate to Increasing β III Tubulin Expression.....	99
4.5	Other Possible Mechanisms of Drug Resistance Explored	108
4.6	Changes in miRNA-200c Expression within Resistant Sub-Lines.....	114
4.7	Changes in Expression Profile in Other microRNAs as Potential Contributors to Drug Resistance.....	115
5.	Discussion and Conclusions.....	118
5.1	Amino Acids Implicated in Intermediate Binding are Not the Sole Determinants of Taxane Binding.....	118
5.2	The Role of β III Tubulin in Paclitaxel Analog Binding at Site 275 and 278	123
5.3	P-gp as a Mechanism of Resistance to Paclitaxel and Analogs.....	125
5.4	Verapamil as an Inhibitor to P-gp Mediated Drug Resistance	128
5.5	Development of a Panel of SKBR-3 Paclitaxel Resistant Sub-Lines: Expression Patterns of β III Tubulin and Associated Resistance	130
5.6	The Role of miRNA Expression in Mediating Resistance to Paclitaxel	132

5.7	Conclusion.....	136
6.	Future work	140
6.1	Analog <i>In Silico</i> Binding Analysis and <i>In Vitro</i> Subcellular Localization Provides Insight into Actual Functions	140
6.2	β Tubulin Mutagenesis and Its Role in Taxane Drug Resistance	142
6.3	Quantitatively Determining Ratios of β Tubulin Isotype Found within Resistant Cell Lines	144
6.4	Effects of β III Tubulin Expression on Drug Resistance in the Resistant SKBR-3 Sub-Lines	145
6.5	Understanding the Roles of 40 Differentially Expressed miRNAs within the Resistant Cell Lines.....	147
	References	149
1.	Appendix I.....	184
1.1	<i>In Vitro</i> Tubulin Polymerization using Paclitaxel and Synthesized Analog.....	184
2.	Appendix II.....	191
2.1	Recombinant Tubulin Purification and Polymerization	191

List of Tables

Table 3-1. Summary of Drug Titrations Showing 50% Inhibitory Concentration, IC_{50} , in Breast Cancer Cell Lines Treated with Paclitaxel and Analogs (source Figure 3-1).....	64
Table 3-2. Determination of IC_{50} Values for P-gp \pm Expressing Cell Lines Treated with Paclitaxel and Analogs and \pm Verapamil.....	70
Table 4-1. Summary of the IC_{50} Values (source Figure 4-3) of Resistant SKBR-3 Sub- Lines Treated with Paclitaxel and Analogs.....	108
Table 4-2. Top 40 miRNA With Significantly Altered Expression (Normalized Counts).....	116

List of Figures

Figure 1-1. Crystal Structure of α/β Heterodimer	12
Figure 1-2. Microtubule and MBA Binding Sites.....	15
Figure 1-3. Chemical Structure of Paclitaxel and Docetaxel	17
Figure 1-4. Locations of Putative Intermediate Binding Site within Microtubule Structure	33
Figure 1-5. Structure of Custom Synthesized Paclitaxel Analogs	37
Figure 1-6. Predicted Chemical Interactions between Paclitaxel and Analogs with Amino Acids Located within the Intermediate Binding Site	38
Figure 2-1. Method for Creating Panel of Paclitaxel Resistant Sub-Lines	41
Figure 2-2. Schema for the Preparation of the “WT” Whole Cell Lysates for Western Blot Analysis.....	44
Figure 2-3. Schema for the Preparation of the Whole Cell Lysates for Western Blot and NGS Analysis	46
Figure 3-1. IC_{50} Values for Paclitaxel and Analogs in Assays using Breast Cancer Cell Lines	63
Figure 3-2. Western Blot Analysis of Expression of β Tubulin Isoforms and P-gp Expression in Breast Cancer Cell Lines	65
Figure 3-3. Cell Viability Assays of P-gp \pm Expressing Cell Lines Treated with Paclitaxel and Analogs	74
Figure 3-4. Western Blot Analysis of β Tubulin Isoforms and P-gp Expression in P-gp \pm Expressing Cell Lines	76

Figure 3-5. Differential Cytotoxicity of Paclitaxel Analogs in Presence of Verapamil Administered to MESSA/DX5 Cells.....	84
Figure 3-6. Rank Order of Cytotoxic Efficiency of Paclitaxel Compared to Analogs in MESSA/DX5 Cells in Presence of Verapamil	85
Figure 3-7. Differential Cytotoxicity of Paclitaxel Analogs in Presence of Verapamil Administered to K562/R7 Cell Lines	90
Figure 3-8. Rank Order of Cytotoxic Efficiency of Paclitaxel Compared to Analogs in K562/R7 Cells in Presence of Verapamil	91
Figure 4-1. Phenotypic Changes Observed of SKBR-3 Sub-Lines Showing Incremental Resistance to Paclitaxel	96
Figure 4-2. β Tubulin Isotype Protein Expression in a Panel of Resistant SKBR-3 Sub-Lines.....	98
Figure 4-3. Effects of β III Tubulin Expression on Profiles of Cytotoxicity from Paclitaxel and Analogs	107
Figure 4-4. Hierarchical Clustering Analysis of SKBR-3 Resistant Sub-Lines ...	111
Figure 4-5. Differential Expression of miRNAs Correlated to Increased Paclitaxel Resistance in SKBR-3 Sub-Lines.....	113
Figure 4-6. Changes in the Expression of miR-200c Shows Reciprocal Expression Patterns with β III Tubulin Protein.....	115
Figure A1-1. Dose Dependent Polymerization of Purified Bovin Brain Tubulin, Facilitated by Paclitaxel and Analogs.....	189
Figure A1-2. Assessing the Dynamics of Polymerizing Microtubules in the Presence of Paclitaxel and Analogs.....	190

Figure A2-1. Representative SDS PAGE and Western Blot Analysis of the Fractions Collected from the Purification of Wild Type Recombinant Tubulin.....	193
Figure A2-2. Recombinant Tubulin Polymerization Assay.....	194

List of Abbreviations

α	Alpha
β	Beta
γ	Gamma
δ	Delta
ε	Epsilon
ζ	Zeta
η	Eta
ABC	ATP binding cassette transporters
Ala	Alanine
ATP	Adenosine triphosphate
ATCC	American Type Culture Collection
ANOVA	Analysis of Variance
Bax	Bcl-2-associated X protein
BCRP	Breast cancer resistance protein
bp	Base pair
BRCA-1	Breast cancer type 1 susceptibility protein
BSA	Bovine serum albumin
CCNB1	Cyclin B1
C-7/10	Carbon 7/10
C-cpn	Cytosolic chaperonin complex
<i>C. elegans</i>	<i>Caenorhabditis elegans</i>
C terminal	Carboxylic terminal

Da	Dalton
DNA	Deoxyribonucleic acid
<i>E. coli</i>	<i>Escherichia coli</i>
EDTA	Ethylenediaminetetraacetic acid
EGTA	Ethylene glycol tetraacetic acid
EMT	Epithelial to mesenchymal transition
ER	Estrogen receptor
FISH	Fluorescent <i>In situ</i> hybridization
g	Gravity
g_{av}	Gravities average
GDP	Guanosine diphosphate
GTP	Guanosine triphosphate
h	Hours
Her 2	Human epidermal growth factor receptor 2
His	Histidine
IC ₅₀	Inhibitory Concentration 50% of cells
Ile	Isoleucine
I _Q	Quasi-native intermediate conformation
Ki-67	Kiel-67
MBA	Microtubule binding agent
<i>MDR-1</i>	Multidrug resistance protein 1
min	Minutes
miRNA	microRNA

mRNA	Messenger RNA
MRP	Multidrug resistance associated protein
MTS	3-(4,5-dimethylthiazol-2-yl)-5-(3-carboxymethoxyphenyl)-2-(4-sulfophenyl)-2H-tetrazolium
MYBL	Myb-related protein B
NGS	Next generation sequencing
Ni-NTA	Nickel nitrilotriacetic acid
nt	Nucleotide
P	Probability
P53	Protein 53
PAGE	Polyacrylamide Gel Electrophoresis
P-gp	P-glycoprotein
PR	Progesterone receptor
Q-RT-PCR	Quantitative- real time-polymerase chain reaction
Ran	Ras related nuclear protein
RIPA	Radio Immuno Precipitation Assay
RISC	RNA induced silencing complex
RNA	Ribonucleic acid
RPM	Revolutions per minute
RPMI-1640	Roswell Park Memorial Institute-1640
s	Seconds
SDS	Sodium Dodecyl Sulphate
SE	Standard error

Ser	Serine
siRNA	Small interfering RNA
TBC	Tubulin binding cofactor
<i>T. Brevifolia</i>	<i>Taxus Brevifolia</i>
TBST	Tris buffered saline, Tween 20
TBSMT	Tris buffered saline, milk, Tween 20
TEMED	Tetramethylethylenediamine
TN	Triple negative breast cancer
Tx	Taxol
UTR	Untranslated region
Val	Valine
v/v	Volume/volume (ml/100ml)
WT	Wild Type
w/v	Weight/volume (g/100ml)

1. Introduction

1.1 Cancer

Cancer is a term used to define a large number of related neoplastic diseases. This group of diseases affects a large proportion of the population, and according to the Canadian Cancer Society, 40% of people will develop cancer in their life-times resulting in 25% of people prematurely losing their lives. In 2013 there will be an estimated 187, 600 new cases of cancer across Canada and 75, 500 deaths.

Understanding the biology of cancer is a critical first step to being able to treat the disease. In a review by Hanahan and Weinberg published in 2000 (1), six characteristics shared by all cancers were identified: viz., (i) sustaining proliferative signaling; (ii) evading growth suppressors; (iii) activating invasion and metastasis; (iv) enabling replicative immortality; (v) inducing angiogenesis and (vi) resisting cell death. In 2011 (2) the same authors published a second review that added two enabling characteristics (viz., (vii) genomic instability and mutation; and (viii) tumor-promoting inflammation) and two emerging characteristics of cancer (viz., (ix) deregulating cellular energetics and (x) avoiding immune destruction). These characteristics are gained randomly, through processes of the two enabling characteristics, resulting in a foundation in which cells become malignant.

There are **two major enabling characteristics** that drive the progressive development of each of the hallmarks of cancer. **The first is**

genomic instability and mutations. Normal cells have a remarkable genome repair system that maintains correct DNA sequence. However changes can occur that are missed, resulting in cells with selective survival and proliferative advantages that deviate from, and outcompete normal cells (3). As cells move to a more tumorigenic state, mutations accumulate at an increasing rate, eventually giving rise to cancerous cells (4,5).

The second characteristic that enables the development of cancer is tumor promoting inflammation. Inflammation is a mechanism used by the innate immune systems to protect the host from invasion and repair wounds (6). These mechanisms can be beneficial to developing cancer cells. Many pathways are initiated through inflammation that promote proliferation, inhibit cellular death, development of blood vessels, and extracellular matrix reorganization which promotes invasion and metastases (7-9). These two enabling characteristics work in tandem to facilitate the further progression of each other, as well as initiate progression of the following eight characteristics.

Sustained proliferative signaling is used to provide cells with constitutive growth signals either from the microenvironment or the tumor cells themselves. This allows cancer cells to continuously move through the cell cycle, rapidly increasing the number of cells with developed cancerous traits (10-13). Concordantly, with excess proliferative signaling, cancerous cells also utilize mechanisms in which they **evade growth**

suppressor signals. Ideally these growth suppressors would inhibit a cell's ability to undergo division; however cancerous cells have developed a means by which this can be ignored (14-17).

Cells utilize the mechanisms of programmed cell death, called apoptosis, to implement self-death when signals indicate they are not behaving as expected (18). Cancer cells are able to **resist cell death** and continue to proliferate uncontrollably (19-23). Due to the ability of cancerous cells to divide continuously they have developed a mechanism which enables **replicative immortality**. Normal cells have a finite number of divisions before they enter a state of eternal G_0 or senescence (24). This is dictated by the erosion of non-coding DNA at the ends of chromosomes (telomeres) that occurs with each cellular division. Cancer cells promote the elongation of telomeres using the enzyme telomerase (as one of the mechanisms) to allow for replicative immortality (25-30).

The development of new blood vessels is required for supplying oxygen to the ever increasing number of cancer cells within a tumor. Cancer cells are able to produce the signals that **induce angiogenesis** to supply the tumor with oxygenated blood (31-35). The migration of cancer cells from their microenvironment to the surrounding tissue and to distant tissues is key for the progression of the disease through **activating invasion and metastasis** pathways. Cancer cells are able to reorganize the extracellular matrix through enzymatic means for tissue invasion as well as utilization of blood vessels for the movement of cancerous cells to

distant locations within the host system (36-45). The ability of these cells to **avoid destruction from the immune system** as they develop and relocate to distant sites, allows for the progression of the disease (46-49). And finally, cancer cells are able to **deregulate cellular energetics** to meet the energy demands for proliferation and tumor development (50-54).

These characteristics provided the much needed conceptual framework for researchers to understand and study cancer by invoking or validating hypotheses within this defined premise.

1.2 Breast Cancer

Breast cancer is a type of cancer affecting tissue within the breast region. This region is defined as involving the tissue up to the collar bone and extends laterally from the armpit to the sternum in the center of the chest. Breast cancer is a disease that primarily afflicts women, but does occur in men at a rate of 0.7% of all new breast cancer cases (55), with mortality rates similar to that of women. Breast cancer has the highest incidence rate of all cancers in women with 1 in 9 Canadian women developing this cancer during her lifetime. Worldwide, there are close to 1 million new cases of women developing breast cancer each year, as well as approximately 400,000 (56) deaths, second only to lung cancer. According to the Canadian Cancer Society, 23,800 women will be diagnosed and 5,000 deaths will be attributed to breast cancer in 2013. Survival is dependent on stage of the disease. In the United States, breast

cancer patients with non-invasive tumors have a 98% 5 year survival rate, but drops to 24% in patients with metastatic disease (57,58), with close to 33% of patients developing metastatic disease (58,59). Over the last couple of decades, breast cancer incidence is on the rise while the number of breast cancer related deaths is on the decline, with a decrease of 2.2% per annum (60). This is mainly due to the establishment of screening methods used for early detection and the evolution of treatment options available for breast cancer patients (58,61). Mammography is the standard method of detection but can be accompanied with magnetic resonance imaging and ultrasound methods as well (60,62). Treatment options for breast cancer vary based on several pathological features of the particular disease of an individual. Surgical resection and radiation therapy can be used in combination with systemic therapies such as standard chemotherapy, endocrine therapy or monoclonal antibody therapy as either adjuvant or neoadjuvant options.

1.2.1 Hormone Receptor Status

The prognosis of breast cancer has classically been through morphological characteristics including tumor size, number of lymph nodes infiltrated and presence of distant metastases within the patient. More recently immunohistochemical analyses have been used to identify expression of specific receptors to determine the prognosis and chemotherapeutical options for a specific patient (63,64). The three receptors of interest are human epidermal growth factor receptor 2 (Her2),

estrogen receptor (ER) and progesterone receptor (PR). Based on the presence or absence of these receptors within breast cancer tissues, the patient's breast cancer can be separated into 4 major groups (64).

1.2.1.1 Triple Negative Breast Cancer

Triple negative (TN) breast cancer is classified as the name suggests for being negative (in subsequent text we also use receptor negative status as synonymous with very low expression) for Her2, ER, and PR receptors. This hormone receptor state occurs in 15% of breast cancer cases (65-67). These types of breast cancer have a poor prognosis, generally having high risk of early recurrence within the first three years following diagnosis (68). The metastatic potential is high in these types of tumors. Lymph node association is high even with small local tumors (69). The development of distant metastases generally occurs prior to local recurrence. These tumors metastasize to the brain and liver, which in turn results in a quick progression from development of metastasis to death (68). These subtypes of tumors have a high risk of relapse at 20% (70). Because of the absence or highly under expressed hormone or Her2 receptors, there are fewer treatment options for these patients. These types of tumors are typically chemosensitive, allowing for preferential and successful treatment using taxanes (65) and anthracycline combination therapies (71), as well as platinum based therapies (72-74). There are other subtypes of cancers within the TN, described recently using the combination of transcriptomic and next generation sequencing

technologies and knowledge gained from these are yet to be translated in to clinical practice (75,76).

1.2.1.2 Her2+ Breast Cancer

Her2+ enriched breast cancer is negative for ER and PR expression but positive for the human epidermal growth factor receptor 2, a membrane protein receptor tyrosine kinase. Approximately 15 – 20% (65) of breast cancer cases present with over-expression of Her2, 90% of which is attributed to gene amplification (77). The over-expression of Her2 can be determined through immunohistochemical analysis to identify protein expression or through fluorescent *In situ* hybridization (FISH) analysis to detect the number of gene copies within the cell (64). This subtype is generally characterized as having poor prognosis. This poor prognosis is attributed to higher percentage of recurrence and higher mortality rate (64,77,78). Her2+ breast cancers have a high rate of relapse, comparable to TN cancers (up to 20%). Recent advances in monoclonal antibody treatment have allowed specific targeting of these receptors with drugs such as trastuzumab (Herceptin), and have shown better patient outcomes in combination with chemotherapy compared to chemotherapy alone (79-81). Antibodies bind cell surface receptor, Her2 and are inhibitors of the receptor, preventing epidermal growth factor from binding and activating signal transduction events.

1.2.1.3 Luminal A Breast Cancer

Luminal A breast cancer is classified as being ER and/or PR positive, Her2 negative and having low expression of Ki-67 protein, a marker for highly proliferating cells (82,83). Patients with these characteristics for expression of markers have good prognosis and generally mean better outcomes for patients, with strong response to hormonal therapy (84,85). Luminal A cancers also have the lowest relapse rate of the four subtypes with only 12.7% of patients having recurrent disease. Beyond treatment of luminal A breast cancer with hormonal therapy, there is little added benefit to treating these cancers with common cytotoxic agents due to low levels of cellular proliferation indicated by low Ki-67 protein (86). However adjuvant radiation therapy has been shown to be very effective in treating luminal A type cancers, and has been shown to reduce the risk of recurrence (56,70). This may be due to the cells dependence on estrogen which has been shown to decrease the time required for cells to transition from G1 to S phase of the cell cycle, allowing cells less time to repair DNA damages caused by radiation (56).

1.2.1.4 Luminal B Breast Cancer

Luminal B breast cancer is characterized by being ER and/or PR positive, having occasional expression of Her2 and having high expression (> 14% of cells) of Ki-67 (85,87). Other proliferative markers such as CCNB1 and MYBL are more highly expressed in luminal B breast cancer compared to luminal A (88,89). This subtype of breast cancer makes up

about 10 – 20% of breast cancer cases (90), and has a poorer prognosis due to high proliferative rates (84,85). Treatment of these tumors is difficult; with patients responding well to neoadjuvant treatment but not as well as other subclasses of breast cancer (90), resulting in poorer outcomes.

1.3 Microtubules

1.3.1 Microtubule Composition, Mechanisms and Functions

Microtubules are hollow cylindrical polymeric macromolecules. They are comprised predominantly of repeating α (alpha) and β (beta) tubulin heterodimers (91,92). Microtubules are dynamic structures, continuously in phases of either elongation or shortening. This stochastic dynamic feature is termed “dynamic instability” and contributes itself to the architecture, motility and division of the cell. Dynamic instability is characterized by two phases, one in which elongation is unexpectedly interrupted by fast shrinkage, known as “catastrophe.” The growth phase of the microtubule is recovered in a process called “rescue.” These two processes contribute to the function of the microtubule in the cell, and with any one of the above processes dominating, leading to loss of microtubule function and potential cell death (93).

Both of these functions are believed to be regulated, in that microtubule growth or shortening events do not occur by chance. It is believed that the structure of, or proteins that interact with microtubules, are determinates for microtubule fate. Catastrophe is accepted to occur

following a single, not well understood event in the growth of the microtubule. A random event occurs in which the protective end structure of the microtubule disassociates, causing the sudden and rapid disassembly of microtubules (93) .

Microtubule growth tends to be in a unidirectional manner mediated by the polarity of the structure. Microtubules have plus and minus ends, which direct the polarity of the structure. The plus end contains a cap, consisting of heterodimers that are GTP bound. When heterodimers within the cap interact with free heterodimers, GTP bound to β tubulin is hydrolyzed to GDP and the microtubule is elongated. Elongation can occur at both ends but is favored at the plus end. Furthermore, an event known as tread milling can occur in which the plus end undergoes polymerization and the minus end depolymerization resulting in a consistent tubulin mass, but results in the movement of the centre of mass in a single direction (94,95).

1.3.2 Tubulin

As was previously stated, microtubules are polymers of repeating tubulin heterodimers. Tubulins are a family of globular proteins that are made up of seven known tubulin isoforms. α , β and γ (gamma) are conserved evolutionarily and found in all eukaryotic cells. Isoforms δ (delta), ϵ (epsilon), ζ (zeta), and η (eta) have been discovered more recently and are not found in all eukaryotic cells, attributed to either the loss of the gene over the course of evolution or not acquiring the genes in

the first place (96,97). α and β tubulin are the isoforms that are found within the heterodimers that make up the microtubule structure. γ is important for nucleation of microtubules, forming a ring structure which provides the foundation for microtubule elongation. This protein is mainly found within the centrioles of the microtubule organizing center (98-102). Each of these three proteins represents a sub-family of similarly structured isotypes with slight variations in the amino acid sequence, most of which are found in the C terminal region of the protein. To date there are eight known α tubulin proteins originating from four genes, nine β tubulin proteins originating from splice variant of eight genes, and seven γ tubulin proteins originating from six genes. Many of these isotypes are tissue specific, being present or absent with variable expression ratios between tissue types. The functions of the remaining four isoforms of tubulin (δ , ε , ζ , and η) are not well understood. δ and ε are found within centrioles and are thought to potentially play a role in microtubule polymerization but this remains to be substantiated. The functions of ζ and η are still unknown (96,97).

α and β tubulin are the most well studied of the tubulin isoforms in which heterodimers, especially β tubulin, are a focal point of this thesis. The folding of tubulins and formation of heterodimers for use in microtubules are complex. α and β tubulin proteins do not fold into their native complexes through random folding events. These proteins require a myriad of other proteins and cofactors to achieve their final native

conformation. Newly translated tubulin proteins interact with cytosolic chaperonin complexes (c-cpn) to achieve the first stage of folding. Chaperonins are large multi subunit protein complexes that fold tubulin proteins into a quasi-native intermediate (I_Q) conformation using an ATP dependent mechanism (97,103-105). The I_Q then interact with isoform specific proteins, known as tubulin binding cofactors (TBC), that complete the folding process as well as join α and β monomers together to form

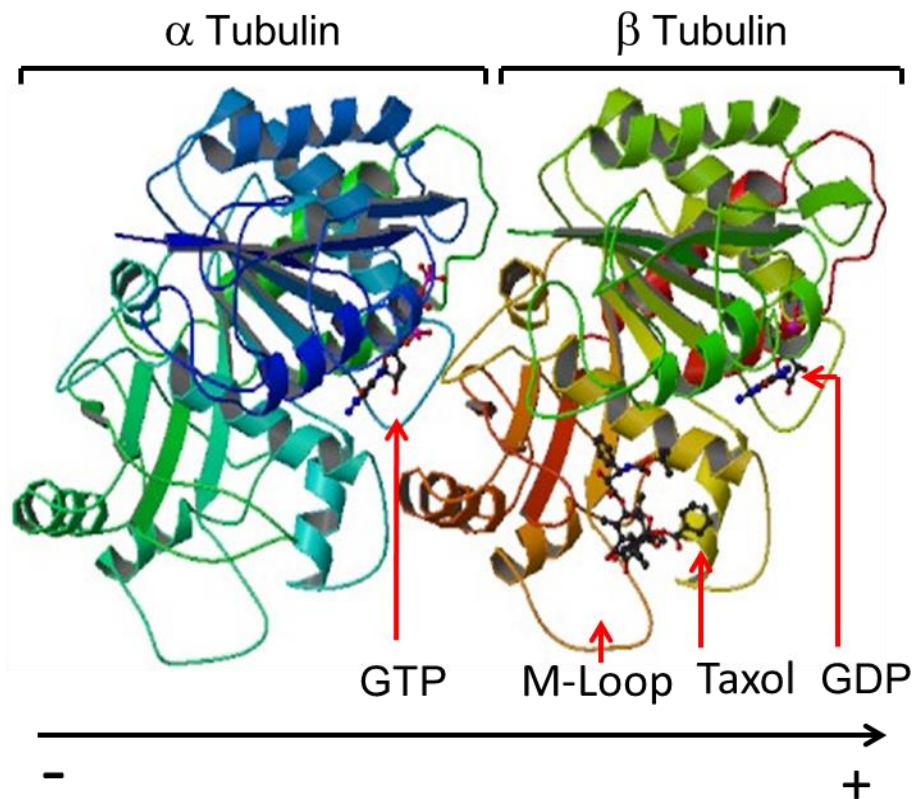


Figure 1-1. Crystal Structure of α/β Heterodimer

Image from Protein Data bank at http://www.rcsb.org/pdb/explore.do?structureId=1_tub.
Provided by Nogales et al 1998 (106)

dimer structures. From the c-cpn complex α tubulin can interact with either cofactor B (TBCB/F_B) or cofactor E (TBCE/F_E) with the possibility to exchange from TBCB to TBCE. Similarly β tubulin interacts with cofactor A (TBCA/F_A) or cofactor D (TBCD/F_D) with the possibility to exchange from TBCA to TBCD. These processes are reversible and reserves of α and β tubulin can be developed in the I_Q conformation bound to these cofactors. Once α and β tubulin are bound to the TBCE and TBCD cofactors, respectively, they form a complex. This complex then interacts with cofactor C (TBCC/F_C) and the hydrolysis of a GTP occurs to create the final native tubulin within a heterodimer (103,107,108). These processes are also reversible as TBCE and TBCD can separate heterodimers, sequestering them into pools of monomers (108). This mechanism can be used to create tubulin monomers even under conditions when *de novo* tubulin protein synthesis is non-operating or functional.

1.3.3 Targeting Microtubules with Anti-Cancer Therapeutic Agents

Because of the immense reliance on microtubules by a living cell, but more importantly an even greater reliance by cancerous cells, microtubules are a critical and fundamental target for anticancer therapy. Natural compounds that promote microtubule polymerization or destabilization of microtubules are known as Microtubule Binding Agents (MBA). These compounds are a class of anti-cancer drugs that are continuously being explored and redeveloped to improve treatment options.

There are three known target sites for anti-microtubule compounds to bind within the microtubule structure. The first is the vinca alkaloid binding domain and is located on β tubulin of the heterodimer. This class of drug originated from the naturally occurring compounds vincristine and vinblastine, both isolated from the leaves of the periwinkle plant (109). These drugs promote microtubule stabilization and disassembly in a dose dependent manner. They bind with high affinity to the growing end of the microtubule at low concentrations to inhibit microtubule dynamics, stabilizing the microtubule structure. At higher concentrations vinca drugs promote the disassembly of microtubules, preventing the formation of the mitotic spindle required for mitosis.

The second class of MBAs also promotes disassembly of microtubules. These are the drugs that bind to the colchicine binding domain within β tubulin. Colchicine is a drug used in the treatment of gout. Due to the high toxicity of colchicine it is not used as an anticancer drug but provides a secondary site for microtubule binding. At low concentrations, colchicine binds to free tubulin and is incorporated into the growing microtubule which slows the elongation of microtubules, stabilizing their dynamics. At high concentrations, the incorporation of colchicine bound tubulin destabilizes the overall microtubule structure and causes depolymerization of the microtubule (109).

Finally the third class of MBA are the taxanes (e.g., Taxol or paclitaxel; Taxotere or docetaxel). This class of drugs binds to the interior,

or lumen, of microtubules at the β tubulin subunit. Similar to the other two classes of drugs, taxanes promote microtubule stabilization at low concentrations, however at high concentrations of drug function differently from the other two by promoting polymerization and elongation of microtubules. This class of anticancer drug will be explained in further detail to follow.

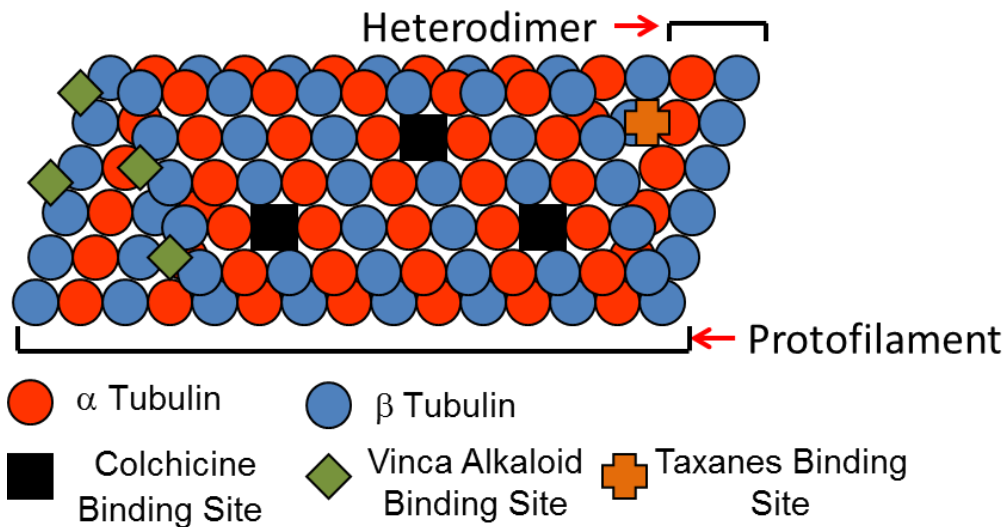


Figure 1-2. Microtubule and MBA Binding Sites

Modified figure adopted from Jordan et al. 2004 (109)

1.4 Taxanes

1.4.1 Origins of Paclitaxel

This class of anti-cancer drugs originated from the discovery of the parental compound, paclitaxel, originally described in 1967. It was discovered as part of a National Cancer Institute program to identify anti-cancer agents found within randomly selected plant species, and was given the name Taxol (61,110). Taxol was originally isolated from the bark

and stems of the Pacific yew tree, *Taxus Brevifolia*. Only 500 mg was originally purified from 12 kg of dried bark and stems, resulting in a yield of approximately 0.004%. This approach continued and taxol was isolated from the bark of *T. Brevifolia* during the 70s and 80s as it underwent pre-clinical and clinical phase trials for treating many solid tumors including ovarian, breast, lung and AIDS related Kaposi sarcoma (111-113). Taxol gained FDA approval in 1992 and was distributed by Bristol-Myers Squibb. The generic name was changed to paclitaxel and it was marketed under the trade name Taxol. Due to low yields of paclitaxel from the bark and declining populations of *T.Brevifolia* (61), a new method to develop the drug was adopted resulting in the creation of the first paclitaxel analog, docetaxel (61). Precursor molecules, baccatin III or 10-deacetylbaccatin III, were used as foundational structures for the semi-synthetic development of docetaxel and paclitaxel. These precursor molecules are found within the needles of other species of yew trees, specifically *Taxus baccata*, or European yew. These types of yew grow at much faster rates and the recovery of precursors from needles is much higher, and because the plant does not have to be destroyed to harvest needles, became an attractive option and as a renewable resource for the development of paclitaxel (110).

Second generation drug docetaxel is altered at two positions of paclitaxel. Docetaxel has a hydroxyl group at the C-10 position instead of an acetate ester, and tert-butyl carbamate ester on the phenylpropionate

These drugs have been developed with the goals to; improve water solubility, tumor permeability, and cellular retention, thereby resulting in better outcomes and longer survival times in patients (61).

1.4.2 Mechanisms of Action

Taxanes are classified as MBA, in that their main mechanism of action is through targeting microtubules. Specifically, this family of drugs are microtubule polymerizing agents. They are responsible for dose dependent promotion of nucleation, elongation and stabilization of microtubules. At low concentrations of drug, they promote the stabilization of microtubules; however at increasing drug concentrations, taxanes can promote elongation of microtubules, eventually leading to organization of microtubule bundles, and changes to cellular architecture (116). However there is also evidence that off-target interactions occur in which regulation of genes are altered due to treatment.

1.4.2.1 Protein Target of Taxane Drugs

Taxanes specifically target β tubulin of the α/β heterodimer (117,118). The location of this active site is found on the interior, or lumen, of the hollow microtubule structure. Given that microtubules are composed of repeating globular proteins, interstitial spaces (“nano-pores”) are located along the length of the microtubule, located between adjacent protofilaments. It is through these pores that taxanes have been shown to move and gain access to its active site on the interior lumen (119,120). Once bound to the active site, a conformational change occurs, wherein a

motif of β tubulin known as the M-loop, is stabilized preventing the disassembly of the microtubules (Figure 1-1). Taxanes bind in a 1:1 ratio with heterodimers along the length of the microtubule (109). Although taxanes can potentially be bound to each heterodimer found within a microtubule structure, only one taxane molecule is required to inhibit depolymerization of hundreds of tubulin heterodimers (109,116).

This type of mechanism is useful for the inhibition of mitosis. Microtubules are required for the separation of sister chromatids during the progression of the cell cycle from metaphase to anaphase (121). Cells that are unable to divide sister chromatids slip into mitotic arrest. Without a resolution to this problem cells will initiate the pathways that lead to programmed cell death, or apoptosis (122). This type of mechanism does not discriminate between healthy and cancerous tissue, however, since cancerous tissue is generally in a state of much higher cell division, this mechanism by default targets cancer cells at a much higher frequency.

1.4.2.2 Taxane Mediated Changes in Gene Expression

Changes in gene expression in cells treated with paclitaxel have been identified. Differential expression may originate due to off-target effects or due to the initiation of signal transduction cascades. Differentially expressed genes encoding proteins or cytokines in pathways related to inflammation, cell cycle arrest, apoptosis, and inhibition of angiogenesis have been reported (61). There have been 85 genes identified in which their expression has been altered in the presence of

docetaxel (123) and an indeterminate number of genes activated by paclitaxel. Several of these genes encode components of signal pathways related to apoptosis or regulation of the cell cycle. However there are several cases in which genes such as *BAX* are also activated due to paclitaxel treatment that ultimately lead to cell survival and chemotherapeutic resistance (124).

1.5 MicroRNAs

1.5.1 MiRNA Origins and Biosynthesis

MicroRNAs are small non-coding RNAs of 18-25 nucleotides in length. They are evolutionarily conserved, having functions in simple organisms such as *C. elegans* as well as more complex organisms such as plants and mammals (125). The conservation of this mechanism of regulating gene expression suggests that it dates back to the last common ancestor of these organisms (126). Most miRNAs function by binding to the 3' untranslated region (3'UTR) of the mRNA of a gene, and silence the gene by inhibiting messenger translation.

MicroRNAs reside in three locations within the genome. They can be found in the intronic or exonic regions of genes and likely regulate the genes in which they are located, or a gene in relatively close proximity. The remaining miRNAs are located in regions where no genes are present and are likely transcribed from their own promoters as individuals or as families of miRNAs (poly-cistronic) with similar functions. There are five steps required for the production of a mature miRNA, beginning in the

nucleus and moving to the cytoplasm where they confer functional activity. The first step is the generation of a single stranded primary miRNA (pri-miRNA) of ≥ 200 bp and even upwards of 1 kb in length (125). This is thought to be a process carried out by either RNA polymerase II (125,127), when located in the region of a gene, or RNA polymerase III (127) when transcribed using their own promoters. The second step includes endonuclease excision of shorter precursor –miRNAs (pre-miRNA) of 60-110 nt in length. This is performed by Drosha RNase III endonuclease (128). Pre-miRNAs are then exported from the nucleus to the cytoplasm by Ran –GTP through recognition using Exportin- 5 receptor. Following transport to the cytoplasm, Dicer endonuclease cleaves the pre-miRNA into a mature miRNA, double stranded and 18-25 nt in length. The mature miRNAs are incorporated as a single strand into a ribonuclear particle to create the RNA induced silencing complex (RISC) through interactions with Argonaut protein, a family of proteins integral to the RISC complex and miRNA induced gene silencing. The strand from the RNA duplex not incorporated into the RISC complex is denoted as miRNA*. A mature miRNA can induce silencing by two ways: (i) through binding to a complete homologous sequence within the target transcript, wherein the mRNA is degraded; or (ii) through incomplete homology of mature miRNA with the target mRNA. Incomplete homology of the miRNA with the mRNA stand results in two distinct mechanisms: (i) blocking translational machinery and (ii) mRNA de-adenylation (129,130). The

incomplete homology is the dominant mechanism by which mammalian systems induce gene silencing. Due to the number of possible incomplete base pair interactions between a mature miRNA and a transcript, a single miRNA has the potential to target many mRNAs with incomplete homology resulting in down regulation of the targets. Members of the miRNA family have the ability to target the same transcript, resulting in a redundancy of regulation. The ability of miRNAs to regulate many transcripts is known as hetero-silencing, a distinction that separates miRNAs from siRNAs which typically undergo auto-silencing, or same gene silencing. Additionally, the widespread post transcriptional regulation by miRNAs has led to the belief that about a third of the entire genome is regulated by miRNAs. There have been over 1000 human miRNAs identified to date (125,127,131,132).

1.5.2 MicroRNAs Deregulation in Breast Cancer

Similar to mRNAs and the genes from which they are encoded, miRNAs are also regulated at the genomic, epigenomic and transcriptional levels. Given that a large number of miRNAs are located in regions of the genome that are highly susceptible to genomic instability, the propensity of these miRNAs to become deregulated is high (127,131). Aberrant expression of miRNAs has been linked to several types of cancer. Differential expression found between breast cancer tumor types has led to the use of miRNA profiles for specific cancer as predictive and prognostic markers for patient outcomes. MicroRNAs have been shown to function as oncogenes or as tumor suppressors, and have been seen to

be over or under-expressed in tumors (133-135). Acting as either oncogenes or tumor suppressors, miRNAs have activity in many cancer related pathways affecting proliferation, anti/pro apoptotic machinery, invasion and metastasis, and cellular differentiation. Given that miRNAs are rather simple to detect in circulation as well as in paraffin embedded tissue samples they are becoming more widely used and implicated as potential biomarkers for the detection, prognosis and with potential to tailor treatment decisions. Several studies have been performed that show the differential expression of miRNAs between healthy and cancerous tissue, as well as between many pathological characteristics related to breast cancer. Many of these studies have been carried out using breast tissue in which they found miRNAs, both up and down regulated related to tumor development (136), ER status, PR status, tumor stage, vascular invasion, lymph node metastasis and rate of proliferation (137). This knowledge of the characteristics of breast cancer can be extended to use miRNAs for the classifications of the subtypes of breast cancer (as with mRNA differential expression profiles), for better understanding of an individual's molecular heterogeneity of the tumor, and likely aid treatment decisions to improve outcomes.

Given the ability of a single miRNA to regulate multiple mRNA targets or multiple miRNAs regulating a single mRNA target, leads to redundancy or pleiotropy of targets or functions. As a result, common pathways may be involved in the aetiology of different types of cancers.

There is also the possibility of a single miRNA functioning as a biomarker for a tumor suppressor in one cancer type and as an oncogene in another. This variability and redundancy offers a more global outlook for understanding the interactions between mRNA and cognate miRNAs. Since biology operates as networks and not through single gene/mRNA entities, the global regulation of mRNAs by miRNAs at the whole genome level should eventually help design drugs targeting pathways and not the single gene products, provided mechanisms of resistance to drugs in a treatment setting is fully delineated. Until then, model systems will continue to provide the mechanistic and functional insights to address mechanisms of drug actions.

1.6 Mechanisms of Taxane Mediated Drug Resistance

The success of taxanes has been overshadowed by intrinsic or acquired resistance of tumors upon exposure to the drug. Resistance to taxanes has hampered clinical efforts to achieve a full response. Several mechanisms have been proposed to explain drug resistance, both with *in vitro* model systems and also to explain the observations in the clinic.

1.6.1 Over-Expression of Drug Efflux Pumps

Cellular retention of anti-cancer drugs is key to their success as effective therapeutics. There are inherent mechanisms used by the cell to eliminate harmful toxins from the cytoplasm. A family of membrane proteins known as the ATP binding cassette (ABC) transporters is responsible for the expulsion of toxins from within cells. There are 49

genes and their encoded products belonging to the ABC family are divided into seven sub families (ABCA – ABCG), all of which are expressed under normal cellular conditions (138,139). In cancerous cells, expression of many of these efflux pumps is up-regulated, and contributes to enhanced expulsion of different classes of cancer drugs from within cells. These protein efflux pumps include P-glycoprotein (P-gp), which is the protein product of the gene *MDR-1* (ABCB1), *MRP1/2* (multidrug resistant associated protein/ABCC1/2) and breast cancer resistance protein (BCRP/ABCG2) (140,141).

P-gp is one of the more widely studied efflux pumps that contribute greatly to the observed *in vitro* and *in vivo* drug resistance. This protein binds hydrophobic substrates with either a positive or neutral charge and expels them from the cell in an ATP dependent manner. P-gp expression often increases following treatment resulting in a high chance of treatment failure. It has been shown that roughly 41% of breast tumors express P-gp, with as little as 29% of patients with primary disease but up to 71% in relapsed patients (142-144). Although patient data has been reported, the link between patient tumors and drug resistance due to P-gp expression is weak. The majority of evidence implicating this protein in drug resistance has been from *in vitro* studies with cultured cells.

1.6.2 Variable Tubulin Isotype Expression

As previously stated, β tubulin family consists of nine different isotypes. These isotypes are tissue specific and are expressed with

variable ratios among the tissues of the body (145). Each of these isotypes has a different amino acid sequence, which can result in slight differences in the native conformation of folded protein, contributing to differences in taxane binding affinity. It is these differences that influence a particular isotype's ability to promote microtubule stabilization or destabilization. There is extensive evidence linking tubulin isotype expression to drug resistance and sensitivity (see below).

1.6.2.1 β I Tubulin

β I tubulin isotype is the most prominent isotype in a variety of tissue types. Both *in vitro* and *in vivo* experimental work has been done to show that elevated expression of β I tubulin is associated with paclitaxel and docetaxel resistance. Studies have shown an increase in β I expression in both MCF-7 breast cancer and paclitaxel resistant A549 lung cancer cell lines. This increase in expression was observed simultaneously with the increase in expression of β II, III and IV isotypes (146,147). Kavallaris et al. validated their findings when paclitaxel resistant ovarian tumors were analyzed for expression of tubulin isotypes. Similar to their cell line work, these investigators reported a 3.6-fold increase in β I isotype expression in tumor samples, although the authors attributed this increase to the variety of cell types found in ovarian tumors (146). Others have also shown that ovarian tumors exhibit a marked increase in the expression of β I. Ohishi et al. used immunohistochemistry to characterize the expression of tubulin isotype levels in 77 ovarian tumors. In addition to

high expression of β I, the investigators of this study also found high expression of β IV and medium expression of β III (148). β I tubulin expression has been shown to be increased in taxane resistant cells, although increased expression of this isotype is accompanied by altered expression of other isotypes, potentially decreasing the significance of β I tubulin in taxane resistance.

1.6.2.2 β II Tubulin

β II gene produces two different splice variants, IIa and IIb, which encode protein isotypes found mainly in the brain but with limited expression in a variety of tissue types. Previous cell line and *in vivo* work has shown that β II tubulin is decreased or completely absent in taxane resistance (146,148). Others have shown that there is an increase in β II mRNA but no detectable levels of protein were found (149). Additionally, evidence has also been published that shows β II protein levels increased in taxane resistant cell lines. The authors do note that these resistant cell lines also show large increases in P-gp expression, which indicates that the observed resistance is due to efflux pumps and changes in isotype expression may be a coincidence (150).

1.6.2.3 β III Tubulin

β III tubulin isotype is found only in neuronal tissue and the testes, and has been shown to destabilize microtubule polymerization due to its highly dynamic properties (151-153). There is abundant evidence in the

literature, from both *in vitro* and *in vivo* work, that shows that over expression of β III isotypes is responsible for taxane resistance as an individual entity (154-160). In one study, patient data shows that individuals with high expression of β III were resistant to treatment (69.2% of patients) compared to those with low expression of β III tubulin (30.4% of patients) (161). Relapsed patients following curative surgical resection of lung cancer treated with paclitaxel and platinum based regimens and showing low β III expression, had a better median progression free survival time compared to those with high expression (162). Work has been done that has shown opposite findings to these. Patients with ovarian clear cell adenocarcinoma respond better to paclitaxel/platinum combination therapies when expression of β III tubulin is high (151). Findings such as these are the exception to the norm, as there is an overwhelming number of publications that provide evidence that high expression of β III tubulin as an individual factor increases resistance to taxane based therapies.

1.6.2.4 β IV Tubulin

β IV tubulin gene produces two protein products as the result of alternative splicing. These two proteins are IVa and IVb. IVb is expressed at high levels in a wide variety of cell types (145,146), while IVa is highly expressed in the brain with limited expression in other tissue types. *In vitro* and *in vivo* experiments have been published showing that increased levels of β IV are correlated with taxane resistance (146-148). Similar to β

I, changes in expression of β IV tubulin is accompanied by changes in other isotype expression, specifically I and III. β IV, to my knowledge, has not been shown to be a singular factor in influencing taxane resistance.

1.6.3 β Tubulin Mutations

Amino acid substitutions induced by gene mutations alters the sequence of tubulin proteins. These sequence alterations can affect taxane's ability to induce microtubule polymerization. *In vitro* work has been done by a number of groups that showed single point mutations conferred increased paclitaxel resistance within a number of human cell lines. Yin et al. summarized 26 different amino acid substitutions distributed across 14 different residue positions, spanning the entire protein sequence, and these residues were shown to be important in the interactions with paclitaxel (or other tubulin binding drugs). The majority of the mutations have been discovered in β I (163,164), but other studies have discovered mutations in β II and β III that confer paclitaxel resistance (165) or cause neurological disorders due to improper microtubule formation (166). A review of the literature for mutations within tubulin genes suggests that many, but not all, of the mutations discovered to date can confer resistance to taxane drug treatment. The mechanisms by which these mutations induce taxane resistance are variable. Some of these mutations are located within the paclitaxel binding site, precluding drugs from binding (167). Other mutations and the resulting amino acid changes appear to effect microtubule stability. These amino acids are involved in

proper lateral protofilament interaction and microtubule heterodimer binding, which prevent taxanes from stabilizing microtubules (168-170). The evidence found within the literature implicating specific, individual amino acid substitutions causing paclitaxel resistance is from the cell line models and from *in vitro* characterizations. There is limited evidence supporting major involvement of β tubulin gene mutations in drug resistance in patients; however efforts are underway to continue to discover mutations that correlate to resistance in clinical samples and associated isotype expression patterns (114). It is also of interest to look for determinants of resistance beyond tubulin gene mutations and/or changes in expression of specific isotypes. To this end, I have undertaken a genome wide scale search for markers for a comprehensive understanding of taxane resistance mechanisms, a theme addressed in this study.

1.7 *In Silico* Design of Paclitaxel Analogs and the Rationale

1.7.1 Nano Pore

As previously stated, experimental evidence has been provided to show that paclitaxel moves through the interstitial spaces, known as nano-pores, located between heterodimers (171). Considering the possible structures of microtubules, there are four possible nano-pores originating from two microtubule conformations (Figure 1-2). The first conformation is the A lattice, in which adjacent heterodimers are offset by a single

monomer, resulting in an antiparallel association among heterodimers running the length of the microtubule. This type of lattice results in two different nano-pores, the 1s and the 2s. The 1s pore is created at the inter-dimer space of two heterodimers of one protofilament and the intra-dimer space of a single heterodimer of the other protofilament. The 2s nano-pore is created by similar configurations of heterodimers, the only difference being that each protofilament involved takes on the opposite role in the 2s pore, compared to the 1s pore. As a result, the 2s nano-pore is located within close proximity of the taxol binding site whereas the 1s nano-pore is away from the taxol binding site.

The second conformation, and the one that occurs with a much higher frequency in nature, is the B lattice. This microtubule conformation results in adjacent protofilaments orientating themselves in a parallel fashion such that heterodimers line up with like monomers associated with each other. This conformation also results in two nano-pores being formed. The 1 nano-pore is created at the inter-dimer space of both adjacent protofilaments. This nano-pore is located proximal to the taxane active site. The 2 nano-pore is created at the intra-dimer space of two adjacent heterodimers and is located one tubulin monomer away from the taxane active site.

Of the four pores, the 1 is the largest (172), providing the most space for taxane compounds to travel through. This pore is also located with close proximity to the taxane active site and given the B lattice to be

the more dominant form by a wide margin; it is believed that taxanes travel through this nano-pore to gain access to their active site. Recent work from Dr. Tuszynski's group has provided evidence of a binding site located within this pore (termed intermediate binding site) to which the taxanes associate with and facilitate movement of drug from the exterior of the microtubule to the interior (unpublished observations). This putative intermediate binding site analysis formed the basis for *in silico* modeling for paclitaxel analogs to stabilize or facilitate a transient interaction with the intermediate binding site (residues in the protein) for eventual migration of taxol to the active site pocket. Efforts were made at custom chemical synthesis of representative paclitaxel analogs described in the ensuing text.

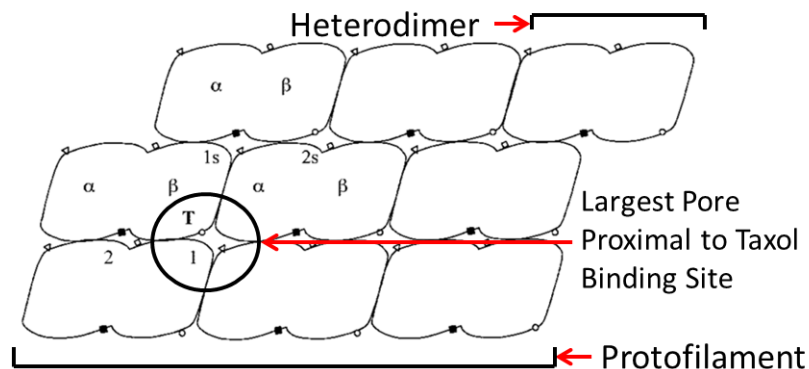


Figure 1-4. Locations of Putative Intermediate Binding Site within Microtubule Structure

There are two possible protofilament conformations within the microtubule. Most common is the B lattice conformation, in which α and β of one heterodimer are parallel with the α and β of a second heterodimer of the adjacent protofilament. Two different pores are created. The nano-pore 1 is the largest one at the inter-dimer space of both protofilaments and the nano-pore 2, is at the intra dimer space between two adjacent heterodimers (shown in figure as 1 and 2). The second conformation occurs when heterodimers within adjacent protofilaments are offset by a single monomer making the structure antiparallel; this is called a seam structure. Two different pores are created, 1s and 2s. Both pores are created at the intra dimer space of one protofilament and the inter dimer space of the adjacent protofilament. Paclitaxel binding site is denoted by "T". Image from Freedman et al. 2009 (172)

1.7.2 Rationale for the Synthesis of Paclitaxel Analogs

Seven paclitaxel analogs have been designed using *in silico* modeling work performed by Dr. Tuszynski's group. However, it is not trivial to synthesize analogs of a drug not knowing the properties of the drug in solution (solubility), availability of precursor molecules for synthesis, the least number of chemical synthesis steps from the starting material and the eventual yield. Custom syntheses of analogs for paclitaxel were out-sourced; Helios Biotech Ltd, Edmonton (Dr. Damaraju, Director, 2008-2013) and the research organizations in India, jointly provided the services. I was successful in procuring the synthesized form

of four of these analogs for use in experiments related to my interests in the microtubule nano-pore; Tx-A, Tx-C, Tx-D and Tx-F (A-F, merely indicates the chronological order of the modeled compounds and only the ones successful in the synthesis are shown here, Figure 1-5).

My interests in this field stem from work done by members of the Tuszynski group as well as others that have suggested the presence of a putative intermediate binding site within the pores of microtubules. Within the pores, two amino acids have been identified by *in silico* methods were hypothesized to play important roles in the binding of taxane drugs to the intermediate binding site and the movement of the drug to its final active site, amino acids 275 and 278. It is important to determine if these two amino acids are indeed involved in binding, polymerization and ultimately cytotoxicity to cancerous cells. These paclitaxel analogs were used to attempt to elucidate the role that amino acids 275 and 278 play in taxane activity, and their potential involvement in conferring β tubulin isotype mediated specificities.

To implicate that amino acid 275 of β tubulin is involved with binding of paclitaxel to the intermediate binding site; two derivatives have been designed to achieve this goal, Tx-A (837.92 Da) and Tx-C (855.91 Da) (Figure 1-5). One key aspect is that the amino acid at residue 275 is variable for a given isotype of β tubulin. This amino acid is Ser 275 in β I and II isotypes but Ala 275 in β III. This distinction should influence the

binding potential of paclitaxel (Figure 1-6A) as well as both these analogs, depending on the dominant isotype being expressed within the cells. Both derivatives were designed with binding affinities lower than that of paclitaxel at the Ser 275 position of β I and II, with the expected induction of polymerization and cell kill potential of these novel analogs to be lower than those of paclitaxel. This decrease in binding potential should be further influenced by the presence of Ala 275 native to β III. It is hypothesized that Tx-A will be unable to bind to the side chain hydroxyl group of Ser or methyl group of Ala due to the removal of the hydroxyl group and replacement with a hydrogen atom at the C-7 position of paclitaxel (Figure 1-6B). Tx-C is hypothesized to have an intermediate binding with Ser 275 as compared to paclitaxel. This is due to the lower binding affinity of fluorine at C-7 with the hydroxyl group of Ser 275. Paclitaxel has a binding energy with Ser 275 of 5 kcal/mol whereas the binding energy of Tx-C with Ser 275 is 3 kcal/mol, which should lead to an intermediate assembly rate and cytotoxicity in cell line models (Figure 1-6C). Again this effective loss of binding will be greater in the presence of β III tubulin Ala 275. I hypothesize that a reduction in the binding potential will result in a decrease in tubulin polymerization, vis-a-vis., less cell kill. This loss of function would implicate amino acid 275 in intermediate binding.

Tx-D (869.92 Da) and Tx-F (883.94 Da) (Figure 1-5) are designed to interact with amino acid 278 located within the intermediate binding site.

This amino acid is Ser in β I, II, and III isotypes. It is hypothesized that if this interaction is made stronger as part of intermediate binding it will stabilize the interaction for quicker movement of the compound to the taxol active site, an effect that should enhance the ability of these drugs to induce microtubule polymerization and cytotoxicity. Manipulations made at the C-10 position of paclitaxel to elongate the side chain enable the derivatives to span the 4-9 Å gap required to make the interaction with Ser 278 (Figure 1-6D). Given the role I postulated for amino acid 275 in intermediate binding, the presence of Ala 275 in β III tubulin should still have an effect on binding of these drugs at their C-7 hydroxyl group, in addition to the changes made at the C-10 position. Previous work has provided no additional information on which of these two manipulations will result in the greatest interaction. The extent to which cytotoxicity may be improved by elongation of the C-10 side chain will be determined from cell line based cytotoxicity assays. I hypothesize that amino acids 275 and 278 are important in intermediate site binding and translocation of taxane drugs to their active site, as well as β III tubulin induced resistance. Paclitaxel analogs will be used to assess the validity of this claim using both *in vitro* tubulin polymerization assays and cytotoxicity assays. Positive findings correlated to the above predictions will confirm predicted role of these two amino acids.

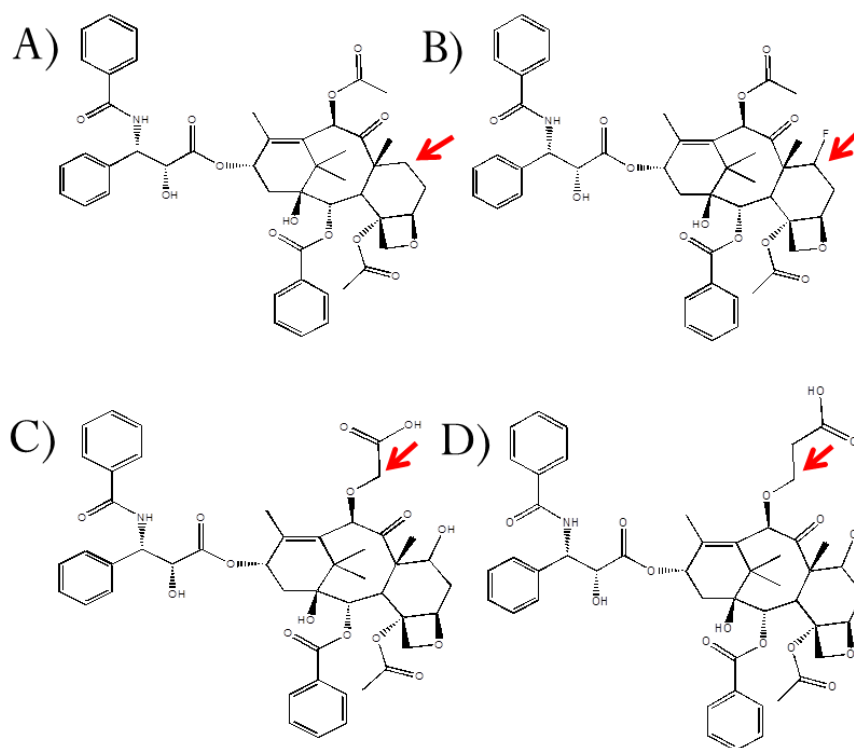


Figure 1-5. Structure of Custom Synthesized Paclitaxel Analogs

Four analogs of paclitaxel have been created, manipulated at a single location to interact with amino acids, 275 and 278 within β tubulin. (A) Tx-A and (B) Tx-C; these have been manipulated at the C-7 position, designed to interact with Ser 275 of β tubulin. In Tx-A the hydroxyl group has been removed and replaced with a hydrogen atom and In Tx-CB the hydroxyl group has been replaced by a fluorine atom. (C) Tx-D and (D) Tx-F; these have been manipulated at the C-10 position, designed to interact with Ser 278 of β tubulin. In Tx-D the side chain at C-10 position has been extended by a single carbon, whereas in Tx-F the side chain at C-10 has been extended by two carbon atoms.

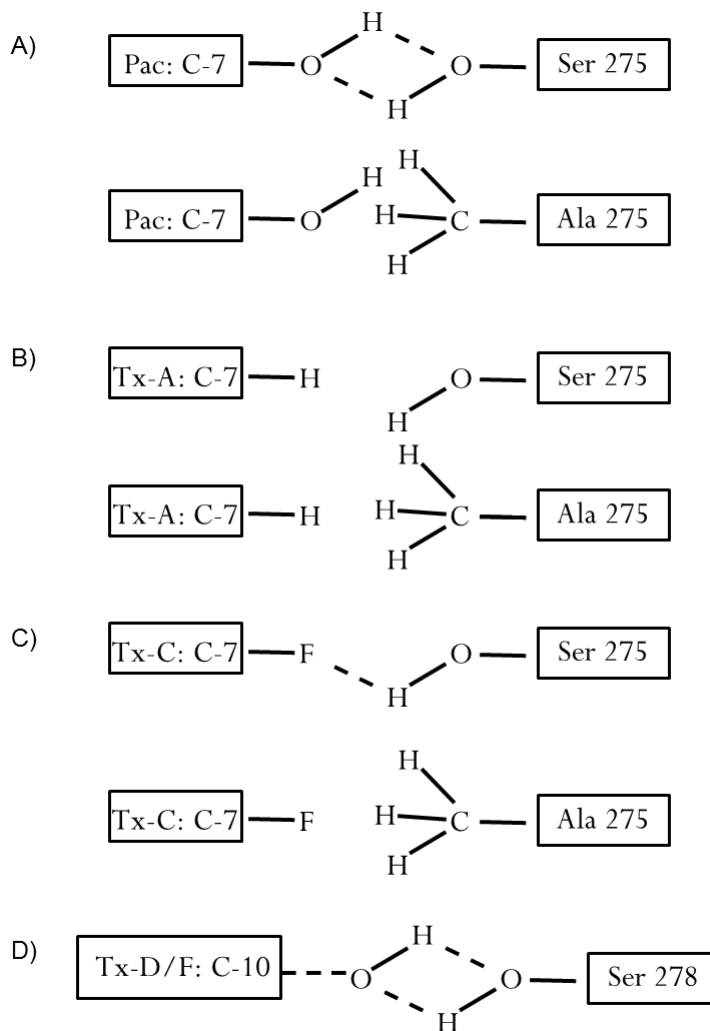


Figure 1-6. Predicted Chemical Interactions between Paclitaxel and Analogs with Amino Acids Located within the Intermediate Binding Site

(A) Paclitaxel C-7 was predicted to interact with the amino acid at the 275 position and its interaction is dependent on isotype specific expression of β tubulin; amino acid at 275 position is Ser in β I tubulin and Ala in β III; (B) Tx-A is manipulated at C-7 position, in that a hydroxyl group was replaced with a hydrogen atom. Putative Tx-A interactions if any were shown with the β tubulin at 275 position; (C) Tx-C is manipulated at C-7 position, in that a hydroxyl group was replaced by a fluorine atom. Putative Tx-C interactions if any were shown with the β tubulin at 275 position; (D) Tx-D and Tx-F were manipulated at C-10 position, in that chain elongation was achieved by one and two carbon bonds respectively. A replacement of the ketone moiety in the structure by a carboxylic acid potentially mediates interactions with the amino acid 278. Chain elongation should in principle result in shortening of the distance between amino acid side chain and taxane moiety.

2. Materials and Methods

2.1 Cell Culture

Breast cancer cell lines, SKBR-3, MDA-MB-231, and T-47D cell lines were kindly provided by Dr. Ing Swie Goping (University of Alberta, Canada). MESSA (*MDR-1* negative) and DX5 (*MDR-1* positive) uterine sarcoma cell lines, and K562 (*MDR-1* negative) and R7 (*MDR-1* positive) chronic myelogenous leukemia cell lines were kindly provided by Dr. Charles Dumontet (University of Lyon, France). All cell lines were maintained in RPMI 1640 media supplemented with 10% fetal bovine serum, at 37°C, 5% CO₂ and in a humidified environment. Adherent cells were maintained in media until ~90% confluent. Cells were trypsinized in a solution of Trypsin-EDTA (Gibco, Life Technologies Corporation, Carlsbad, CA, USA) at a final concentration of 0.25% and were re-seeded based on the perceived growth rate of each cell type.

2.2 Paclitaxel Resistant Derived Sub-Lines

I reasoned that incremental resistance to paclitaxel if developed in a cell line model would serve to (i) correlate tubulin isotype expression levels (or P-gp) to paclitaxel resistance levels and (ii) minimize variations due to differences among the cell types to facilitate comparisons of IC₅₀'s. Since commercial sources of cell lines exhibiting resistance to paclitaxel were not available I chose to develop the resistant sub-lines. To address these objectives, I selected the breast cancer cell line, SKBR-3, Her2+ cell line with no expression of ER and PR for the development of a series of

sub-lines with incremental resistance towards the anti-microtubule drug paclitaxel (Hospira Inc., Lake Forest, IL, USA). TN breast cancer cell lines tend to have intrinsic resistance to multiple drugs and luminal breast cancer cell lines are not of immediate interest due to their good prognosis and low rates of recurrence in affected populations. Her2+ enriched breast tumors inherently offer the advantage to administer targeted therapies (Herceptin), show considerable recurrence and further cytotoxic therapies are warranted. This method was adopted using previously described techniques (173,174). Using an experimentally determined IC_{50} value for SKBR-3 cells treated with paclitaxel, "WT" SKBR-3 cells were treated with a concentration of paclitaxel 1000-fold less than this known IC_{50} . The cells were maintained in this initial concentration of drug for two passages after which they were re-seeded into two populations of cells, the first to be maintained at the same drug concentration, grown to confluency and cryopreserved for future experimentation. The second population of cells was grown in a new concentration of drug three-fold greater than the previous drug concentration. This pattern of drug exposure continued until a maximum tolerable dosage was obtained. For subsequent experiments using these derived cell lines, media containing the same drug concentration the cells were developed and used at all times to maintain growth of cells. All cells were developed and maintained in verapamil (167), a known inhibitor of the multidrug resistance pump, P-gp, to prevent P-gp mediated resistance as a dominant mechanism within these cell

lines. Media containing both drug and verapamil was replaced every 2 - 3 days with fresh drug containing media.

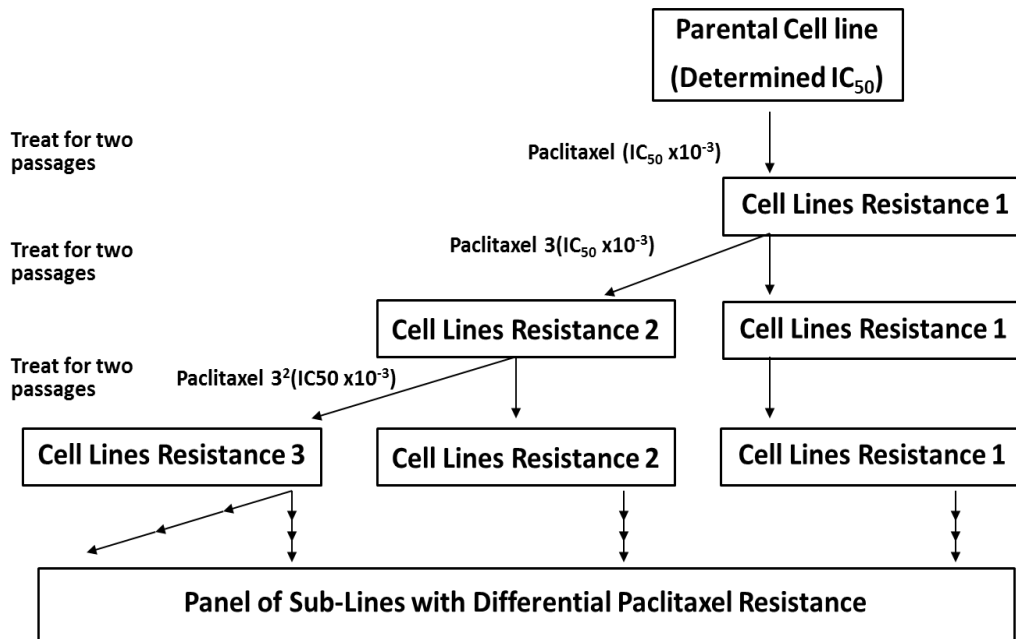


Figure 2-1. Method for Creating Panel of Paclitaxel Resistant Sub-Lines

2.3 Cell Imaging

Images of all cell lines were obtained using a Zeiss Axiovert 200M microscope as seen through a 10x/0.3 Zeiss Plan-NEOFLUAR camera. Images were captured using a Cooke SensiCam^{QE} camera and Metamorph Version 7.7.7.0 software (Molecular Devices LLC., Sunnyvale, CA, USA). WT cell lines were maintained in drug free media before images were taken. Resistant cell lines were maintained in drug containing media at the same concentration in which they were originally developed.

2.4 Cytotoxicity Experiments

Cell viability in the presence of paclitaxel or each of the four analogs, Tx-A, Tx-C, Tx-D, and Tx-F, was determined using the CellTiter 96® AQueous Non-Radioactive Cell Proliferation Assay (MTS) (Promega, Madison, WI, USA). Cells were seeded in 96-well plates (Nalge Nunc International, Rochester, NY, USA) at levels proportional to their growth rate (ranging from 5 to 10 thousand cell per well) at a volume of 100 µl and allowed to adhere to the plate overnight. The following day the cells were treated with a range of 100 µl of 2x drug concentrations for a final 1x drug concentration per well. Each drug concentration was administered to six different wells, to ensure correct pipetting of cells and drug containing media in each well. This treatment was maintained unchanged for a 72 hour period. Following 72 hours of treatment, 30 µl of MTS reagent was added to each well. The plates were incubated at 37°C for a time period of 30 minutes to 4 hours, depending on colour development, a rate which was variable from cell line to cell line. Relative cell viability was determined by measuring the absorbance of each well at 490nm and converted to a percent of total viability compared to an untreated control. Experimental results are an average of at least n=3 experiments.

2.5 Cell Pellet Preparation from Wild Type Cell Lines

Total protein cell lysates were used to carry out western blot analysis. SKBR-3, MDA-MB-231, T-47D, MESSA, DX5, K562, and R7 cell

lines were used. Cells were always allowed to grow to ~90% confluency, followed by trypsinization. Each cell line was seeded into two separate T-125 flasks (Corning Incorporated Life Sciences, Tewksbury, MA, USA) according to growth rates. (i) One flask was administered drug containing media to a concentration of $\frac{1}{2}$ IC₅₀ (drug treatment began 24 hour prior to trypsinizing the cells), to determine the effects of acute drug exposure on levels of β tubulin within each cell line (175) and (ii) cells were maintained in the second flask in drug free media. Re-seeding of flask for a replicate analysis was achieved by using cells grown in drug free media. The process was repeated to have as many replicates as needed. Cells were counted and pelleted by centrifugation to remove media prior to liquid nitrogen freezing. Cells were lysed using a Radio Immuno Precipitation Assay (RIPA) (150mM NaCl, 1.0% Triton X-100, 0.5% sodium deoxycholate, 0.1% SDS, 50mM Tris HCl, pH8.0) lysis buffer. Protein levels for each sample were determined using a modified Lowry protein assay.

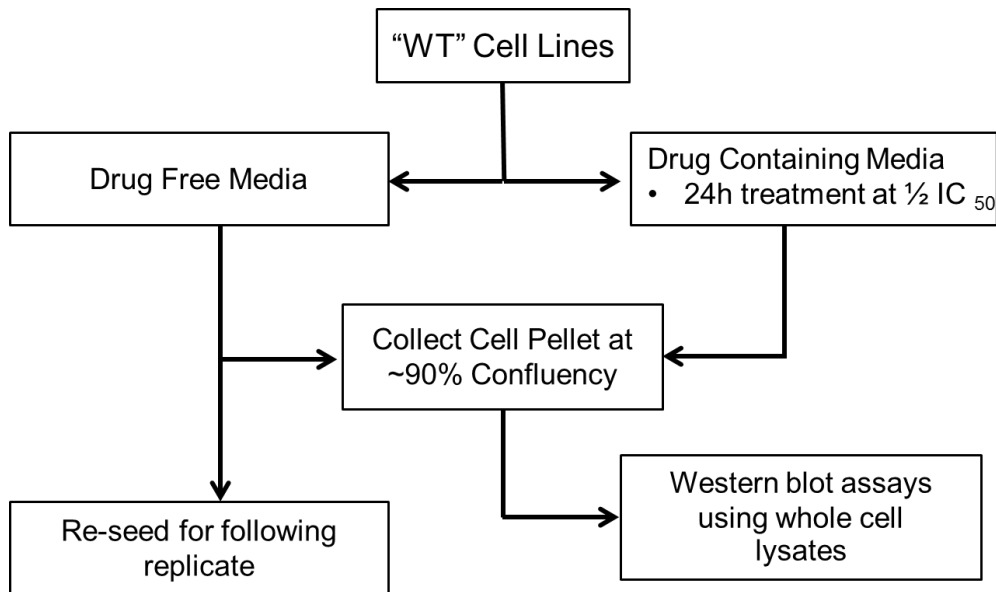


Figure 2-2. Schema for the Preparation of the “WT” Whole Cell Lysates for Western Blot Analysis

2.6 Cell Pellet Preparation from Resistant Sub-Lines

Total protein cell lysates from a subset of derived resistant sub-lines (selected four cell lines representing the extremes of sensitive to highest resistance) were prepared for use in western blot experiments and for miRNA analysis using Next Generation Sequencing (NGS). Characteristics of the four cell lines were as follows: Cell lines selected went through equal passages in cell culture media (with or without the drug during selection of resistant cell lines). Numbers in parenthesis indicate the IC_{50} values of SKBR-3 for paclitaxel divided by 1000; this low drug concentration was to ensure that cells were gradually exposed to drug in multiple steps. The number outside of parenthesis is the fold increase in drug concentration to achieve the next higher dose which was always a 3-fold increase. The first two sequential drug increases within the

media would translate to $3 \times 3 = 9 = 3^2$, the third three sequential drug increase would be $3 \times 3 \times 3 = 27 = 3^3$, and so on with each subsequent change in drug concentration. Cell lines used were $(IC_{50} \times 10^{-3})^3$, $(IC_{50} \times 10^{-3})^4$, $(IC_{50} \times 10^{-3})^5$, $(IC_{50} \times 10^{-3})^7$. “WT” SKBR-3 and SKBR-3 cell having gone through the same number of passages as the highest drug resistant cell line were used as controls. All cell lines were seeded in T-125 flasks for western blot analysis or T-75 flasks when cell lysate requirements were modest as in total RNA preparation for use in conjunction with NGS experiments. Control cells were maintained in drug free media for the entire growth period. Each resistant cell line was grown in two separate flasks. Paclitaxel resistant cells were grown in either drug free media or drug containing media, at the same concentration in which each cell line was developed, for the entire growth period. All resistant cell lines were also grown in the presence of 5 $\mu\text{g/ml}$ verapamil. Different growth conditions for resistant cells were used to determine if removal of media caused reversion of any drug related resistance phenotypes. Cells were allowed to grow to ~90% confluency. Re-seeding of flasks for resistant lines used cells from drug containing media to generate replicates to ensure that any reversions of drug resistant phenotypes were not propagated into the following replicates. Cells were trypsinized, counted and pelleted, followed by removal of media and liquid nitrogen freezing. Pellets used for NGS were shipped following this step to the University of Lethbridge (Alberta, Canada) for RNA extraction, and preparation of

samples for small RNAome sequencing from which miRNA profiles were extracted. Cells used for western blot analysis were lysed using four repeat freeze thaw cycles with liquid nitrogen and a 37°C water bath. Protein levels of whole cell lysates for each sample were determined used a modified Lowry protein assay.

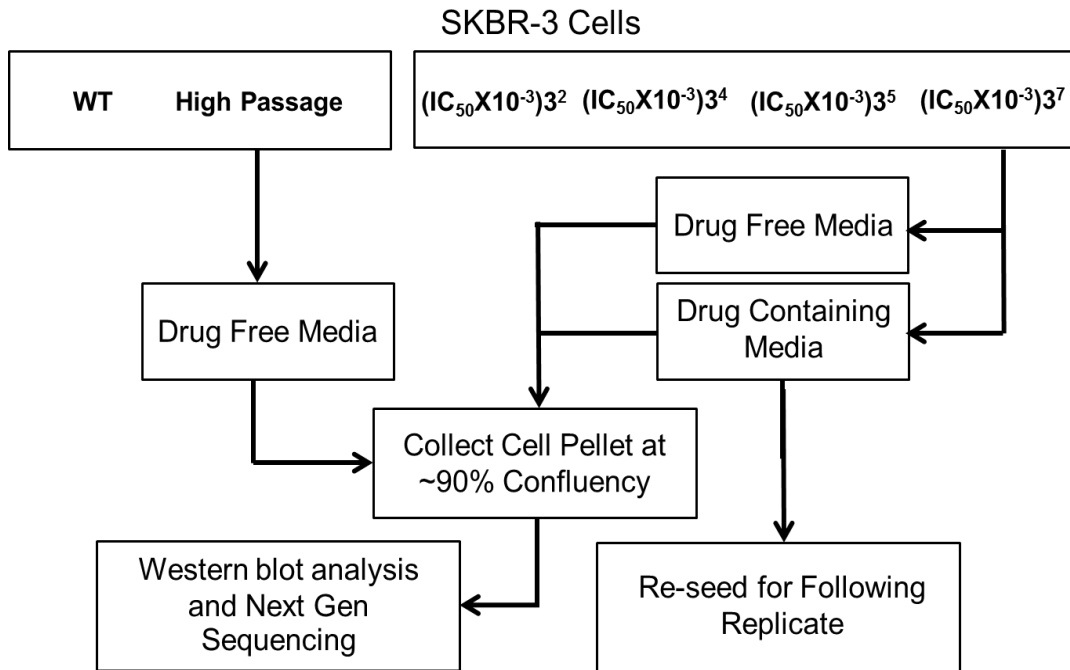


Figure 2-3. Schema for the Preparation of the Whole Cell Lysates for Western Blot and NGS Analysis

2.7 Sodium Dodecyl Sulphate (SDS) Polyacrylamide Gel Electrophoresis (PAGE) Analysis

SDS PAGE analysis was performed for western blot and protein purification experiments. Ten % polyacrylamide gels (from a stock solution of 40% 29:1 acrylamide/bis solution, 0.375M Tris, 0.1% (v/v) SDS, 0.1% (v/v) ammonium persulphate, 0.1 % (v/v) TEMED, water to volume) were used for all western blot experiments and for assessing the composition of

the proteins during partial purification of human recombinant tubulin proteins expressed in bacterial systems. Polyacrylamide (7.5%) gels were used for western blot analysis of P-gp protein (170 kDa) for the required resolution of protein bands in this size range. Total protein lysates (25 μ g) were loaded into 10 or 15 well polyacrylamide gels using 1x Laemmli Sample Buffer (Bio-Rad Laboratories Inc., Hercules, CA, USA). Gels were run at 200V for ~1h in 1x Tris/Glycine/SDS run buffer (ICN Biomedicals Inc., Irvine, CA, USA) before being removed and stained with Coomassie Blue or transferred to nitrocellulose membrane for western blot analysis. Coomassie-stained gels were destained using a solution of 50% H₂O, 40% methanol, and 10% glacial acetic acid. Destained gels were scanned on a CanoScan LiDE 600F (Canon Inc., Tokyo, Japan) and visualized using Adobe Photoshop 6.0 software (Adobe Systems, San Jose, CA, USA).

2.8 Western Blot Analysis

Following gel electrophoresis and transfer of proteins to nitrocellulose membranes, the membranes were blocked with 5% Tris buffered saline, milk and Tween (TBSMT) (154mM Tris HCl, 1.37M NaCl, 0.1% (v/v) Tween20, 5% (w/v) milk) solution for 1 hour. Proteins on membranes were exposed overnight to primary antibody-TBSMT solution. On the following day, membranes were washed in Tris buffered saline, Tween (TBST) (154mM Tris HCl, 1.37M NaCl, 0.1% (v/v) Tween20, pH 7.6), for 6 cycles with 5 min wash/incubation for each cycle in TBST to

remove unbound antibody. Membranes were further exposed to secondary antibody in TBST for 30 min. Following secondary antibody incubation, membranes were washed in TBST for 12 cycles with 5 min wash/incubation for each cycle in TBST to remove any unbound secondary antibody. Proteins were detected following a 5 min exposure to either ECL Prime Western Blotting Detection Reagent (GE Healthcare, Little Chalfont, England) or Lumi-Light Western Blotting Substrate (Roche Diagnostics, Indianapolis, IN, USA) and the exposed film was developed using a KODAK m35A X-OMAT Processor (Eastman Kodak, Rochester, NY, USA).

Proteins detected using primary mouse anti-human antibodies (Abcam, Cambridge, England) were: β tubulin I (ab 11312) used at a dilution of 1 in 100,000, β II (ab 28035) used at a dilution of 1 in 2000, β III (ab 14545) used at a dilution of 1 in 1000, β IV (ab 11315) used at a dilution of 1 in 400, β V (ab 21754) used at a dilution of 1 in 1000, P-gp (ab 3366) used at a dilution of 1 in 2000 and goat anti-human actin (sc-1616, Santa Cruz Biotechnology Inc., Dallas, TX, USA) used at a dilution of 1 in 4000. Secondary antibodies were goat anti-mouse (115-035-003), at a dilution of 1 in 10,000 and rabbit anti-goat (305-035-045, Jackson ImmunoResearch Laboratories Inc., West Grove, PA, USA) used at a dilution of 1 in 40,000.

2.9 Lowry Protein Assay

Total protein content was determined for both western blot experiments and recombinant tubulin experiments using a modification of the original Lowry et al. (1956) method. Bovine serum albumin (BSA) was used as a standard for all protein assays. A new standard curve was created for each set of experiments performed on a day to day basis. To establish a standard curve, 0, 10, 20, 30, and 40 μl of 1mg/ml BSA stock was added to enough water to bring the total volume to 250 μl . The standard curve contained 0 to 40 μg of protein. Assays from unknown samples were established by adding 50 μl of unknown at a range of dilutions (1/2 to 1/100) to 200 μl of water, for a final volume of 250 μl . Blanks were created containing the appropriate concentrations of buffers used in the unknown samples to correct for any changes in colour that may have occurred independently of protein content. To begin the reaction, 250 μl of Blue Goodies reagent (2mM $\text{CuSO}_4 \cdot 5\text{H}_2\text{O}$, 4mM Na-tartrate, 943mM Na_2CO_3 , 500mM NaOH, prepared fresh every 2-3 weeks) was added to each tube at 10 s intervals and immediately vortexed. Tubes were left undisturbed for 10 min followed by the addition of 1 ml of 1/18 Folin and Ciocalteu's phenol reagent (Sigma Aldrich, St. Louis, MO, USA) to each tube with immediate vortexing. This too was done at 10 s intervals to ensure equal timing for all samples. Tubes were left undisturbed for 30 min at room temperature. Reaction contents in tubes were read at 10 sec intervals using a Beckman Coulter DU 730

spectrophotometer (Beckman Coulter, Inc. Pasadena, CA, USA) at 650 nm against zero protein containing blank. Total protein in each experimental sample was read/determined using the protein standard curve.

2.10 Recombinant Protein

Wild type and mutant recombinant human β I tubulin was expressed in *Escherichia coli* BL21(DE3) and cell pellets were provided by Dr. David Wishart, University of Alberta. All recombinant proteins were histidine (His) tagged to facilitate protein purifications.

2.11 Protein Purification

Wild type α , β and mutant β tubulin proteins were purified using a modified hybrid protocol for a nickel nitrilotriacetic acid (Ni-NTA) Purification System (Life Technologies Corporation, Carlsbad, CA, USA). *Escherichia coli* BL21 (DE3) cells transformed with expression constructs for human recombinant α and β tubulins were harvested from culture media, washed and stored in 10mM Tris, pH 8.8 at -20°C until ready for use. When ready for use, cells were thawed and centrifuged at 15,000 rpm (11,300 g_{av}) for 15 min using a Beckman JA-20 rotor. Supernatants were removed and kept for future SDS PAGE analysis. Pellets were re-suspended in 8 ml of Native Binding Buffer (50mM NaH_2PO_4 , 500mM NaCl, pH 8.0) and ~8 mg of lysozyme was added to cell suspensions. Cell lysates were sonicated using Bioruptor Sonication System (Diagenode, Liège, Belgium). One cycle of 30s on, followed by 30s cool down for ten

cycles was performed for thorough lysis of cells. The lysate was centrifuged at 12,000 rpm (11,300 g_{av}) for 30 min to pellet cellular debris (including inclusion bodies; see text below); the supernatants were transferred to fresh tubes and stored at 4°C for future SDS PAGE analysis. Tubulin protein was in inclusion bodies at this point, as determined by SDS PAGE and western blotting profiles for tubulin proteins.

Cell pellets containing inclusion bodies were washed four times with four different inclusion body wash buffers containing denaturants and detergents to remove as many impurities as possible before adding to Ni-NTA column. Inclusion body wash buffer I contained: 50mM Tris, 50mM MgSO₄, 50mM NaCl, 0.1% Triton X-100, pH=8.8. Inclusion wash buffer II contained: 50mM Tris, 50mM NaCl, 1mM CaCl₂, 25% glycerol, pH=8.8. Inclusion wash buffer III contained: 50mM Tris, 500mM NaCl, 50mM MgSO₄, pH=8.8. Inclusion wash buffer IV contained: 50mM Tris, 50mM NaCl, 50mM MgCl₂, 2M urea, pH=8.8. Each pellet was re-suspended in 8 ml each wash buffer followed by centrifugation at 12,000 rpm (11,300 g_{av}) for 20 min at 4°C. Supernatants were removed and kept at 4°C for future SDS PAGE analysis. To remove tubulin proteins from inclusion bodies, pellets re-suspended in 8 ml of Inclusion Body Solubilization buffer (50mM Tris, 50mM NaCl, 1mM CaCl₂, 8M urea, 10mM beta-mercaptoethanol, pH=8.8) were incubated overnight at room temperature with constant rotation stirring. Next morning, incubation mixtures were spun and

supernatants were subjected for further purification using the Ni-NTA affinity systems.

Individual Ni-NTA column(s) were prepared under denaturing conditions. Resin Slurry (2.5 ml) was pipetted into each column and phase separated using low speed centrifugation (800xg), and the supernatants were aspirated and discarded. Sterile distilled water (6 ml) was added to the column and resin was re-suspended, followed by low speed centrifugation step, supernatant was aspirated and discarded. Denaturing Binding Buffer, 6 ml (8M urea, 20mM sodium phosphate, 500mM NaCl, pH 7.8) was added to each column and the resin was re-suspended and centrifuged as above for two cycles.

Cell lysate(s) were added to column(s), and the resin was re-suspended, allowing protein to bind to resin for 1 h with gentle agitation to keep resin from settling. Low speed centrifugation was used to separate resin from supernatant; supernatants were removed and stored at 4°C for future SDS PAGE analysis. Column(s) were washed twice with 4 ml of Denaturing Binding Buffer for 2 min before separating the resin from wash supernatants. Column(s) were washed twice with Denaturing Wash Buffer (8M urea, 20mM sodium phosphate, 500mM NaCl, pH 6.0) for 2 min and the process of separating the resin and supernatants was followed as described above. Proteins bound on the column(s) were then subjected to re-naturation under native conditions and the composition of the wash buffers used were selected to aid refolding of the protein(s) approaching

native globular configurations. Column(s) were washed four times with 8 ml of Native Wash Buffer (50mM NaH₂PO₄, 500mM NaCl, 20mM imidazole, pH 8.0) for 2 min before separating the resin from the supernatant(s). Supernatant(s) from all wash steps were kept at 4°C for SDS PAGE analysis. Settled resin was treated with Native Elution Buffer (46mM NaH₂PO₄, 458mM NaCl, 250mM imidazole, pH 8.0) to remove the His tagged tubulin protein from the resin-Ni moiety. Twelve, 1 ml fractions were collected from the column. 10µl of each fraction was run on a 10% SDS PAGE gel to monitor protein elution patterns. Fractions containing proteins were desalted using multiple Zeba Spin Desalting Columns (Thermo Fisher Scientific, Waltham, MA, USA) to remove high concentrations of salt within the elution buffer. The desalted samples from each fraction were concentrated individually using a vacufuge to near dryness. The concentrated material from each fraction was re-dissolved in 500 µl of General Tubulin Buffer (Cytoskeleton Inc. Denver, Co, USA). A small fraction of protein was kept for protein assay and SDS PAGE analysis. The remaining protein was frozen as individual droplets in liquid nitrogen to prevent repeated freeze thaw cycles, and appropriate amounts of frozen material were used as needed.

2.12 Tubulin Polymerization Assay

Reagents used for the assays were purchased from Cytoskeleton Inc. Experiments were carried out at a final concentration of 2.5mg/ml total recombinant protein as suggested by the manufacturer. However, since

proteins from affinity purification steps were merely enriched for tubulin proteins and were not purified to homogeneity, the fractions used included contaminating proteins of unknown identities. Therefore the final concentrations of tubulin protein(s) used for assays is only an estimate and will likely represent <2.5 mg/ml, deviating from the recommended amounts of purified proteins for polymerization assays. Paclitaxel and colchicine were prepared to 11 times final concentration in General Tubulin Buffer (80mM PIPES, MgCl₂, 0.5 mM EGTA, pH 6.9). Tubulin Polymerization Buffer (80 mM PIPES, 2 mM MgCl₂, 0.5 mM EGTA, pH 6.9, 1 mM GTP 10.2% glycerol) or drug were preheated in separate wells of half area 96 well plates for 2 min. Immediately before running an assay, both α and β tubulin were thawed in a 37°C water bath for one min and put on ice separately. Appropriate volumes of α and β tubulin were added to each well at a concentration of 1.25 mg/ml estimated protein to a combined final concentration at 2.5mg/ml in 110 μ l total volume. Assays were run for 45 min at 37°C, with absorbance measurements taken every 30 s at 340 nm using a SPECTROmax 190 (Molecular Devices, LLC. Sunnyvale, CA, USA) plate reader and collected using SOFTmax Pro version 4.0 software.

2.13 Small RNAome Profiling of Resistant Sub-Lines Using Next Generation Sequencing (NGS) Platform

Small RNAome (includes miRNA, tRNA, small ribonuclear RNAs) were profiled using NGS (Illumina GAIIx technology platform) utilizing the

services of PlantBiosis Ltd., at Lethbridge, Alberta, Canada. Total RNA from cell pellets was isolated using Ambion kits as suggested by the manufacturer (Life Technologies Corporation, Carlsbad, CA, USA). Size fractionation of RNA, isolating 200bp RNA for TruSeq small library construction, was as per the established protocols at the facility. All samples were sequenced in duplicates and initial bioinformatics support including normalization of the sequencing reads were obtained from the same facility. The data and the analyses presented are considered preliminary since complete analysis of discovery and annotation of potential novel or new miRNAs and other RNAs was beyond the scope of the current study. Since small RNAs are global regulators of gene expression, my goal was to attempt to identify profiles of global small RNA expression patterns that could discriminate sensitive vs. drug resistant cell lines. The bulk of the experimental work on drug resistance mechanisms was focused on select candidate genes or pathways, and importantly on tubulin isotype expression patterns. There are studies describing mRNA and miRNA expression profiles from cell lines from various drug sensitive and resistant cell lines. However, profiling resistant sub-lines and showing extremes of phenotypes for small RNAome were not reported in literature. In the current study, I have focused only on miRNA (and not other small RNAs) since the question being addressed pertained to specific regulation of β -III tubulin mRNA by miRNA and shed light on the possible mechanisms of β -III regulation by cells. It was well documented that miR-

200c specifically targets β -III tubulin (177-181) and it was my immediate interest to confirm these findings and as well to extend them to identify additional miRNAs associated with the extremes of the phenotypes of drug sensitivity or resistance.

2.14 Statistical Analysis

Graphpad Prism 6 (GraphPad Software, Inc. La Jolla, CA, USA) was used to create figures and perform statistical analysis of results. Standard Student's T-test was used to compare the cytotoxicity results for each of the analogs relative to paclitaxel induced cytotoxic profiles; as also for all cytotoxic assay results with and without other variables (e.g., verapamil). One way ANOVA was used to show the statistical significance between low, intermediate and high drug resistance in SKBR-3 sub-lines treated with paclitaxel and analogs.

3. Characterization of Paclitaxel Analogs and the Influences of β III Tubulin Expression on Resistance

3.1 Determining Cytotoxicity of Paclitaxel Analogs Against a Panel of Breast Cancer Cell Lines

I wished to test my hypothesis regarding the two amino acid residues predicted to be involved in the intermediate binding site for paclitaxel and its synthetic analogs. To do this, *in vitro* cytotoxicity assays were carried out using a selection of breast cancer cell lines that have been previously reported to have varying degrees of resistance towards paclitaxel (18). The three breast cancer cell lines were SKBR-3, MDA-MB-231, and T-47D, each with a different hormone or growth factor receptor status. According to the American Type Culture Collection (ATCC) SKBR-3 cell line represent human epidermal growth factor 2 (Her2) expressor phenotype; MDA-MB-231 cell line does not express or have weak expression of receptors and these are in general represented as negative for progesterone (PR), estrogen (ER) and Her2 receptors and are classified as TN; and T-47D cell line represent ER positive or Luminal A breast cancer phenotype. Each cell line was treated with either paclitaxel or one of the analogs at various concentrations for 72 h. MTS reagent was used to determine relative cell viability at each drug concentration compared to the untreated control (Figure 3-1). The data from drug titration curves for IC₅₀ determinations are summarized in Table 3-1.

Drug titrations with SKBR-3: Dose response curves (Figure 3-1A) clearly showed a rank order for various compounds tested. The rank order

for potency of drugs from the cell viability experiments was paclitaxel < Tx-A and Tx-C < Tx-D and Tx-F.

Drug titrations with MDA-MB-231: This cell line was the most resistant of the three cell lines tested (double the IC₅₀ value for paclitaxel compared to other two cell lines). Dose response curves (Figure 3-1B) showed a clear rank order close to what I observed for SKBR-3 (Figure 3-1A). Only Tx-D and Tx-F showed statistically significant differences in IC₅₀ values, compared to paclitaxel.

Drug titrations with T-47D (Figure 3-1C): This cell line showed comparable IC₅₀ values for paclitaxel compared to the SKBR-3 cell line; also the IC₅₀ values were not statistically different for Tx-A compared to paclitaxel. The other three compounds (Tx-C, Tx-D and Tx-F) showed statistically significant differences in IC₅₀ values compared to paclitaxel. Dose response curves showed the rank order of potency as paclitaxel and Tx-A < Tx-C < Tx-D and Tx-F.

Summary of IC₅₀ values from titration experiments (Figure 3-1) are shown in Table 3-1. All drugs showed statistically significant differences to the parent compound and could be considered as potent since the IC₅₀ values were still in the nM range (4-76 nM range, except for Tx-D treatment in MDA-MB-231 cells).

These trends provide insight into the relationship between modeled compounds and the observed experimental profiles (cytotoxicity). Tx-A

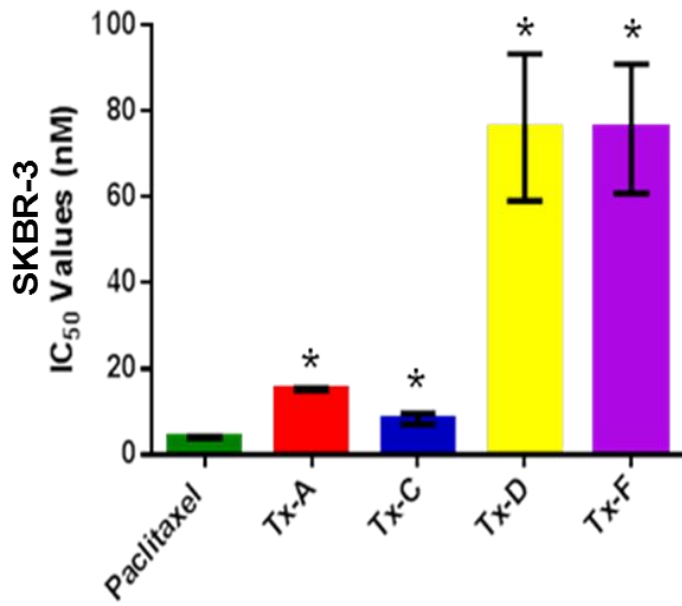
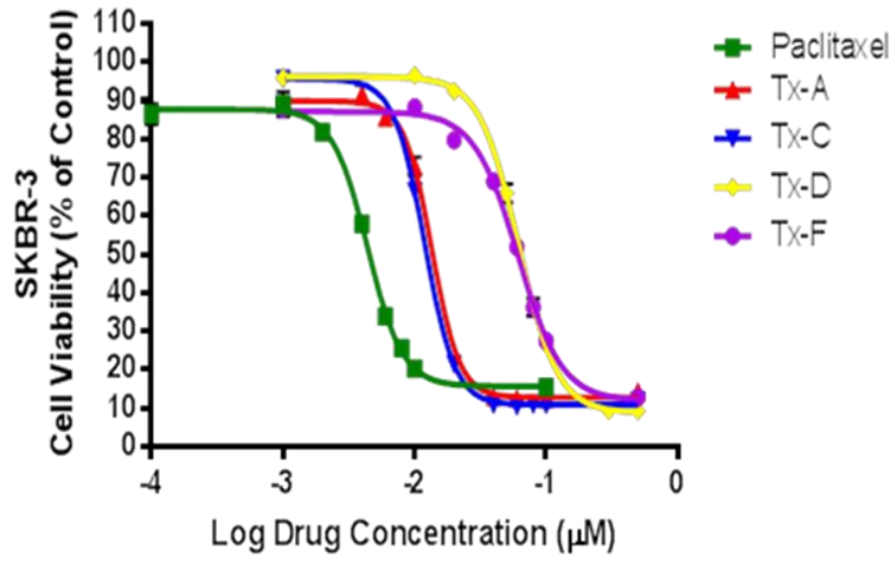
was hypothesized to be the least effective analog given the predicted loss of interaction with residue 275 in the *in silico* design, however it displayed cytotoxicity comparable with that of paclitaxel. Tx-C was predicted to have an IC₅₀ moderately higher than paclitaxel due to the decrease in affinity for Ser 275 by 2 kcal/mol compared to paclitaxel. There was a trend observed for Tx-C effects in T-47D cells, in which this compound showed increasingly higher IC₅₀ values compared to paclitaxel (Table 3-1). Variability of cytotoxicity of Tx-C towards the three cell lines does not allow any conclusions to be made as to the predicted behavior of the drug.

When comparing paclitaxel to the compounds manipulated at the C-10 position, Tx-F and Tx-D, the data showed that there was a large and statistically significant difference. In all three cell lines, there was at least an 8.5-fold difference in IC₅₀ values between paclitaxel and each of these two drugs. The IC₅₀ values obtained for Tx-D and Tx-F in SKBR-3 and T-47D cell lines showed no statistically significant differences. There was a statistically significant ~ 2-fold difference between Tx-D and Tx-F in MDA-MB-231 cell line (Figure 3-1B). This is the only indication thus far that the side chain length of the C-10 moiety in Tx-D and Tx-F may contribute to differences in cytotoxicity. These results refute the original hypothesis, that Tx-D and Tx-F would have greater toxicity than paclitaxel. Given that Tx-D and Tx-F were still relatively effective compared to paclitaxel (from the range of IC₅₀ values observed), it is likely the drug was still entering the nano-pore, accessing the intermediate binding site and eventually making

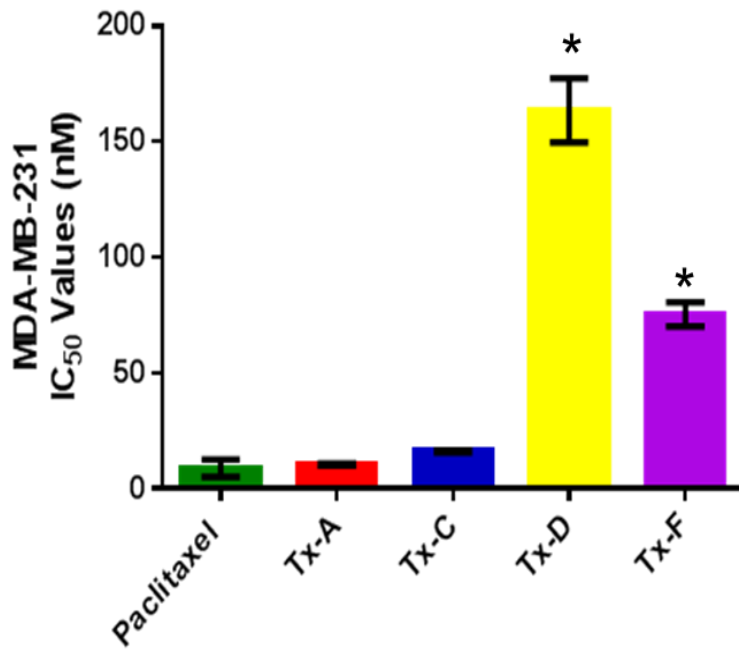
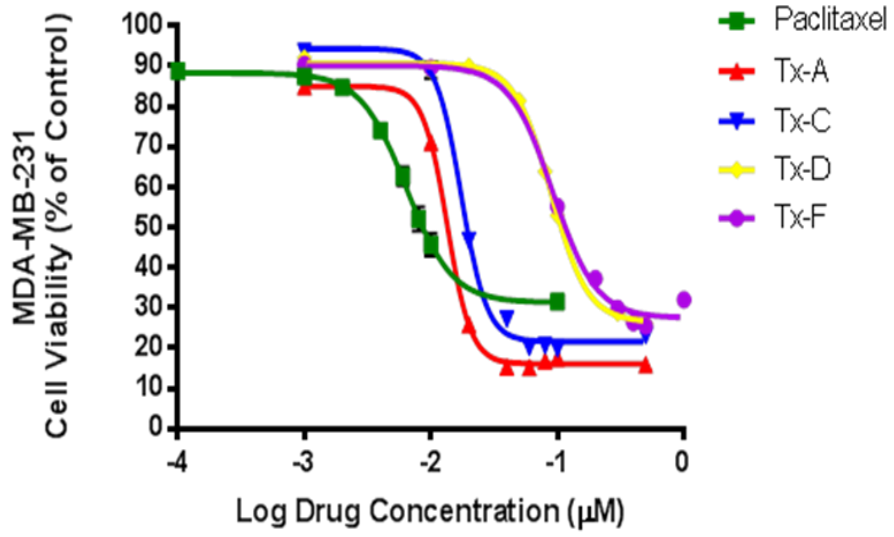
its way to the active site pocket to exert anti-mitotic activity. These results therefore warrant reconsideration of the design of the molecule or recalculation of pore size and the thermodynamic considerations within. It is important to note that modeled compounds based on *in silico* design are in fact amenable for synthesis in sufficient yields to test for activity and the possibility of creating designer drugs in the near future.

Based on the data obtained, it is safe to conclude that the receptor status of the cell lines used did not influence the cytotoxic activity of any of the compounds tested since all cell lines showed cell kill activity as a function of drug concentration and by way of comparable IC₅₀ values.

A)



B)



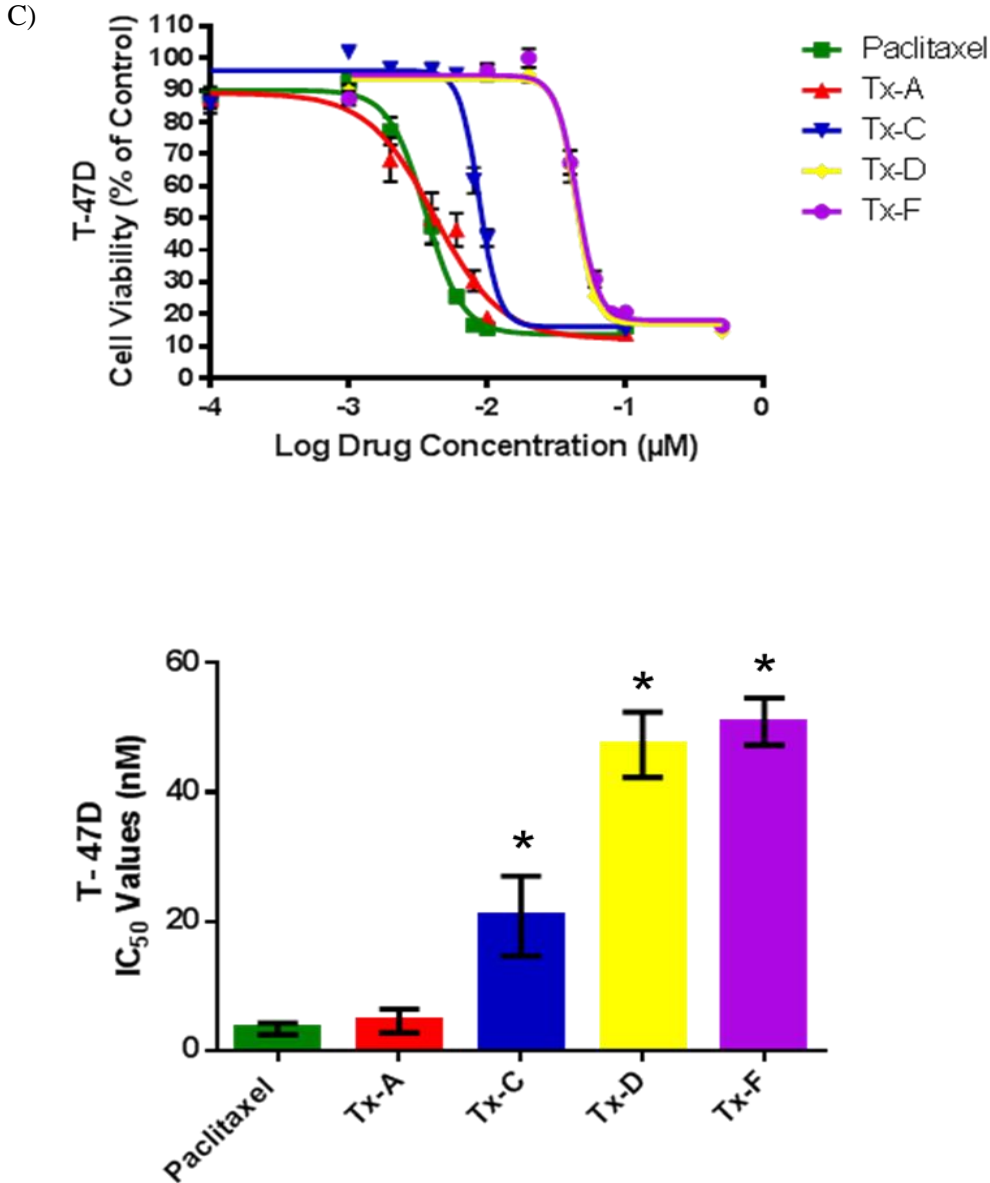


Figure 3-1. IC₅₀ Values for Paclitaxel and Analogs in Assays using Breast Cancer Cell Lines

Cell lines were treated with a range of drug concentrations as indicated (Top figure in each of the panels A-C) to assess the cytotoxic activity of parent, paclitaxel and analogs. Cell lines were exposed to drugs for 72h period. 30 µl of MTS reagent was administered to each well, and absorbance measurements were taken at 490nm. Cell lines studied were: (A) SKBR-3 (Her2+), (B) MDA-MB-231 (Triple Negative) and (C) T-47D (Luminal A). All values (average of replicates) were expressed relative to cell viability values in untreated cells (normalized to 100%). Cytotoxicity curves represent n=3 experiments with 6 replicates per drug concentration for each experiment; Standard deviation, SD, is shown for each drug concentration (Top figure) and for each IC₅₀ determined (bottom figure). Bar graphs (bottom figure in each of the panels A-C) represent IC₅₀ value of n=3 independent experiments. *, P<0.05 determined for IC₅₀ for each analog relative to paclitaxel.

Table 3-1. Summary of Drug Titrations Showing 50% Inhibitory Concentration, IC₅₀, in Breast Cancer Cell Lines Treated with Paclitaxel and Analogs (source Figure 3-1)

	Paclitaxel	Tx-A	Tx-C	Tx-D	Tx-F
SKBR-3	5 _{±1}	16 _{±1} *	9 _{±2} *	77 _{±18} *	76 _{±16} *
MDA-MB-231	9 _{±4}	11 _{±1}	17 _{±1}	164 _{±14} *	756 _{±6} *
T-47D	4 _{±1}	5 _{±2}	42 _{±20} *	48 _{±6} *	51 _{±4} *

The IC₅₀ values (represented in nM) were calculated using the GraphPad Prism 5 program. Values and errors (SE) shown are representative of n=3 independent experiments. *, P<0.05 determined for IC₅₀ for each analog relative to paclitaxel

3.2 Expression of β Tubulin Isoforms and Association with Observed Sensitivity of Cell Lines to Paclitaxel and Analogs

To investigate the role of β tubulin expression within breast cancer cell lines and relate to the observed profiles of cytotoxicity, western blot analysis was performed. It is hypothesized that the differences in β tubulin isotype expression can be correlated with the observed cytotoxicity of paclitaxel and the novel analogs and observed differences, if any, could be correlated to apparent differences in IC₅₀ for the compounds tested. MDA-MB-231, SKBR-3, and T-47D cells were grown in two distinct experimental groups, either in drug free media or in drug free media for all but 24 hours of the growth period. The second group was treated with previously determined $\frac{1}{2}$ IC₅₀ (Table 3-1) concentration of paclitaxel for the remaining 24 h before trypsinizing and pelleting of cells. These two groups were designed to determine the tubulin expression under normal growth

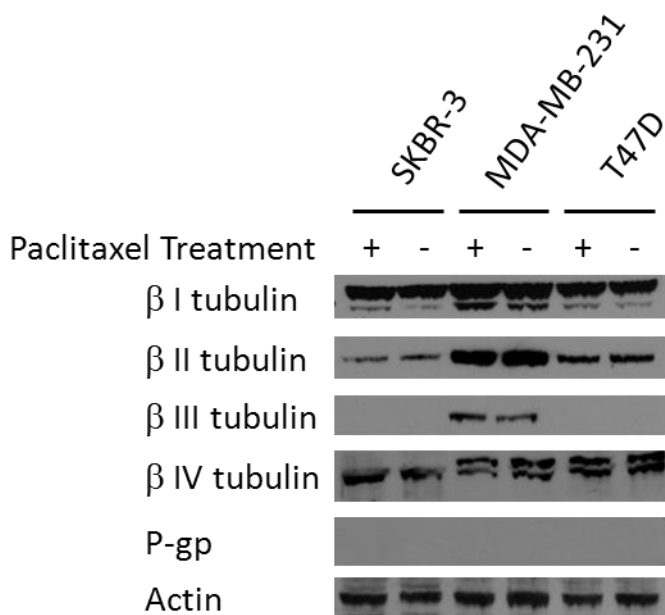


Figure 3-2. Western Blot Analysis of Expression of β Tubulin Isotypes and P-gp Expression in Breast Cancer Cell Lines

Breast cancer cell lines were used to determine expression patterns for β tubulin I – IV isotypes and *MDR-1* efflux pump, P-gp. Experiments were carried out under normal media conditions (-) and acute 24h $\frac{1}{2}$ IC_{50} paclitaxel exposure (+). Data presented is representative of n=3 independent experiments. Actin expression on the blot is used as a loading control.

conditions and also under acute drug exposure. Total cell extracts were collected and western blot analysis was carried out to determine the levels of β tubulin I – IV as well as P-gp as an additional mechanism of drug resistance possibly influencing cytotoxicity. The data showed that there was variability in the β tubulin isotypes, most notable being β -II and β -III across cell lines. β II tubulin was expressed at lower levels within SKBR-3 and T-47D cells, with a greater expression found in the MDA-MB-231 cells. Additionally, MDA-MB-231 was the only cell line of the three to show any expression of β III tubulin (Figure 3-2). This expression may explain

why MDA-MB-231 cells had the highest IC₅₀ value for paclitaxel (Table 3-1) as compared to the other two cell lines.

However this line of interpretation does not hold for the other drugs in question. Based on the predicted interaction of the analogs with Ala 275, found within β III tubulin, the presence of this within MDA-MB-231 results in the opposite effect to both Tx-A and Tx-C. These analogs were predicted to be less cytotoxic under high β III expression but seemed to be functioning better in these conditions. β IV tubulin also appeared to be differentially regulated in MDA-MB-231 and T-47D cells compared to SKBR-3 (Figure 3-2). The presence of an additional band was seen in the western blots of the two former cell lines. A slightly higher molecular weight band is mentioned to occur according to the manufacturer but the identity is unknown.

The data also showed that acute drug exposure had little to no effect on changes in isotype expression. The observed expression was constitutive and the cells do not adjust levels of β tubulin protein to a state of differential expression to influence greater survival under these experimental conditions.

Western blot analysis was used to determine the protein levels within each cell line for the multidrug resistance efflux pump p-glycoprotein (P-gp). The data showed that none of the cells are expressing any levels of P-gp at both normal cellular conditions as well as after acute exposure

to paclitaxel. P-gp expression is not a mechanism of resistance in these cellular models and cannot be attributed to the resistance observed in these cell lines treated with the analogs (Figure 3-2).

3.3 Substrate Specificity of Paclitaxel Analogs to Drug Efflux Pump P-glycoprotein

Two pairs of cell lines were selected to determine if changes made to side chains of novel analogs had changed substrate specificity to the drug efflux pump (P-gp) as well as to provide any additional insight into the behavior of the drugs related to the initial hypothesis. The cell lines used were ovarian MESSA (WT), and derivative of MESSA, DX5 as the drug resistant cell line; CML K562 (WT), and derivative of K562, R7 as the drug resistant suspension cell line. It has been previously reported that DX5 and R7 cell lines which are derived from MESSA and K562 cells respectively, are expected to over-express P-gp protein, and exhibit cross resistance to a variety of chemo therapeutic compounds (182,183). I verified that both DX5 and R7 cell lines express P-gp using western blot analysis (Figure 3-4). Both these cell lines express P-gp whereas MESSA and K562 show no expression. DX5 showed a slight increase in expression, while R7 greatly over-express P-gp.

Cytotoxicity experiments carried out on these cell lines indicate that the paclitaxel and its analogs are substrates for multidrug resistance efflux pumps. The data showed that in all but one of the experiments there is a large fold increase in the IC₅₀ values between pairs of cell lines (Table 3-

2). The only case in which the data showed there is no statistically significant difference on the effect of IC_{50} values due to the presence of P-gp is the case of MESSA/DX5 pair of cell lines treated with paclitaxel (Figure 3-5A). Western blot data showed that DX5 cells have only a modest increase in P-gp and there may not be a large enough increase to affect the cytotoxicity of paclitaxel. However, the analogs showed an increase in IC_{50} and may indicate changes to structures of paclitaxel analogs contributed to greater substrate specificity for drug efflux pumps. The large increase in P-gp found in R7 cell contributes to large increases in IC_{50} treated with all compounds, up to 100-fold difference, compared to K562. The fold difference in IC_{50} values is greatest in cells treated with paclitaxel. This is contradictory to the findings of MESSA/DX5 as it showed the analogs are less specific to P-gp as compared to paclitaxel. Overall, the data supported the conclusion that these analogs are substrates for multidrug resistance (Table 3-2).

3.4 Additional Experimental Evidence in Support of the Cytotoxic Potential of Paclitaxel Analogs

Additional cytotoxicity experiments were carried out using MESSA and DX5 ovarian and K562 and R7 CML cell lines with the intent of further classifying the novel analogs compared to paclitaxel in cell lines systems other than breast cancer. Similar to the results seen in breast cancer cell lines, Tx-A had cytotoxic activity comparable to paclitaxel. In only one cell line, DX5 treated with both drugs, did Tx-A have a statistically significantly higher IC_{50} value (Figure 3-3B). The differences in IC_{50} values in MESSA

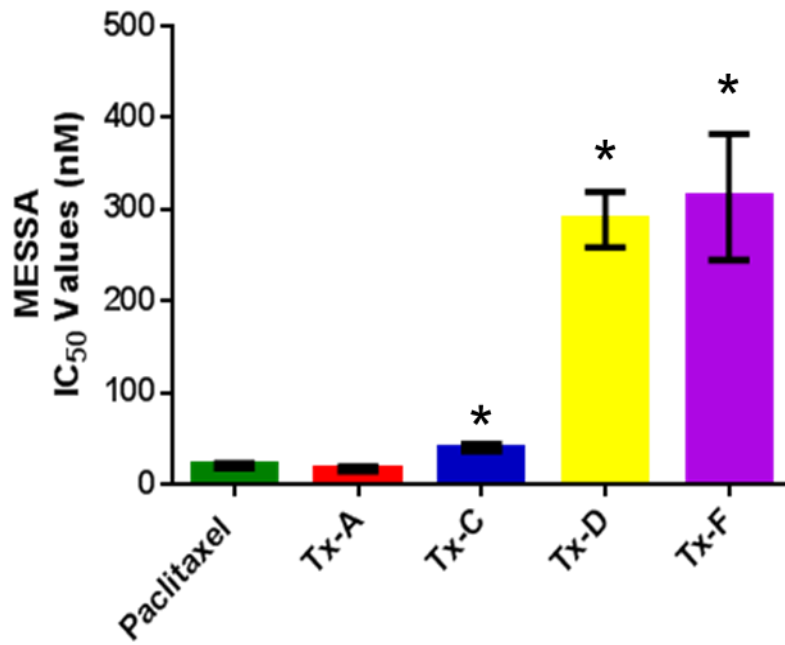
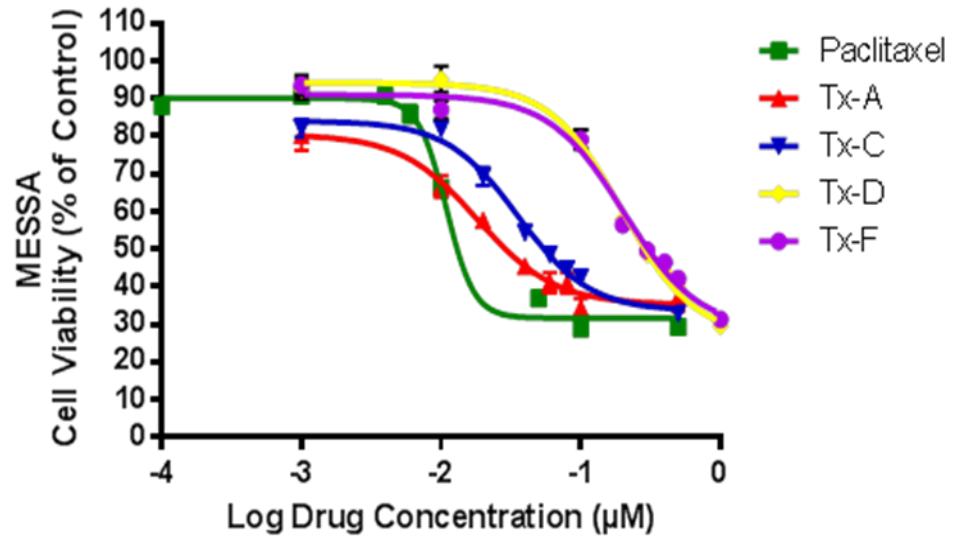
and K562 cell lines were not significantly different, resulting in a cell kill of each drug to be equal. R7 cells on the other hand represent the only cell line of all 7 tested, from among the breast, ovarian and CML lines, which have an IC_{50} value from Tx-A treatment that is statically lower than that of paclitaxel. Paclitaxel had an IC_{50} value 1.6 times greater than that of Tx-A in this particular cell line (Figure 3-3D). The trend observed in the breast cancer cell lines was maintained in these four additional cell lines, Tx-A overall is equally as cytotoxic compared to paclitaxel. The data also showed that in all four of the cell lines treated with Tx-C, Tx-D and Tx-F, the IC_{50} values are all statistically greater than that of paclitaxel. The differences in IC_{50} of these cell lines are similar to that of the breast cancer cell lines. The difference in IC_{50} in Tx-C was at times modest, with only a 2-fold difference as seen in MESSA cells but was as high as 40-fold as in DX5 cells. The difference in IC_{50} values attributed to Tx-D and Tx-F in each of these cell lines compared to paclitaxel is much greater. The differences in IC_{50} for treatment with Tx-D and Tx-F range from 12 and 10-fold in R7 cells, but up to 126 and 118-fold in K562 cells, respectively, consistent with the results obtained from the breast cancer cell lines (Table 3-2). Additionally, this data provided further validation that Tx-C is behaving as predicted, with modest decrease in cytotoxic activity compared to paclitaxel. In each of these four cell lines, treatment with Tx-C results in IC_{50} values that were higher than that of paclitaxel, but exhibit cytotoxicity that is still at nM concentrations.

Table 3-2. Determination of IC₅₀ Values for P-gp ± Expressing Cell Lines Treated with Paclitaxel and Analogs and ± Verapamil

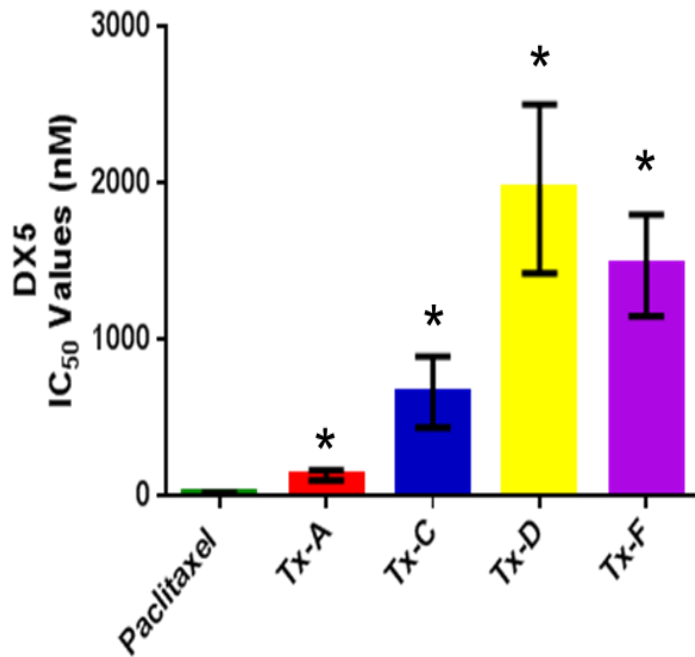
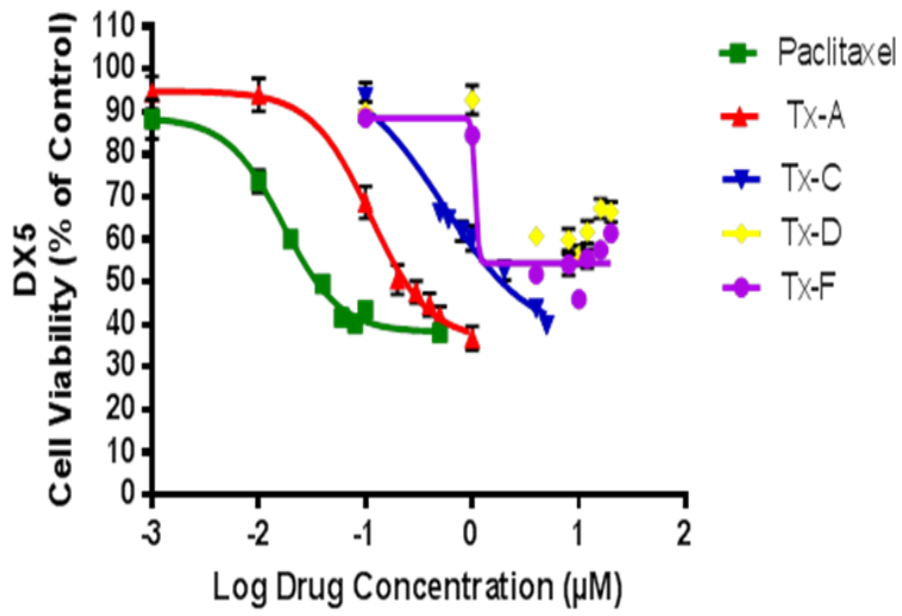
	Paclitaxel	Tx-A	Tx-C	Tx-D	Tx-F
MESSA	21 _{±3}	18 _{±3}	41 _{±4} *	289 _{±31} *	314 _{±69} *
MESSA + VRP	13 _{±1.0}	20 _{±5}	39 _{±4} *	183 _{±13} *	138 _{±11} *
DX5 (MDR-1 +)	18 _{±4}	134 _{±33} *	666 _{±229} *	1963 _{±541} *	1475 _{±324} *
DX5 + VRP	11 _{±5}	15 _{±2}	38 _{±3} *	288 _{±24} *	253 _{±58} *
K562	6 _{±2}	9 _{±2}	57 _{±2} *	669 _{±69} *	593 _{±24} *
K562 + VRP	5 _{±2}	6 _{±1}	10 _{±1} *	23 _{±1} *	24 _{±2} *
R7 (MDR-1 +)	440 _{±26}	266 _{±27} ‡	1482 _{±33} *	5474 _{±81} *	4586 _{±75} *
R7 + VRP	41 _{±7}	22 _{±2}	83 _{±7} *	552 _{±5} *	467 _{±72} *

The IC₅₀ values (represented in nM) were calculated using the GraphPad Prism 5 program. Values and errors (SE) representative of the average IC₅₀ values of n=3 independent experiments. *, P<0.05 determined for IC₅₀ for each analog relative to paclitaxel. ‡, P<0.05 greater cytotoxicity than paclitaxel.

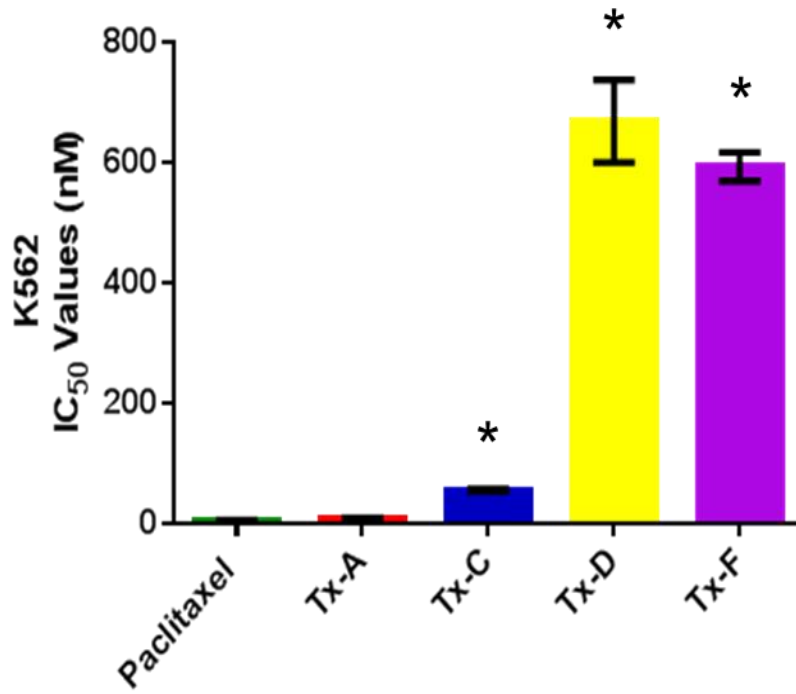
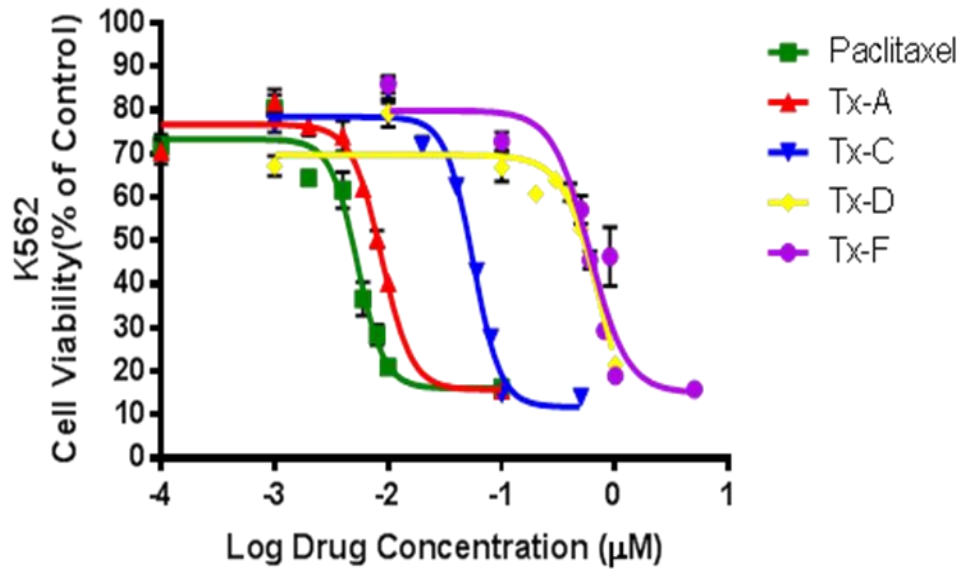
A)



B)



c)



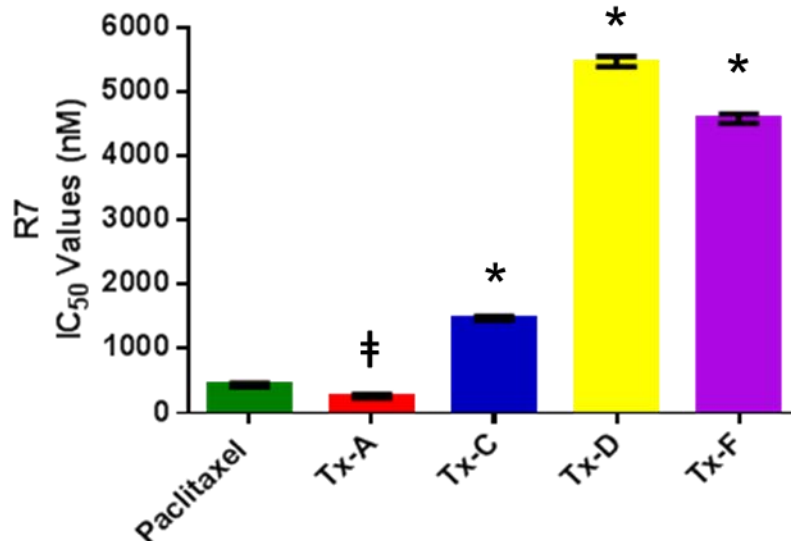
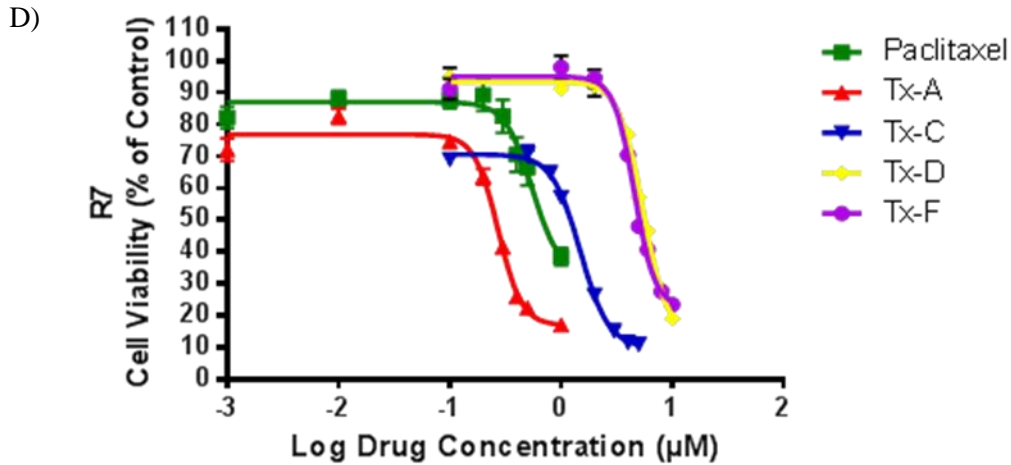


Figure 3-3. Cell Viability Assays of P-gp \pm Expressing Cell Lines Treated with Paclitaxel and Analogs

Cell lines were treated with a range of drug concentrations to assess the cytotoxic activity of the compounds. Cell line pairs, A,B (ovarian cancer cell lines) and C,D (CML cell lines) were tested: (A) MESSA, WT; (B) DX5, P-gp expressing and (C) K562, WT (D) R7, P-gp expressing cells were used to test the affinity of the novel compounds to P-gp- efflux pump. Cell lines were exposed to drugs for 72h period, and at the end, 30 μ l of MTS reagent was administered to each well, and absorbance read at 490nm. All values were compared to the cell viability in untreated cells (normalized to 100%). Cytotoxicity curves represent n=3 independent experiments with 6 replicates per drug concentration for each experiment. Bar graphs represent IC₅₀ value of n=3 independent experiments *, P<0.05 vs. paclitaxel, ‡, P<0.05 greater cytotoxicity than paclitaxel.

3.5 The Contributions of β Tubulin Isozyme Expression for the Observed Resistance within MESSA/DX5 Ovarian and K562/R7 CML Cell Lines

Western blot experiments were carried out using the four non breast cancer cell lines, two pairs with and without P-gp expression. The western blot analyses were carried out to determine levels of tubulin isozymes within the cells and any influence they may have to enable interpretations of cytotoxic activity profiles. Five isozymes of β tubulin (I –IV) were tested for their expression within each of the cell lines.

Constitutive expression (with and without paclitaxel in the growth medium prior to preparation of cell lysates) of β I was similarly expressed in all four cell lines. The levels of β II expression were similar among MESSA, K562 and R7 cells, with a near complete absence of expression seen in DX5 cells. Constitutive β III tubulin was only seen in MESSA cells and expressed at a very high level. β IV was expressed at similar levels between MESSA and DX5 cells. There was a drop in β IV expression from K562 to R7, and both these cell lines also expressed a secondary protein that bound the β IV primary antibody (Figure 3-4), likely the same protein that caused the secondary band observed in both MDA-MB-231 and T-47D breast cancer cells.

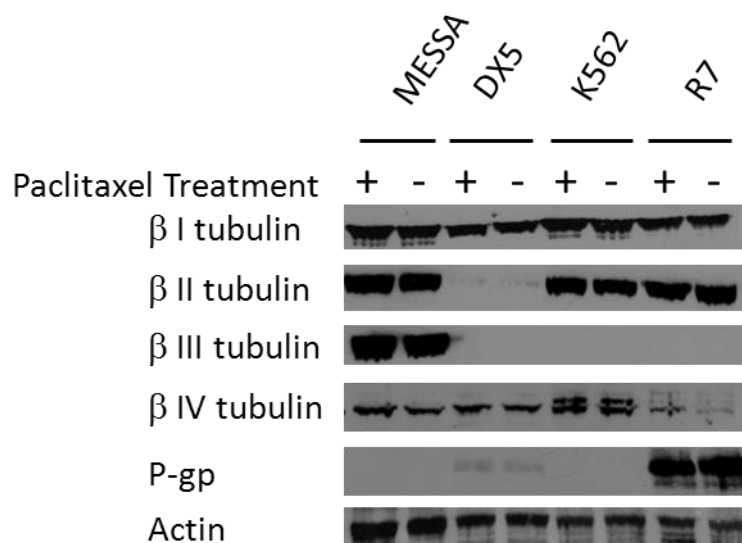


Figure 3-4. Western Blot Analysis of β Tubulin Isoforms and P-gp Expression in P-gp \pm Expressing Cell Lines

Two pairs of cell lines were used to determine β tubulin I – IV isotype expression and *MDR-1* efflux pump, P-gp, expression. Parental cell lines, MESSA (ovarian cancer) and K562 (CML), are P-gp negative, whereas daughter cell lines DX5 and R7 express P-gp and have been characterized in the literature as multidrug resistant lines. Experiments were carried out under normal media conditions (-) and 24h $\frac{1}{2}$ IC_{50} paclitaxel exposure (+). Image is representative of the results from n=3 independent experiments. Actin protein was used as a loading control.

3.6 Combination Treatments Containing Verapamil and Paclitaxel Analogs Contribute to Enhanced Cell Kill

Previous results have shown that the paclitaxel analogs are indeed substrates for P-gp (Table 3.2). It was my intent now to determine if drug resistance to paclitaxel analogs in two cell lines expressing P-gp, DX5 and R7, can be reversed using the known P-gp inhibitor, verapamil. It is my goal to have the IC_{50} s of these two cell lines reach values similar to those seen in MESSA and K562 treated with the same drug. Verapamil was used at a concentration of 5 μ g/ml in combination with variable

concentrations of either paclitaxel or analogs to determine the IC_{50} s under these new conditions (167). The results are then compared to the previously carried out experiments in which no verapamil was present.

The data showed paclitaxel and analogs were more cytotoxic in the presence of verapamil when administered to DX5 and R7 cells. In all but a single experiment group, verapamil inhibits P-gp activity, lowering the IC_{50} of the cell lines expressing the protein to near wild type levels (Table 3-2). Verapamil used in combination with paclitaxel was the lone experiment in which IC_{50} values of the DX5 cells were not statistically altered as compared to the verapamil free conditions. MESSA and DX5 cells with and without verapamil treatments have statistically equal resistances to paclitaxel (Figure 3-5A). Given that DX5 expressed P-gp as a mechanism of paclitaxel resistance, MESSA cells have an intrinsic resistance mechanism which is reflected in the near comparable IC_{50} values for paclitaxel in cells with and without the expression of P-gp. In these cells, resistance is conferred through high expression levels of β III tubulin. Paclitaxel analogs and verapamil administered to these same two cell lines resulted in a decrease of IC_{50} values of the DX5 cells to levels that are similar to that of MESSA cells. MESSA cells treated with paclitaxel (Figure 3-5A), Tx-D (Figure 3-5D), and Tx-F (Figure 3-5E) as well as verapamil contribute to a statically significant drop in IC_{50} values, as compared to the same cells treated without verapamil. Since MESSA cells did not express P-gp there were likely off-target interactions occurring that

contributed to the slight increase in cytotoxicity of these three compounds in combination with verapamil.

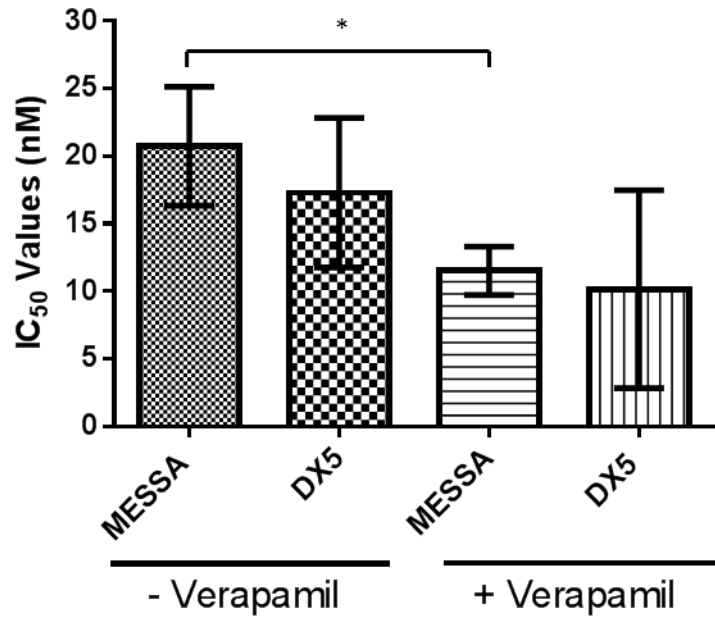
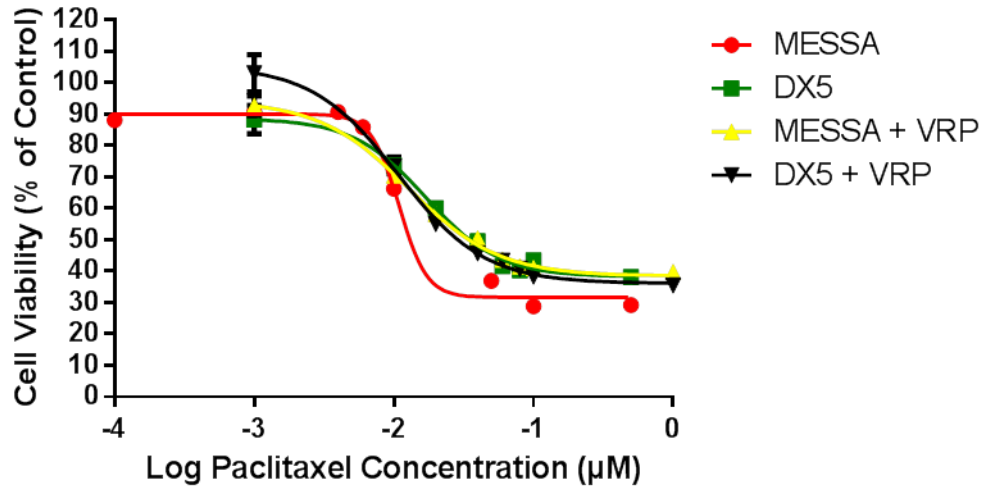
K562 (*MDR-1* negative for expression) and R7 (*MDR-1* positive for expression) cells were treated with paclitaxel or analogs in combination with 5 μ g/ml verapamil to assess the influence of verapamil on the cell lines. Due to the overwhelming expression of P-gp within the R7 cells, combination with verapamil did not result in a complete inhibition of activity. Paclitaxel with verapamil resulted in ~10-fold decrease of IC₅₀ values of R7 cells (41 \pm 7 nM), but was still ~ 8-fold greater than that of parent K562 cells with an IC₅₀ value of 6 \pm 2 nM (Table 3-2). This was also seen in R7 cells treated with Tx-A and verapamil. There was ~12-fold decrease in IC₅₀ from 266 \pm 27 nM to 22 \pm 2 nM, but were still ~2.4-fold greater than the K562 cells treated with the drug (Table 3-2). In combination treatments with verapamil and each of the taxane drugs there was only a slight decrease in IC₅₀ values of K562 cells treated with or without verapamil.

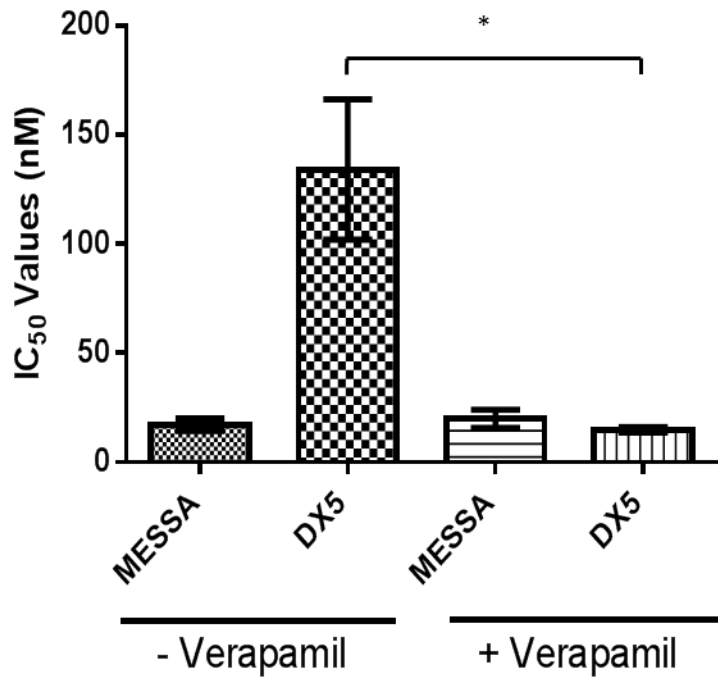
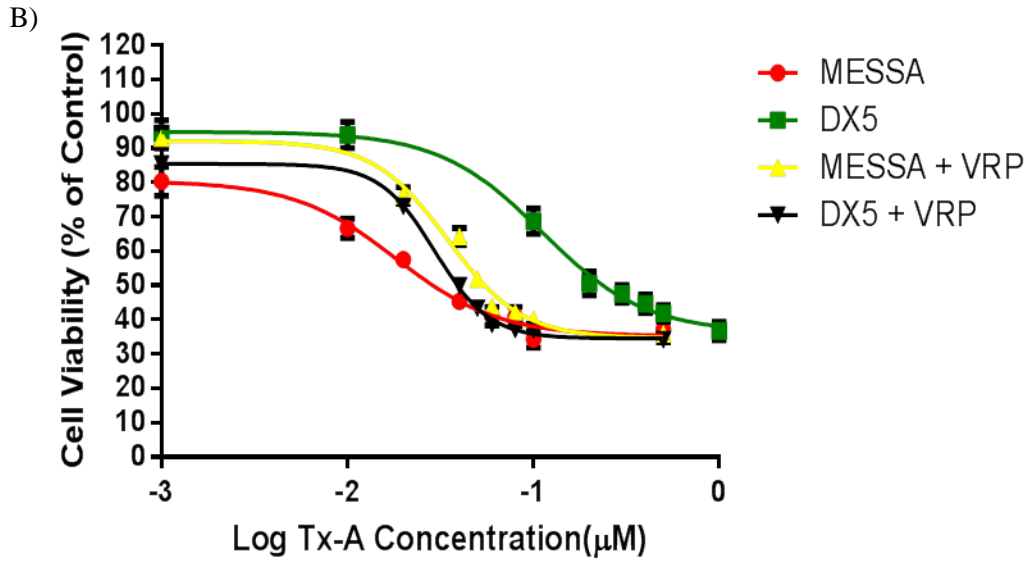
Moreover, combination treatments involving Tx-C, Tx-D or Tx-F with verapamil resulted in a great decreases in IC₅₀ of not only R7 cells but to a greater extent K562 cells. As expected, there was a shift to a lower IC₅₀ in R7 cells over-expressing P-gp, which is to a level similar to that of K562. This indicates that the presence of verapamil is almost completely inhibiting the mechanisms used by the cells to resist Tx-C, Tx-D or Tx-F treatments. However, in addition to these results, there was also a

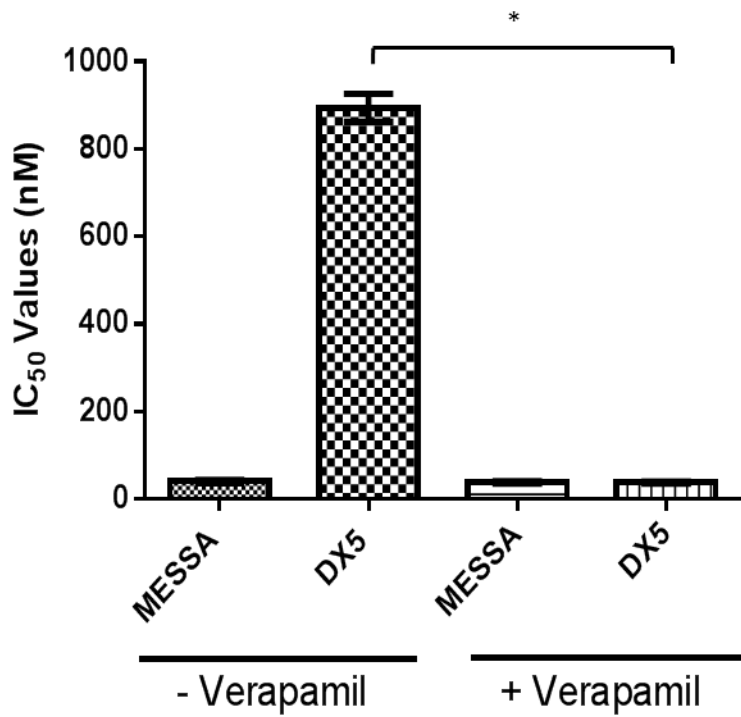
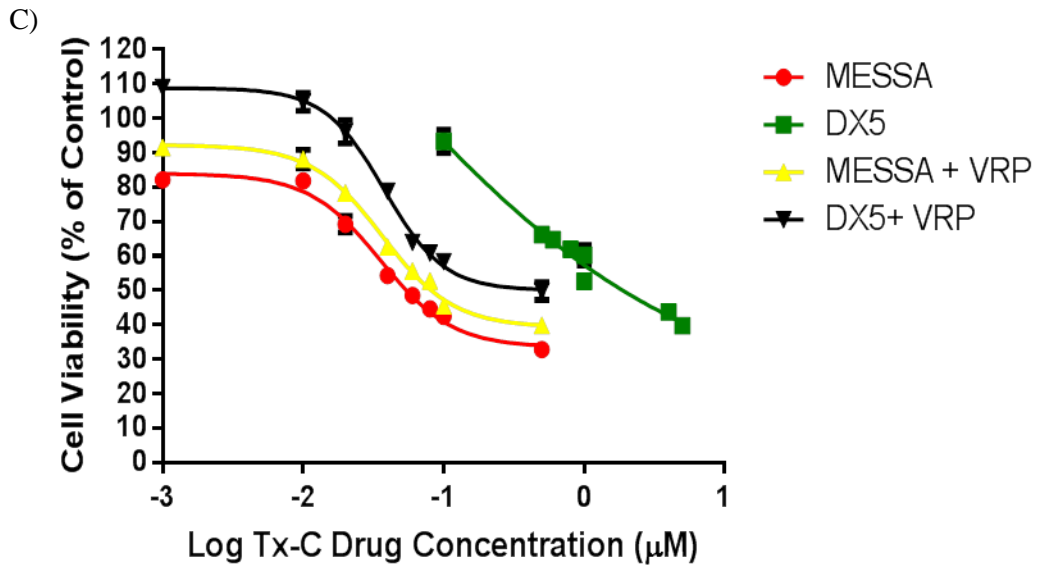
significant decrease in IC_{50} of K562 cells treated with each of these three drugs. Specifically, the decrease in IC_{50} of K562 with and without verapamil treatment was greater than the decrease in IC_{50} of R7 cells treated with Tx-D (Figure 3-7D) and Tx-F (Figure 3-7E). The reduced IC_{50} of K562 cells treated with Tx-C is significantly large but not as great as the difference observed in R7 cells (Figure 3-7C). This suggested that verapamil was interacting with off-targets, which influences the resistance mechanisms of these two cell lines. The off-target interactions may be likely occurring with substrates that influence Tx-C, Tx-D and Tx-F cytotoxicity, and specifically in the cases of Tx-D and Tx-F, mechanisms that influenced their cytotoxicity greater than that of P-gp.

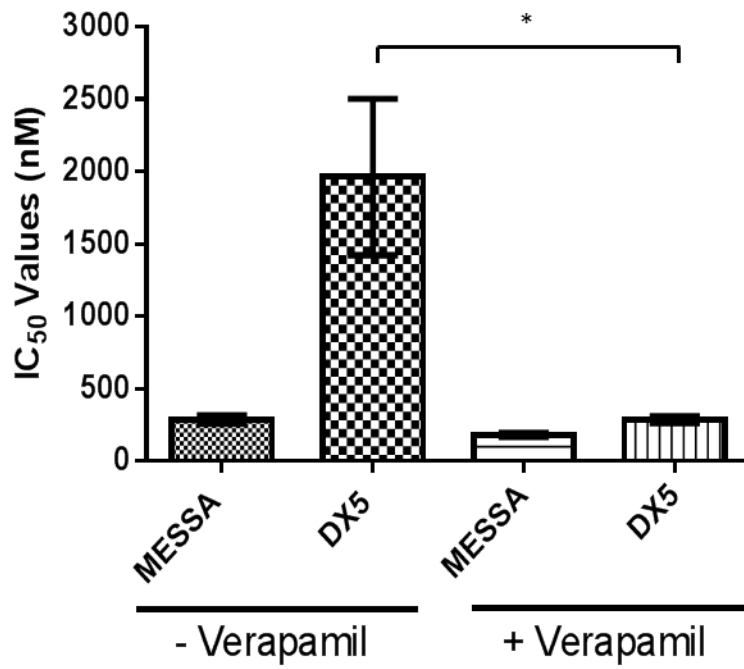
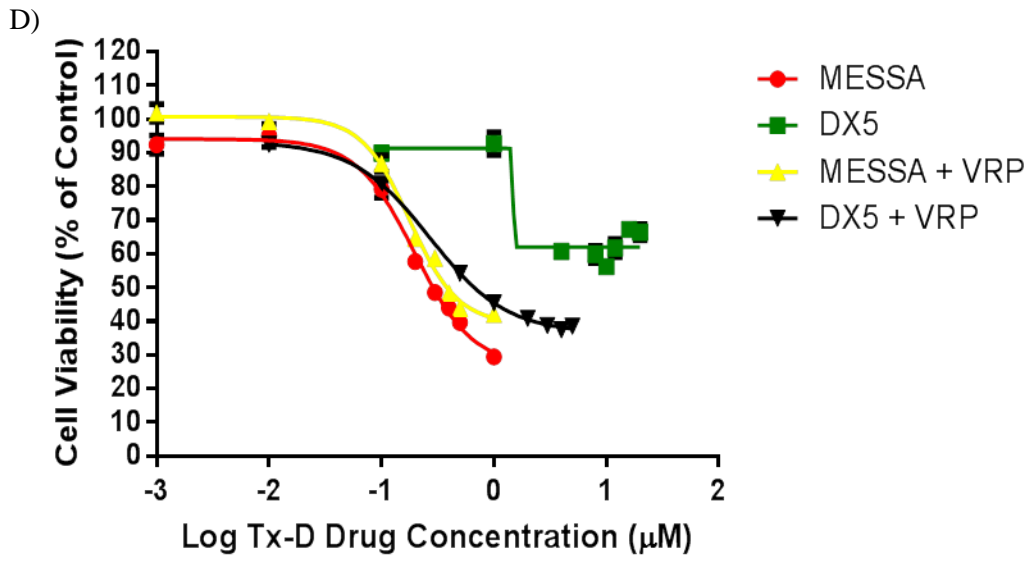
Additional data extracted from the cytotoxicity experiments, again can be used to further validate the original trends observed from the analog experiments performed using the breast cancer cell lines. In conditions in which the paclitaxel, its analogs and verapamil are used, the rank order of each of the compounds as they compare to paclitaxel has remained unchanged with the addition of a new variable. Figures 3-6 and 3-8 show that paclitaxel remained the most cytotoxic of the drugs with Tx-A being statistically not different in all four non breast cancer cell lines. In these four cell lines treatment with Tx-C and verapamil, IC_{50} values were only slightly higher than both paclitaxel and Tx-A but remain statistically distinct. Tx-D and Tx-F remain the analogs with the highest IC_{50} .

A)









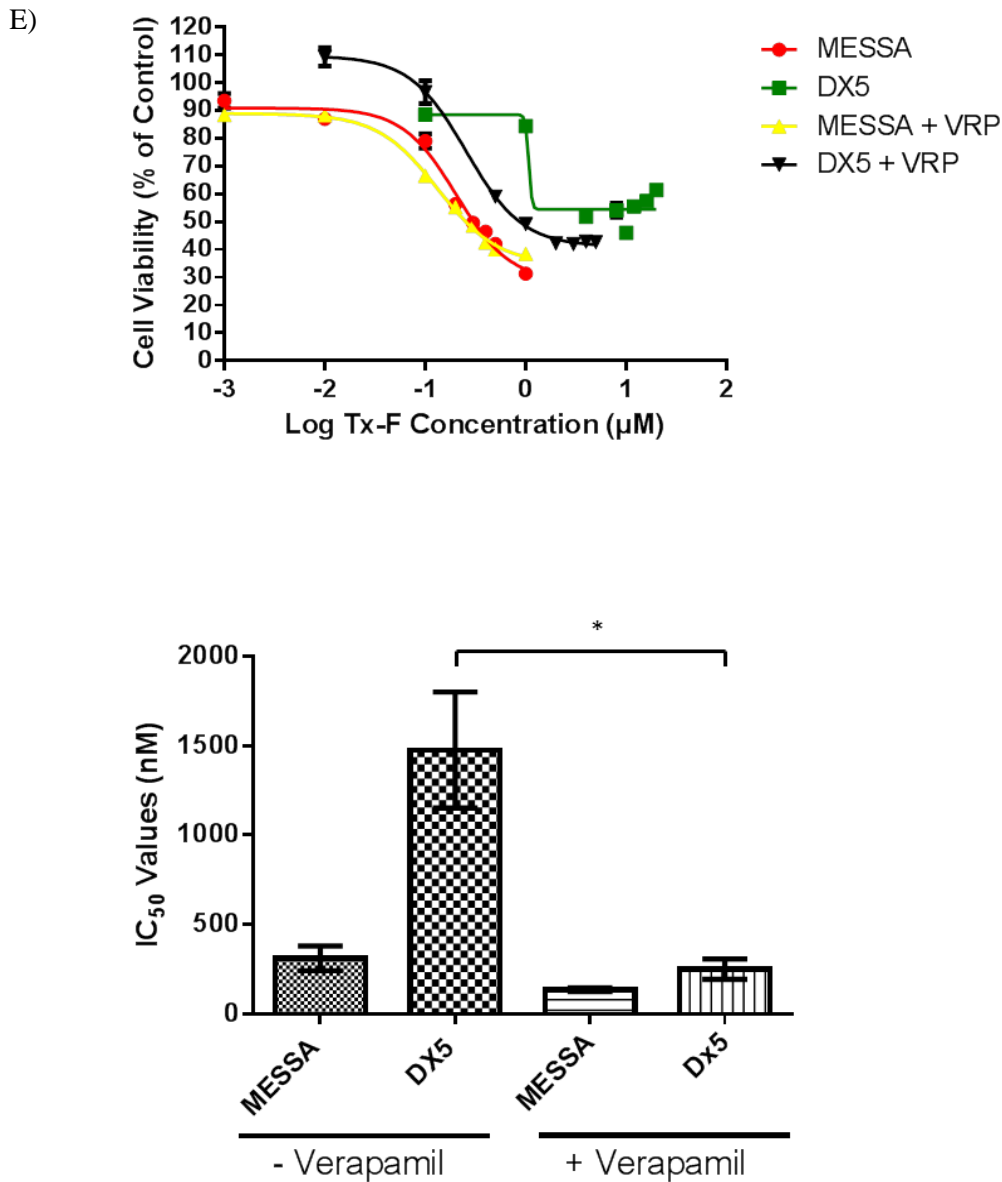


Figure 3-5. Differential Cytotoxicity of Paclitaxel Analogs in Presence of Verapamil Administered to MESSA/DX5 Cells

A range of (A) Paclitaxel, (B) Tx-A, (C) Tx-C, (D) Tx-D, and (E) Tx-F drug concentrations were used to titrate the cytotoxic potential for compounds in MESSA and DX5 ovarian cancer cell lines in the presence and absence of 5 µg/ml verapamil to determine the effects of P-gp and its inhibition on paclitaxel analogs. Cell lines were exposed to drugs for 72h after which 30 µl of MTS reagent was administered to each well, and absorbance measurements were taken at 490nm. Cytotoxicity curves are representative of n=3 independent experiments with 6 replicates per drug concentration for each experiment. Bar graphs represent IC₅₀ values and average of n=3 independent experiments. *, P<0.05

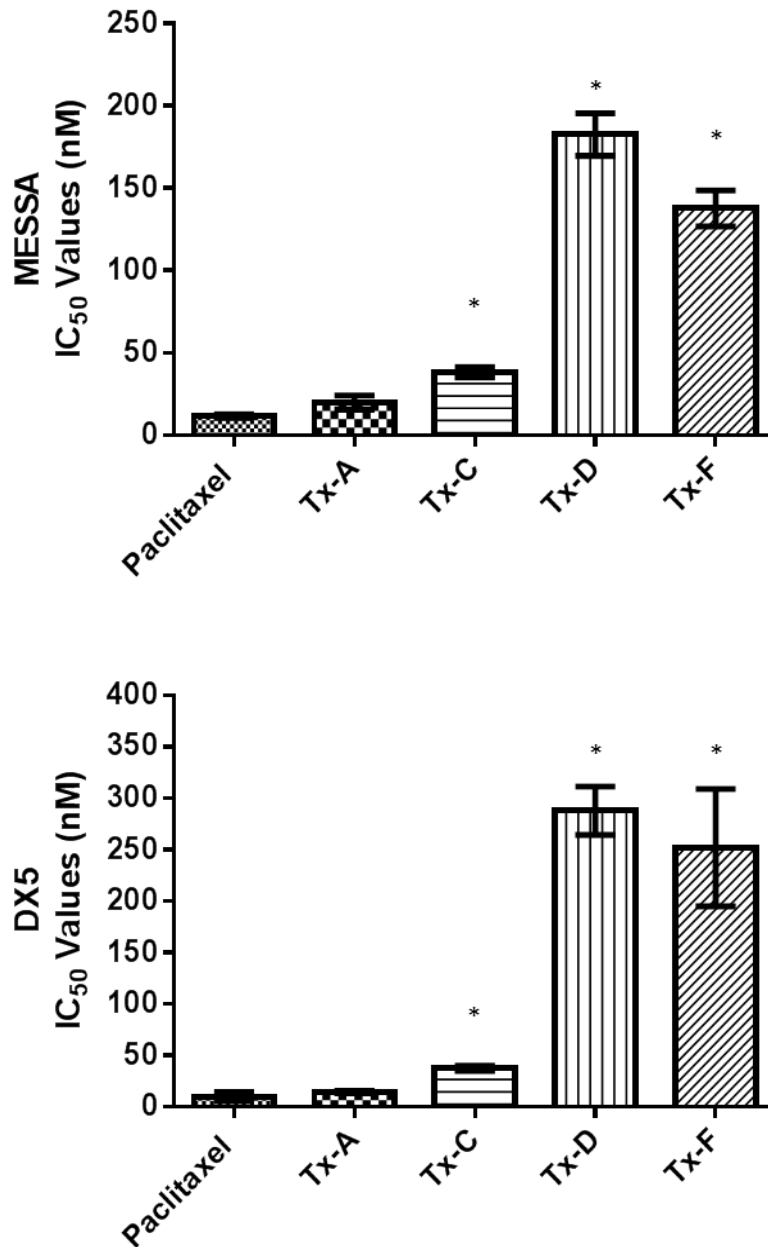
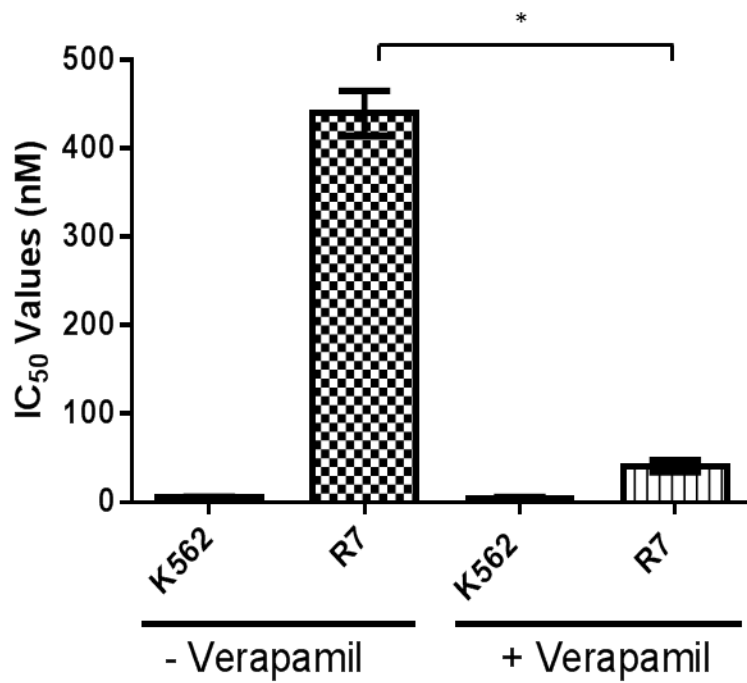
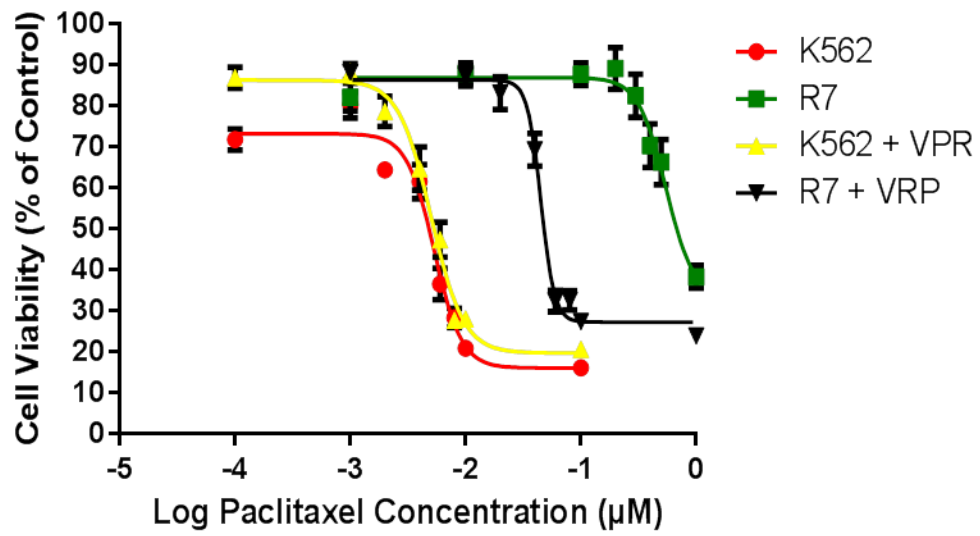
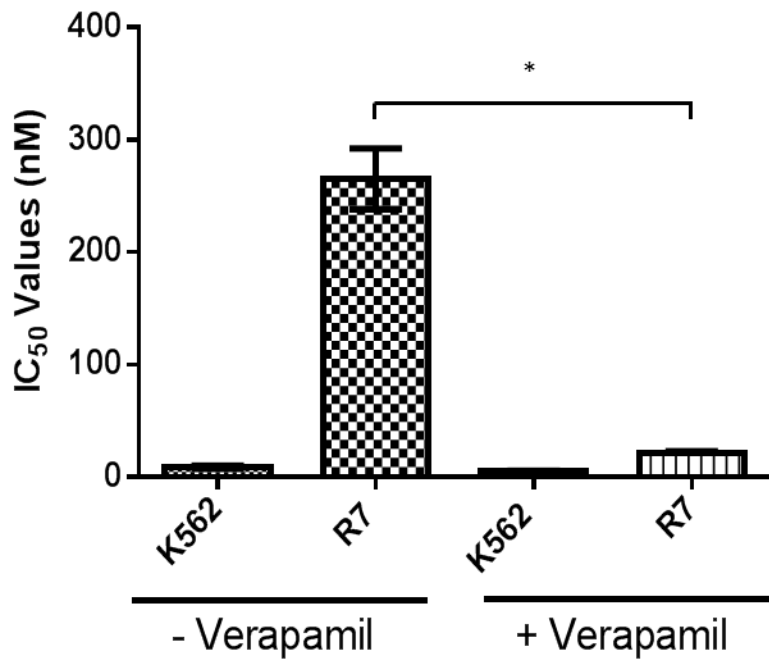
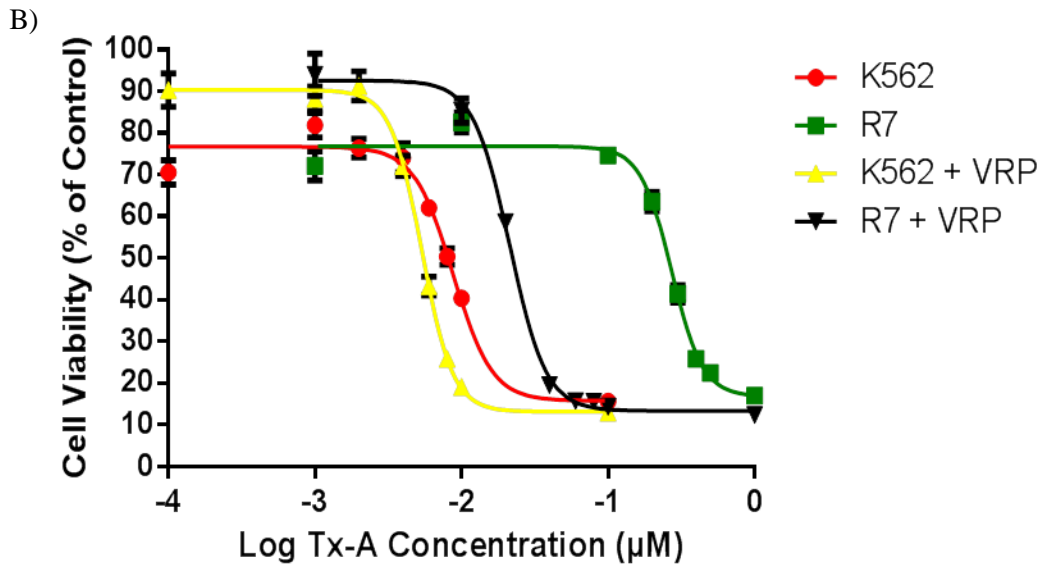


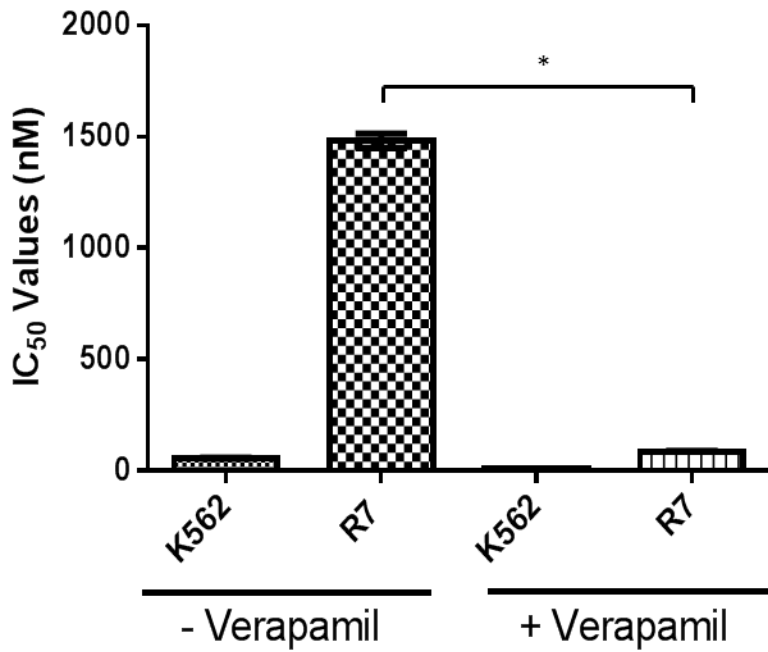
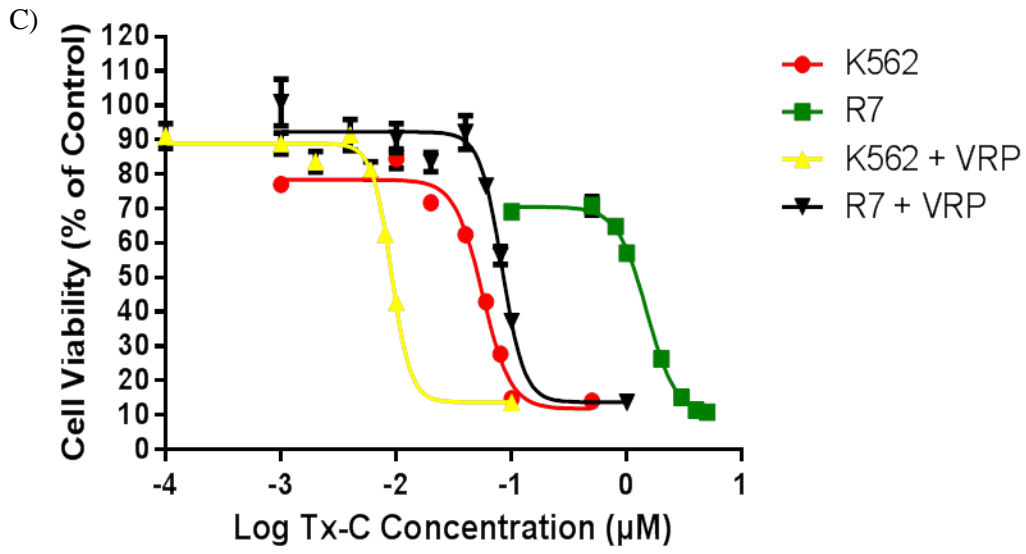
Figure 3-6. Rank Order of Cytotoxic Efficiency of Paclitaxel Compared to Analogs in MESSA/DX5 Cells in Presence of Verapamil

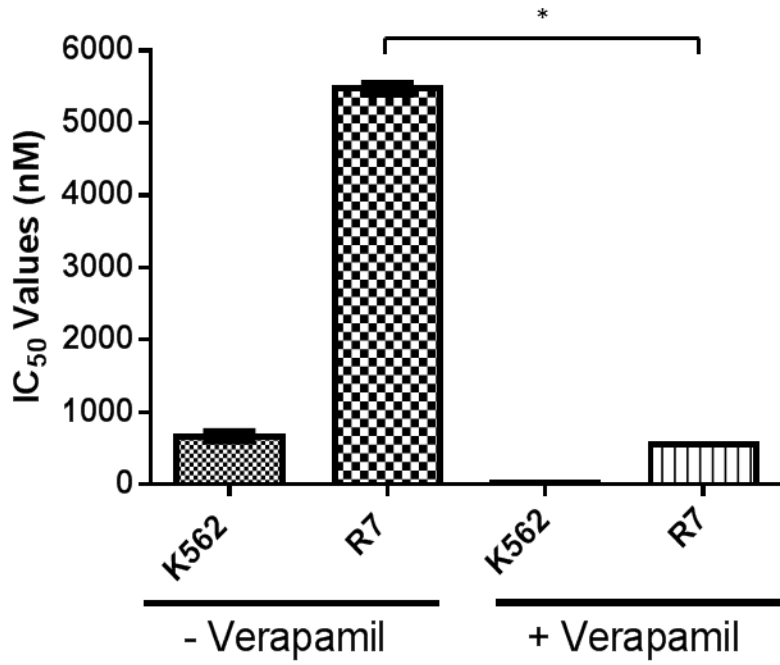
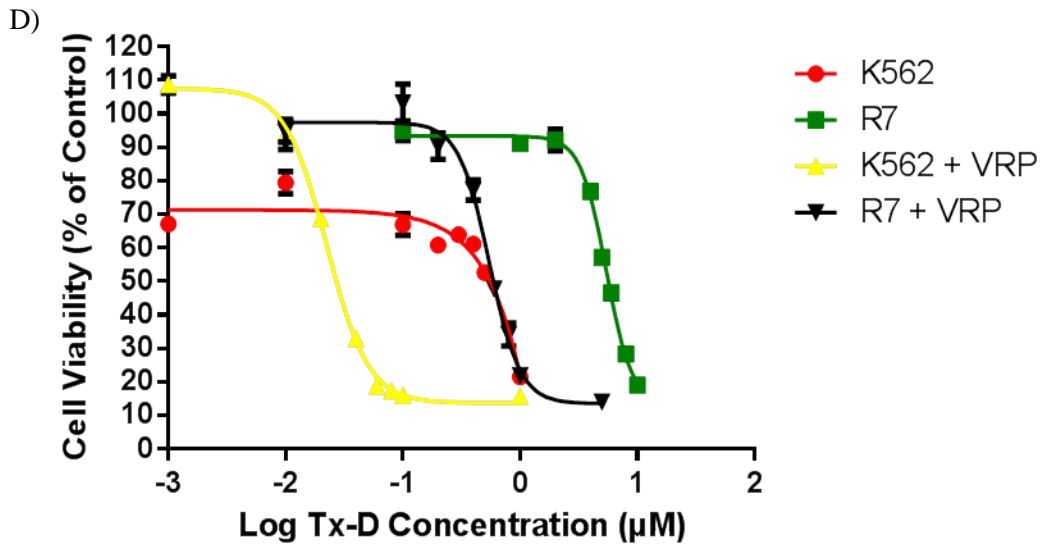
MESSA and DX5 ovarian cancer cell lines were treated with a range of drug concentrations to assess the cytotoxic activity of paclitaxel analogs in the presence of verapamil. Cell lines were exposed to drugs for 72h after which 30 μ l of MTS was administered to each well, and absorbance measurements were taken at 490 nm. All values compared to cell viability in untreated cells (normalized to 100%). Cytotoxicity curves represent n=3 experiments with 6 replicates per drug concentration for each experiment. Bar graphs represent IC₅₀ value from n=3 independent experiment. *, P<0.05 vs. paclitaxel

A)









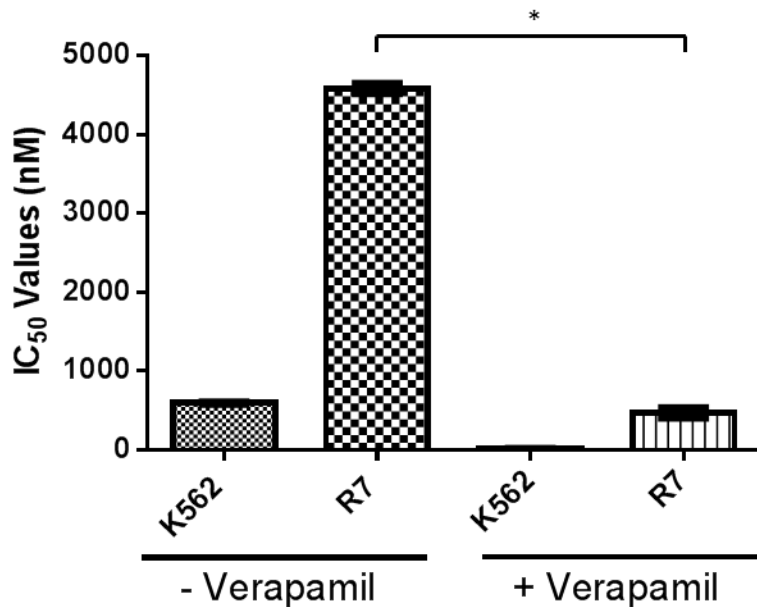
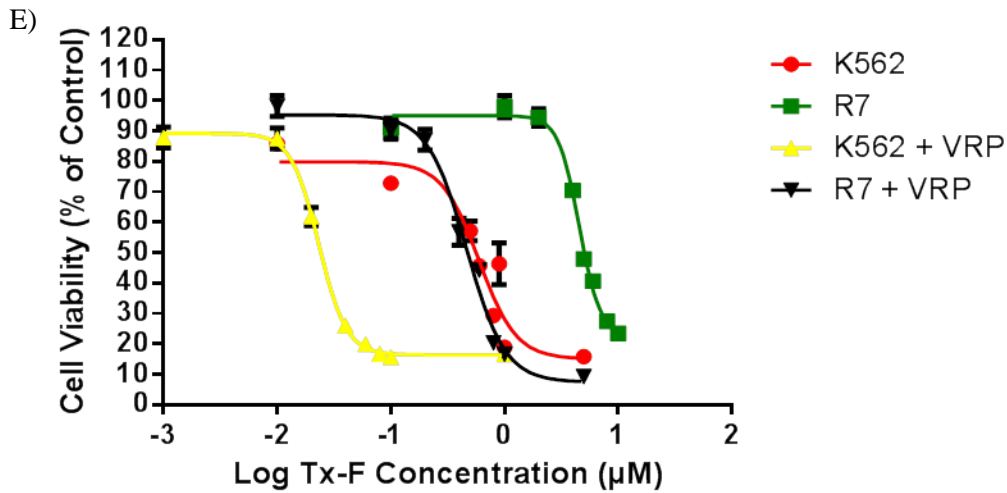


Figure 3-7. Differential Cytotoxicity of Paclitaxel Analogs in Presence of Verapamil Administered to K562/R7 Cell Lines

A range of (A) Paclitaxel, (B) Tx-A, (C) Tx-C, (D) Tx-D, and (E) Tx-F drug concentrations were used to titrate the cytotoxic potential for compounds against K562 and R7 CML cell lines in the presence and absence of 5 $\mu\text{g/ml}$ verapamil to determine the effects of P-gp and its inhibition on paclitaxel analogs. Cell lines were exposed to drugs for 72h after which 30 μl of MTS reagent was administered to each well, and absorbance measurements were taken at 490nm. Viability curves are representative of n=3 independent experiments with 6 replicates per drug concentration for each experiment. Bar graphs represent IC₅₀ value and average of n=3 independent experiments. *, P<0.05

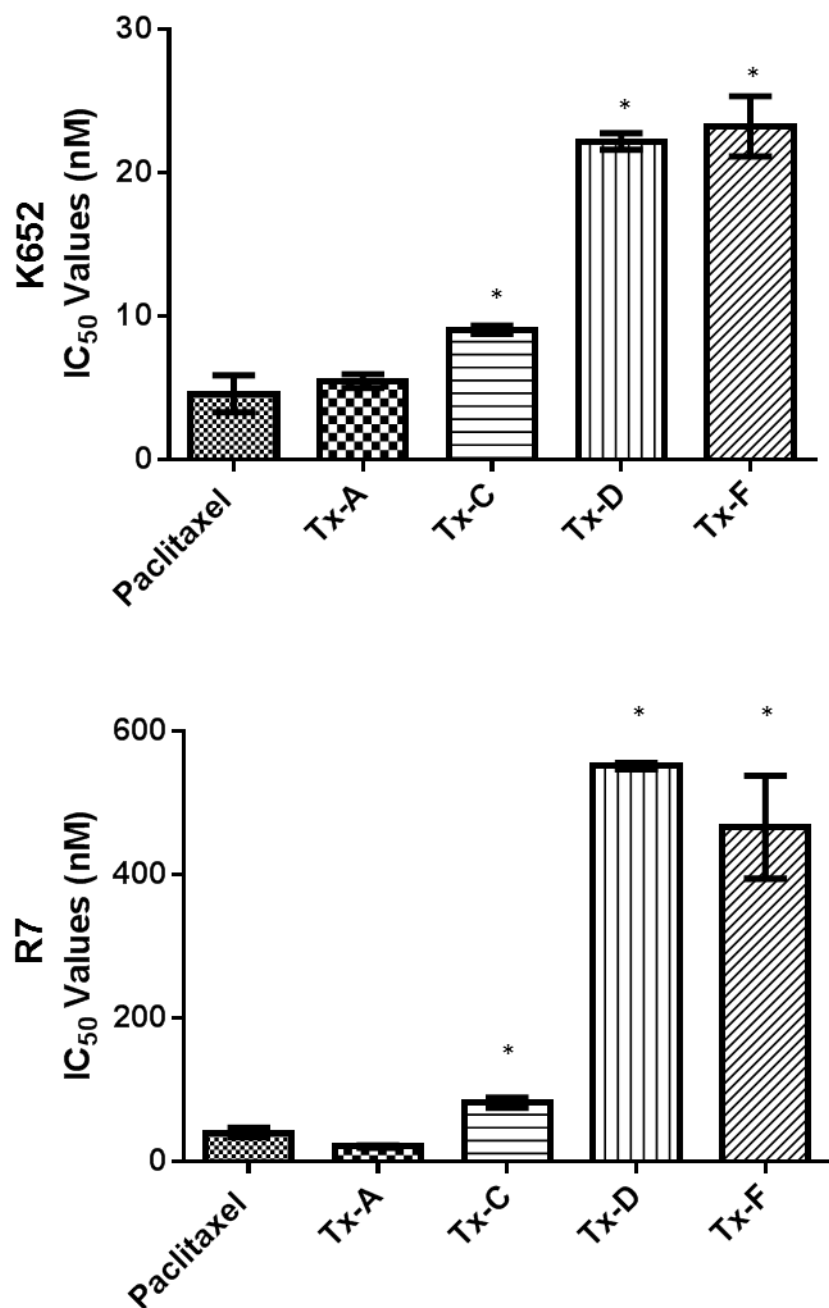


Figure 3-8. Rank Order of Cytotoxic Efficiency of Paclitaxel Compared to Analogs in K562/R7 Cells in Presence of Verapamil

K562 and R7 CML cell lines were treated with a range of drug concentrations to assess the cytotoxic activity of paclitaxel analogs in the presence of verapamil. Cell lines were exposed to drugs for 72 h after which 30 μ l of MTS reagent was administered to each well, and absorbance measurements were taken at 490nm. All values compared to cell viability in untreated cells (normalized to 100%). Cytotoxicity curves represent n=3 experiments with 6 replicates per drug concentration for each experiment. Bar graphs represent IC₅₀ values from n=3 independent experiment. *, P<0.05 vs. paclitaxel.

4. Developing a Panel of Resistant Sub-Lines to Understand Mechanisms of Taxane Resistance

4.1 Development of Paclitaxel Resistant SKBR-3 Sub-Lines

Investigating mechanisms of resistance necessitated developing defined resistant SKBR-3 sub-lines wherein mechanisms mediated by isotypes of β -tubulin could be studied as a function of graded resistance to paclitaxel in the cells, rather than the constitutive expression patterns discerned in the seven cell lines previously studied (Chapter 3). The seven cell lines used were informative in terms of the observed cytotoxic activity of paclitaxel and derived analogs and any constitutive resistance being independent of the cell line of origin (breast cancer, ovarian cancer or leukemia). However, from the seven cell line models used, I was unable to comment on the co-expression requirement, if any, of the β -tubulin isotypes to mediate resistance to paclitaxel, if I was to select cell lines showing moderate resistance vs. high resistance. There were no cell lines available from ATCC with the above defined criteria for drug resistance and access to cell lines developed by other investigators and reported in literature was limited. The concept of a “switch” wherein cells become committed to confer resistance to paclitaxel during the step-wise serial exposure of cells to the drug needed to be determined. Once committed, would the cells show graded expression of β -tubulin isotypes or would the expression remain invariant for a specific tubulin isotype in conferring resistance? Would the “switch” when turned on for resistance to the drug

and tubulin isotype expression patterns go hand-in-hand with P-gp expression? These questions were difficult to address with the panel of cell lines available to me. I therefore undertook creating my own panel of resistant cell lines using a controlled mechanism to better understand *in vitro* resistance to paclitaxel and its analogs. The development of resistant SKBR-3 breast adenocarcinoma sub-lines was achieved through stepwise passage of cells with incremental changes of concentration of drug within the growth media; paclitaxel was used as the drug in all experiments. The intent was to see if there would be a step wise resistance to paclitaxel, instead of all or none given the many steps of serially exposing the cells under different passages to increasing concentrations of the drug. Since β -III tubulin expression was shown to be up-regulated in drug resistant cells (Chapter 3), I was interested if β -III expression would also show proportional increase alongside the step-wise induced drug resistance in serially exposed cells to paclitaxel. Initially, the task of developing a series of sub- lines was undertaken using both SKBR-3 and MDA-MB-231 breast cancer cells. The passage of MDA-MB-231 cells with increased drug concentration (as per the protocol, the starting concentration was 1000-fold lower than the IC_{50} value) did not yield a large enough increase in drug concentration from first passage to final tolerable dose passage to consider using them for future experiments. This is not surprising since MDA-MB-231 cells showed intrinsic resistance to paclitaxel and expressed β -III tubulin. Developing further resistance to paclitaxel above this

background may not add to further insights to understand mechanisms of drug resistance.

4.2 Characterization of Derived Drug Resistance Sub-Lines for Phenotypic (Morphological) Changes

Seven increases in drug containing media were performed to successfully develop a panel of SKBR-3 cell lines each distinguished with a drug concentration in which they were consistently maintained. The sub-lines are denoted by SKBR-3 (IC₅₀ x10⁻³)3^Y, where Y represents the stage of drug concentration to which the cell line was developed as a function of the 3-fold drug increase with the development of each subsequent resistant sub-line (i.e., 0-7). The entire label represents the concentration of paclitaxel in which each cell line was developed and maintained in for all experiments. As seen in Figure 4-1, phenotypic changes were observed over the course of the development. A change in morphology and growth patterns was observed following the development of SKBR-3 (IC₅₀x10⁻³)3⁴. WT SKBR-3 and all cell lines developed up to the (IC₅₀x10⁻³)3⁴ line were large in size, formed a cobblestone pattern when grown to confluency, and grew as a monolayer. SKBR-3 (IC₅₀x10⁻³)3⁴ cells have undergone a morphological change to a round shape, and cells were smaller in size compared to cells of the parental line. They grew as non-monolayer colonies (foci) independent of contact inhibition, as well as showed growth in an anchorage independent manner, with cells floating in suspension within the media. This loss of anchorage dependence is a phenotype of higher malignancy (184), in which a small number of floating

cells can be re-seeded onto another flask for re-adherence, proliferation and creation of a new population with the same phenotypic characteristics. Although there was a select population of cells that grew suspended in media, they were discarded when media was changed. It was assumed that all or most cells in the population shared this trait and therefore discarding these cells did not eliminate a subpopulation of cells with a different phenotype. This was a safe assumption given that when the cells were passaged with only adherent cells there was always a subpopulation of cells that grew in suspension for the reasons mentioned above (loss of contact inhibition and development of anchorage independence). All subsequent cell lines at higher drug concentrations had the same phenotype, and increased growth rate as determined by lower seed numbers and higher rates to which confluency was reached. Cells lines were maintained in drug containing media at constant concentration equal to that in which the cell line was originally selected from, unless otherwise stated, to prevent any reversal or loss of malignant traits. The goal was to establish mechanisms of taxane resistance independent of the activity from multidrug resistance efflux pump P-gp. Due to this desire, all cell lines were created and maintained with the P-gp inhibitor, verapamil. The concentration of verapamil was maintained consistently at 5 μ g/ml, previously identified as a relevant concentration to inhibit P-gp activity (167).

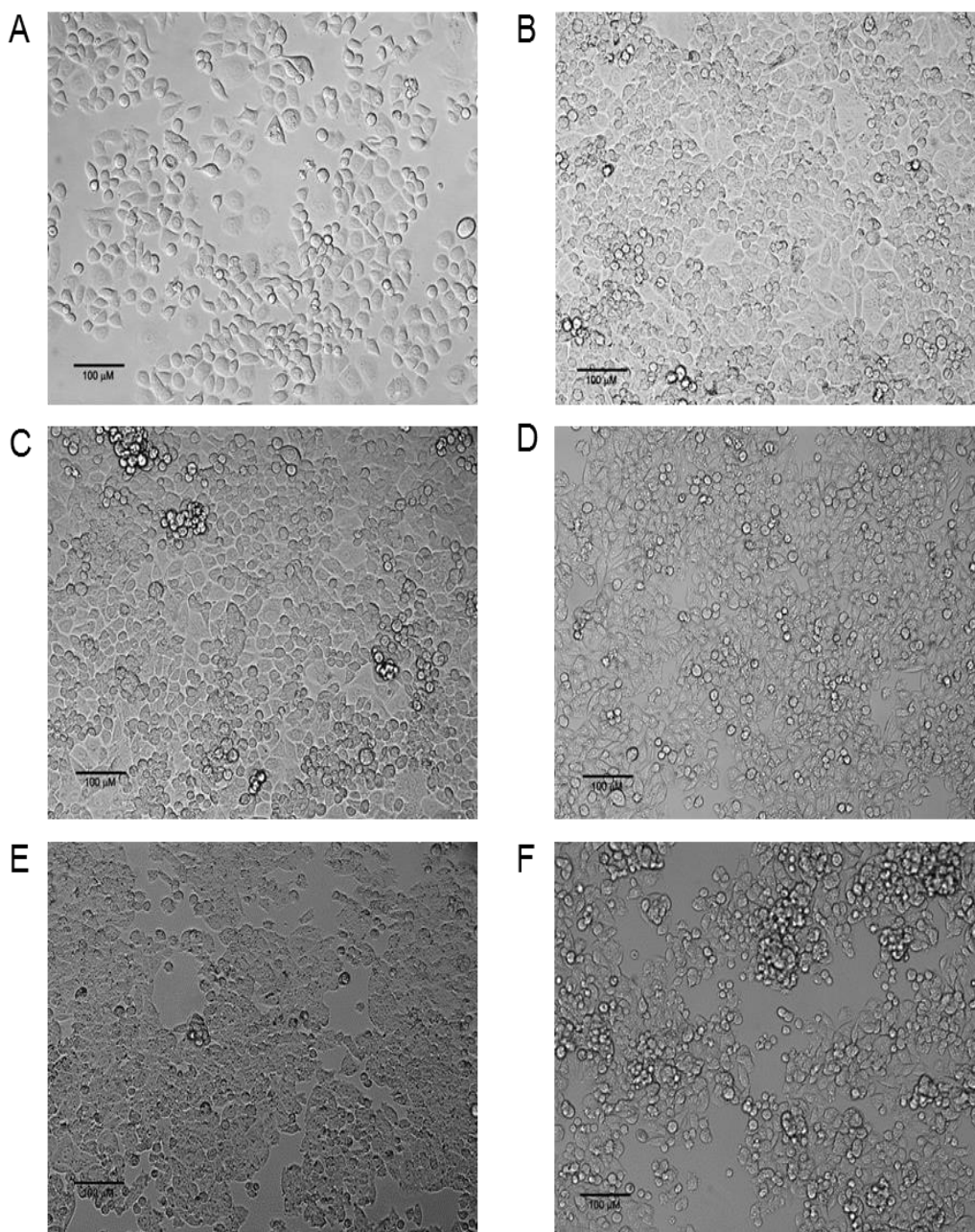


Figure 4-1. Phenotypic Changes Observed of SKBR-3 Sub-Lines Showing Incremental Resistance to Paclitaxel

Four cell lines have been selected from the panel of resistant sub-lines. Two control cell lines have been characterized; (A) SKBR-3 wild type cell line and (B) SKBR-3 cells that underwent high passage during cell culture, as in the drug resistance lines developed. Morphological characteristics of the resistance cell line shown are: (C) $(IC_{50} \times 10^{-3})^2$; (D) $(IC_{50} \times 10^{-3})^4$; (E) $(IC_{50} \times 10^{-3})^5$ and (F) $(IC_{50} \times 10^{-3})^7$. Scale bar represents 100 μm . Images shown were taken using a Zeist AxioVert microscope.

Mechanisms of taxane resistance were investigated in the experiments described in the ensuing section using these cell lines. Of the eight resistance sub-lines created, I selected four cell lines that span a range of drug resistance phenotypes for further experimentation.

4.3 Determining Changes in β Tubulin Isoform Expression from SKBR-3 Resistant Sub-Lines

Using my panel of resistant cell line(s), I performed western blot analysis to investigate differential β tubulin isoform expression, if any, as a function of controlled increase in paclitaxel resistance. This model will provide information on the isoforms that are differentially expressed due to paclitaxel resistance, and may guide the findings and interpretations reported in Chapter 3. I used four of the resistant SKBR-3 sub-lines to identify patterns of expression for tubulin isoforms. Chosen at random, the cell lines used to represent the panel were SKBR-3 ($IC_{50} \times 10^{-3}$)³², ($IC_{50} \times 10^{-3}$)³⁴, ($IC_{50} \times 10^{-3}$)³⁵, and ($IC_{50} \times 10^{-3}$)³⁷. Additionally, two control cell lines were used. The first was the “WT” SKBR-3 cell line from which the panel was created and the second was a SKBR-3 cell line that had undergone a high number of passages, equal to the number of passages the ($IC_{50} \times 10^{-3}$)³⁷ cell line had undergone. Whole cell lysates were used from the controls and resistant cells grown in the presence or absence of drug for western blot analysis. The data shows that as resistance increased there was a sudden appearance of β III tubulin (Figure 4-2). In

both control cell lines as well as in the least resistant of the panel β III protein was completely absent. As drug resistance increased, there was

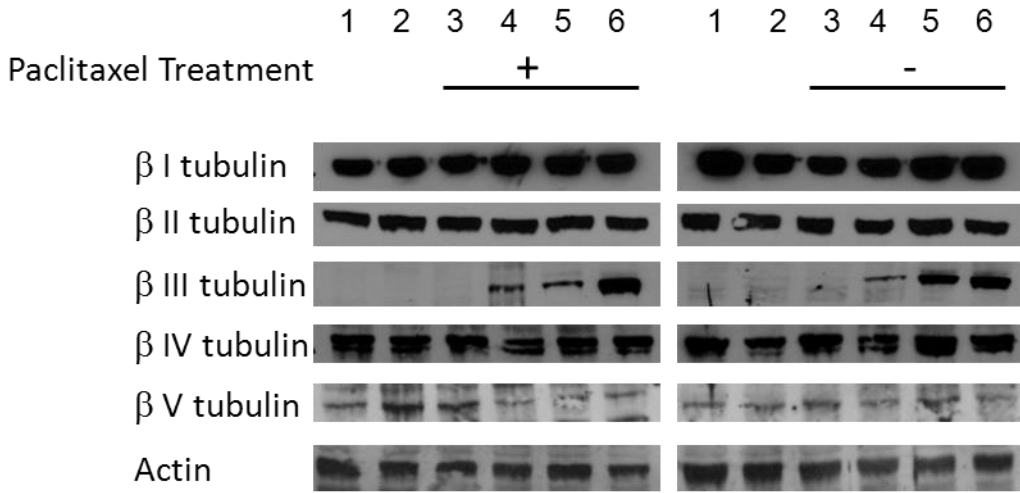


Figure 4-2. β Tubulin Isotype Protein Expression in a Panel of Resistant SKBR-3 Sub-Lines

Four cell lines were selected to determine changes in β isotype I-V expression with cells showing increasing drug resistance. Experiments were carried out under two conditions; drug free media (-) and drug containing media (+) for 7 days. Two controls were used, wild type SKBR-3 cells (1) and High Passage SKBR-3 (2) which have gone through the same number of passages as the highest sub-line. Resistant cell lines used were; $(IC_{50} \times 10^{-3})^3$ (3), $(IC_{50} \times 10^{-3})^4$ (4), $(IC_{50} \times 10^{-3})^5$ (5), and $(IC_{50} \times 10^{-3})^7$ (6). Identical samples loaded into controls wells in both left and right panels. Data shown is representative of $n=3$ independent experiments. Actin was used as a loading control.

a sudden appearance of β III tubulin seen expressed within the $(IC_{50} \times 10^{-3})^4$ sub-line. Expression of β III tubulin continued to rise in $(IC_{50} \times 10^{-3})^5$ cells and was the highest in the most resistant cell line $(IC_{50} \times 10^{-3})^7$. There was an apparent step-wise increase in the expression of β III tubulin within untreated cells (Lanes 4-6, right panel in Figure 4-2) compared to the results shown in left panel in the cells maintained in drug containing media. The step-wise increases in β -III expression from resistant cells

grown in drug free media conform to my original hypothesis. However, a less pronounced effect of such a step-wise increase in expression of β -III was observed in the resistant cells grown in drug containing media, even though the expression reached a maximum in the highest dose of the drug tested. This result was unexpected, and several independent experiments did not provide any further clarity over and above the results summarized here. I therefore speculate at this point that a complex interplay of β -III tubulin expression and external drug concentration may determine the overall balance tipping towards cell survival.

Of the five isotypes tested, β III tubulin was the only one that showed changes corresponding to drug resistance within a range. I was able to clearly demonstrate invariant expression of other β tubulin isotypes; consistent expression was observed in both control cell lines and throughout within the panel of cell lines showing graded resistance. The expression of these isotypes appeared constitutive, and was therefore not influenced by the presence or absence of drug (Figure 4-2). Hence, these remaining four isotypes (β -I, II, IV and V) are considered to not have contributed to the overall resistance observed in these cell lines.

4.4 Cytotoxicity Profiles from Paclitaxel and Analogs Correlate to Increasing β III Tubulin Expression

Using my panel of resistant SKBR-3 sub-lines, I wished to demonstrate that there was indeed a change in IC_{50} values of these cell

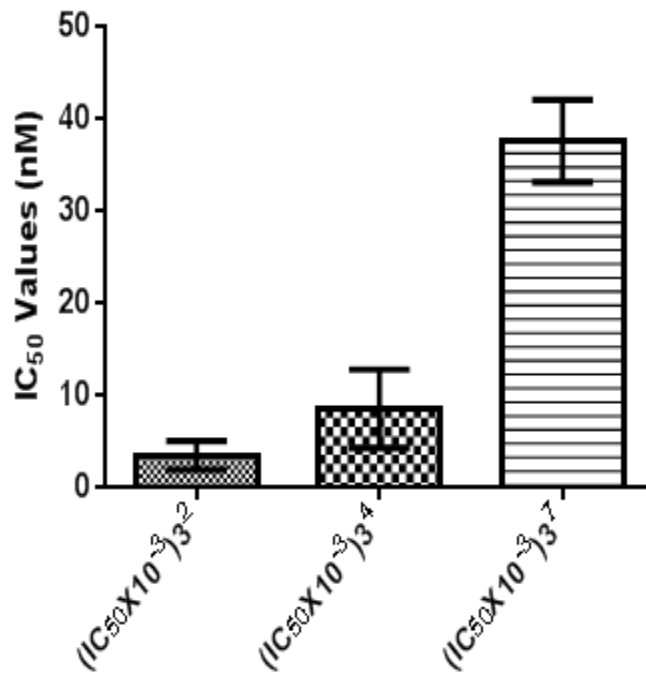
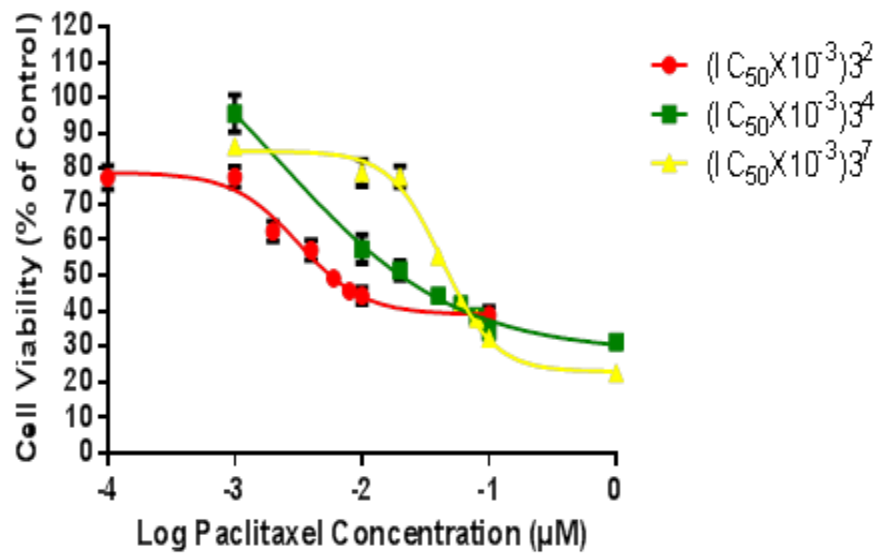
lines to paclitaxel, a function that may be correlated to the changes in β III tubulin expression. Cytotoxicity assays were carried out using paclitaxel as well as the synthetic analogs in the presence of 5 μ g/ml verapamil to determine the changes in three selected cell lines: $(IC_{50} \times 10^{-3})^{3^2}$, the cell line with no expression of β III; $(IC_{50} \times 10^{-3})^{3^4}$, the cell line in which the expression of β III tubulin first appeared; and $(IC_{50} \times 10^{-3})^{3^7}$, the cell line grown in the highest concentration of paclitaxel and expressing the highest amount of β III tubulin protein. Cytotoxicity experiments were carried out over a 72 h period before MTS reagent was administered. The data showed that in each cell line there was a statistically significant increase in IC_{50} value as a function of paclitaxel exposure determined by one way ANOVA (Figure 4-3A).

The $(IC_{50} \times 10^{-3})^{3^2}$ cell line showing no expression of β III tubulin had an IC_{50} equal to or lower than that of the original SKBR-3 WT line. The $(IC_{50} \times 10^{-3})^{3^4}$ cell line, in which β III expression first appeared, had an IC_{50} value of 9 ± 5 nM which was marginally higher than that of the WT cells, although not statistically significant. Finally the most resistant cell line $(IC_{50} \times 10^{-3})^{3^7}$ had an IC_{50} value of 38 ± 5 nM which was a 9.2-fold increase in drug resistance (Figure 4-3A). Similarly, when treated with each of the analogs there was a concomitant increase in IC_{50} values in the cell lines, from the lowest to the highest level of drug resistance. The increases in IC_{50} values also correlated with the expression of β III tubulin. When I

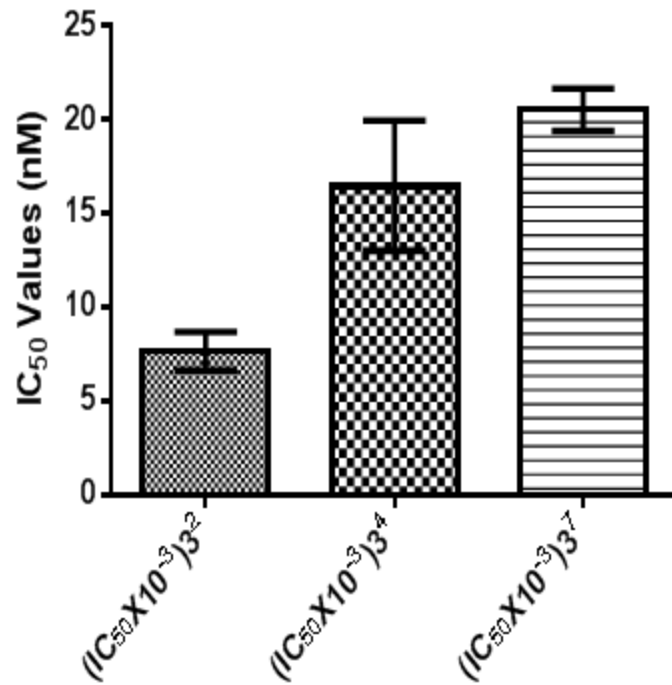
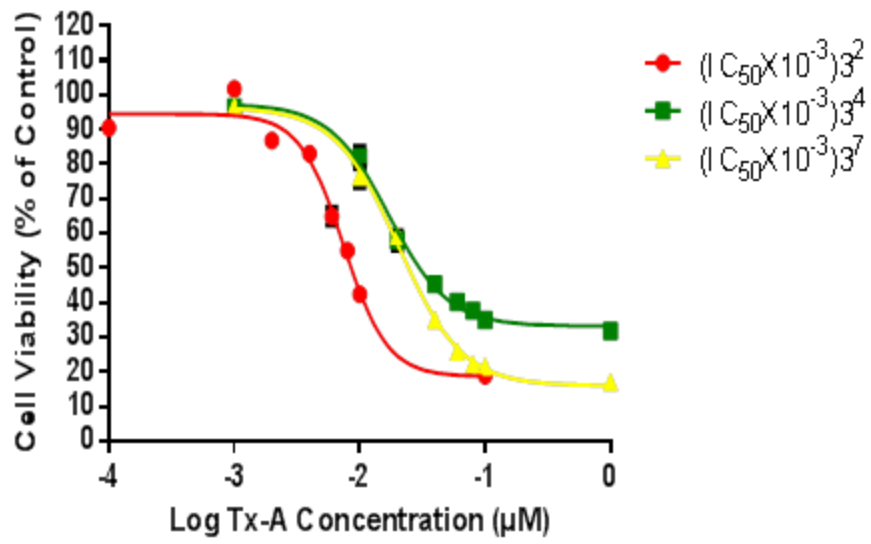
compared the IC_{50} values of the WT with those of the $(IC_{50} \times 10^{-3})3^4$ cell line, except in the case of Tx-A, the remaining three analogs showed IC_{50} values more than 2-fold higher, at 5.7, 2.6, and 2.9 for Tx-C, Tx-D and Tx-F, respectively (Table 4-1). The IC_{50} values increased further, parallel with the higher expression of β III tubulin within $(IC_{50} \times 10^{-3})3^7$ cells (Figure 4-3). This indicates that similar to cells treated with the parent compound, paclitaxel, the IC_{50} values showed expected increases along with increased protein expression levels for β tubulin. It is interesting to note that of the four analogs tested, Tx-C was the only drug in which the IC_{50} value of the $(IC_{50} \times 10^{-3})3^2$ cell line was equal to that of the WT cells (Table 4-1). On the other hand, Tx-A, Tx-D and Tx-F, the IC_{50} values for the WT cells showed more resistance than the $(IC_{50} \times 10^{-3})3^2$ cells (lowest level of resistance among the cell lines developed). This apparent anomaly may be ascribed to the presence of verapamil within the medium of each of the cell lines tested excluding the WT SKBR-3 cells. Verapamil present in the medium was previously shown to exert synergistic effect to that drug under investigation and thus may contribute to lower IC_{50} values than the parent compound, paclitaxel (185). This effect on IC_{50} values was masked in other cell lines showing higher resistance (better signal-to-noise ratio). Since verapamil is an inhibitor of P-gp protein/efflux pump activity, but not an inhibitor of expression of *MDR-1* (P-gp) gene transcription, I evaluated if P-gp protein was expressed in the sub-lines developed. Western blot

analyses revealed expression of P-gp protein in the drug resistant cell lines (data not shown). The simultaneous expression of β -III and P-gp may translate to the resistance to a number of drugs, not only restricted to paclitaxel or analogs and the cell lines I developed need to be further investigated for resistance to other drugs. There appears to be no obligatory co-expression of β -III tubulin protein and P-gp protein, as assessed by the seven cell line models I have used initially (Chapter 3). There were cell lines expressing β -III tubulin independent of P-gp expression and vice-versa (Figure 3-4). MESSA cells showed only β -III expression and R7 showed only P-gp expression. Similar to R7 cells, DX5 cells showed only P-gp expression and not β -III (Figure 3-4).

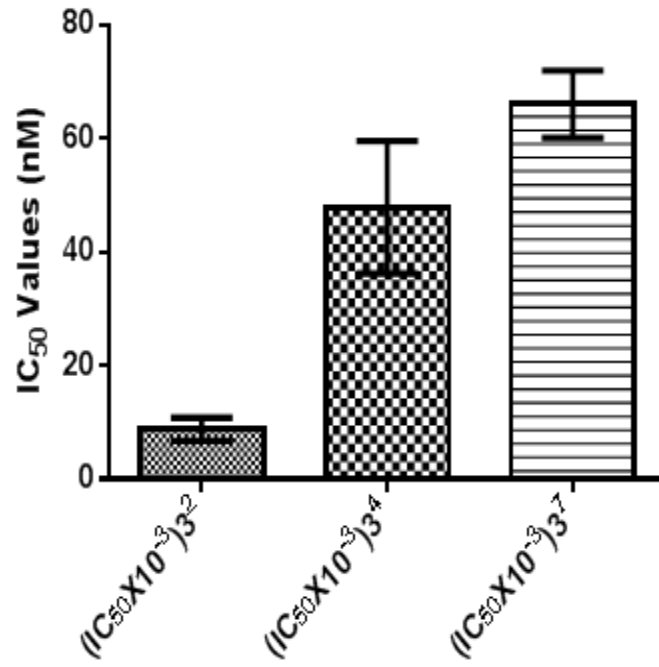
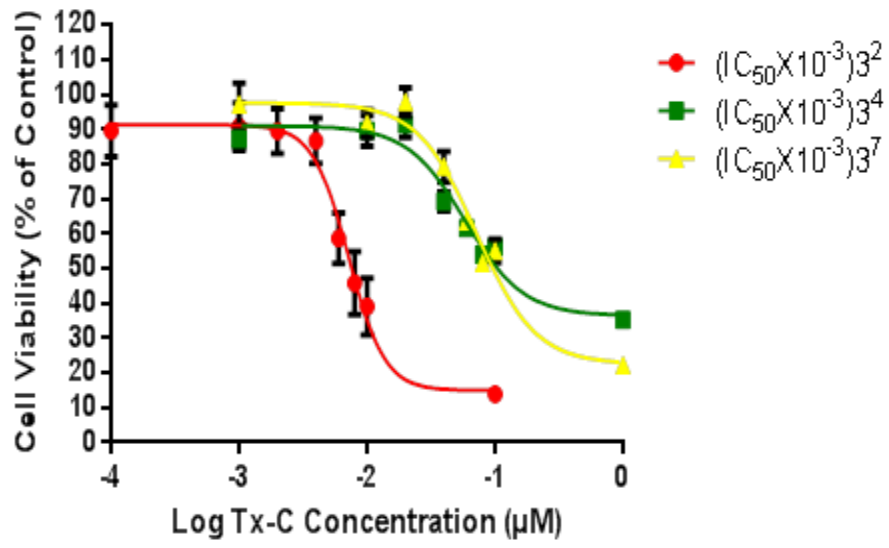
A)



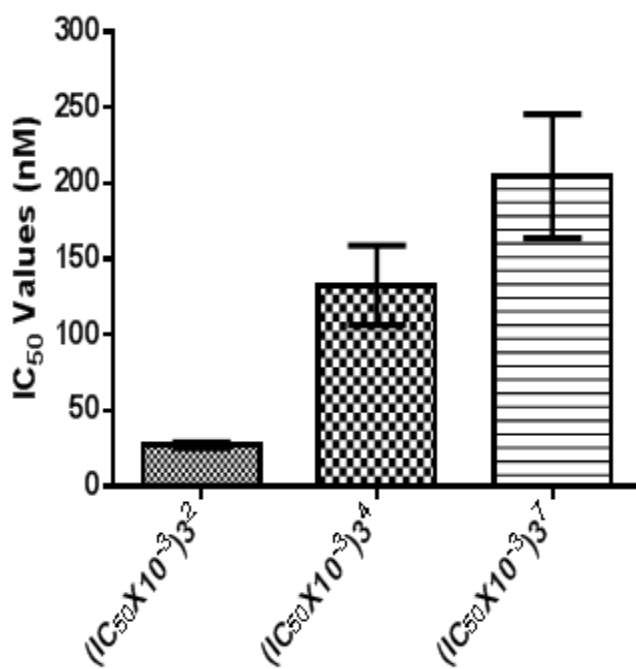
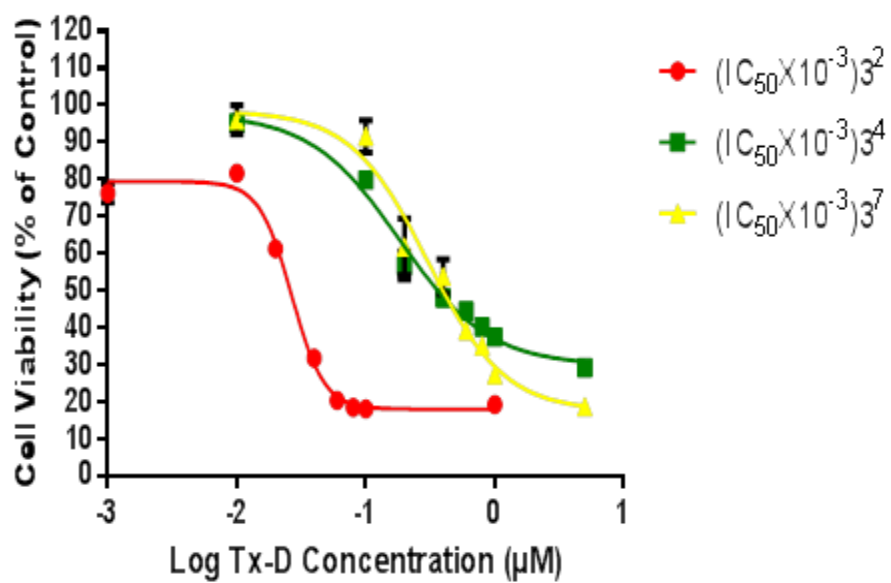
B)



C)



D)



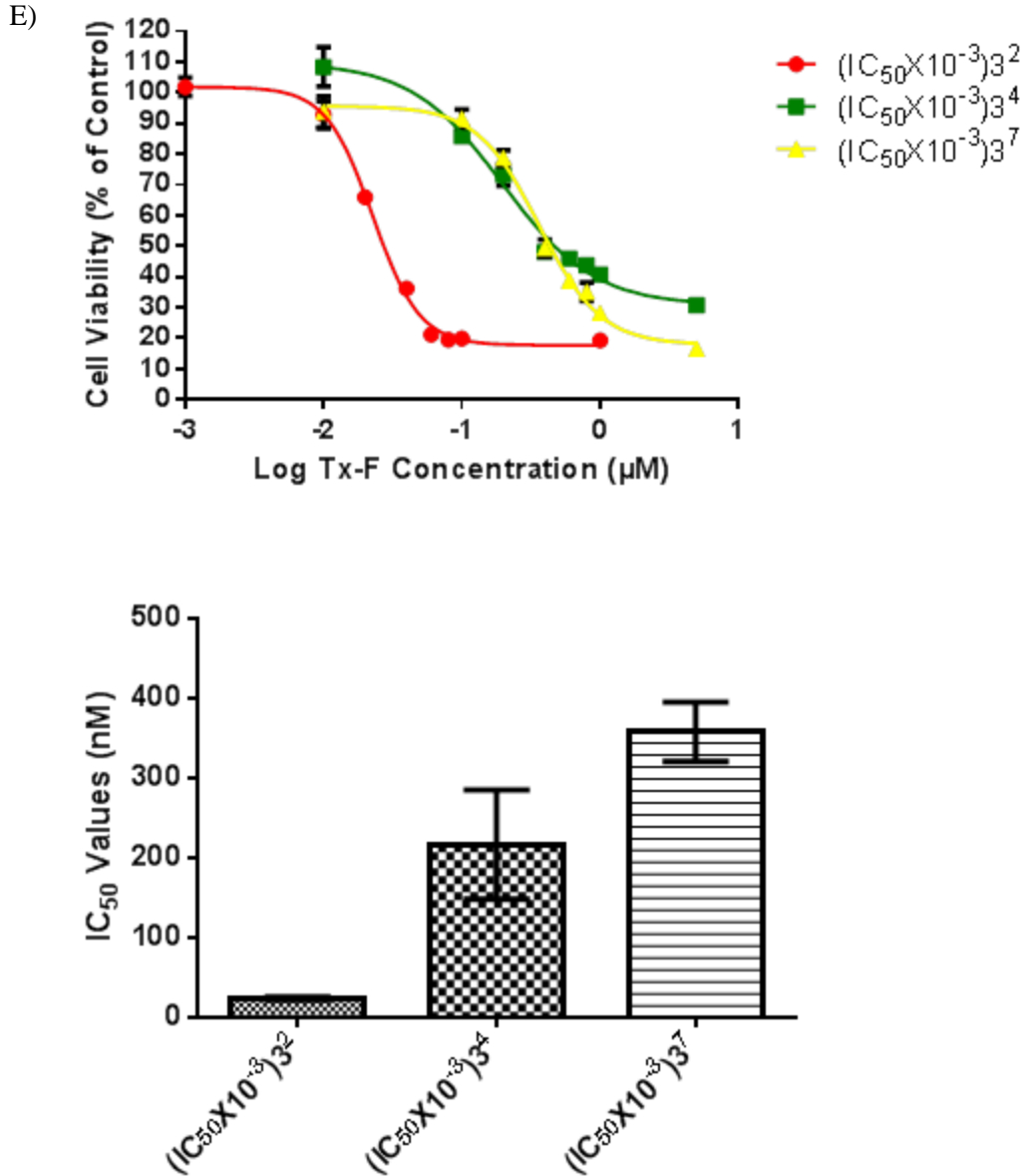


Figure 4-3. Effects of β III Tubulin Expression on Profiles of Cytotoxicity from Paclitaxel and Analogs

Three of the SKBR-3 sub-lines were used to determine the cytotoxicity of paclitaxel and analogs. $(IC_{50} \times 10^{-3})^{3^2}$ cell line was selected as pre β III tubulin induction and $(IC_{50} \times 10^{-3})^{3^4}$ and $(IC_{50} \times 10^{-3})^{3^7}$ were selected for post β III tubulin induction. Cells treated with (A) Paclitaxel, (B) Tx-A, (C) Tx-C, (D) Tx-D, and (E) Tx-F over a range of drug concentrations and 5 $\mu\text{g}/\text{ml}$ verapamil was present in all experiments and treatments to inhibit P-gp activity. Cell lines were exposed to drugs for 72 h after which 30 μl of MTS reagent was administered to each well, and absorbance was read at 490nm. Cell viability data presented is representative of $n=3$ independent experiments with 6 replicates per drug concentration per experiment. Bar graphs represent IC₅₀ of $n=3$ independent experiments. Statistical significance of experimental groups determined using one way ANOVA $p < 0.05$

Table 4-1. Summary of the IC₅₀ Values (source Figure 4-3) of Resistant SKBR-3 Sub- Lines Treated with Paclitaxel and Analogs

	Paclitaxel	Tx-A	Tx-C	Tx-D	Tx-F
WT	5 _{±1}	16 _{±1}	9 _{±2}	77 _{±18}	76 _{±16}
(IC ₅₀ x10 ⁻³) ^{3²}	4 _{±2}	8 _{±1}	9 _{±3}	28 _{±3}	23 _{±2}
(IC ₅₀ x10 ⁻³) ^{3⁴}	9 _{±5}	17 _{±4}	48 _{±12}	199 _{±68}	217 _{±69}
(IC ₅₀ x10 ⁻³) ^{3⁷}	38 _{±5}	21 _{±2}	66 _{±6}	335 _{±133}	358 _{±38}

The IC₅₀ values (represented in nM) were calculated using the GraphPad Prism 5 program. Values and errors (SE) shown are the average IC₅₀ values from n=3 independent experiments. Statistical significance of experimental groups determined using one way ANOVA, p<0.05

4.5 Other Possible Mechanisms of Drug Resistance Explored

Cytotoxicity and western blot experiments showed that the mechanisms of drug resistance in the cell lines could be ascribed to the expression of β III tubulin since expression correlated well with the profiles from cytotoxicity data from paclitaxel as well as its analogs. There is precedence in literature to indicate that global gene expression profiles identified in WT and drug resistant cell lines showed expression changes in a number of genes such as apoptosis (differential expression of pro- and anti-apoptosis family members), cell cycle regulation genes, DNA repair and drug metabolism gene pathways. These observations point to the diverse cellular and molecular mechanisms operating for imparting resistance to drugs and that holistic approach to understand drug resistance is needed (as opposed to single gene approaches) and that biology operates in complex networks. I reasoned that global regulation of

gene expression through microRNAs (miRNAs) may capture a higher level of complexity of biological networks since each miRNA could in principle mediate translational repression of the target genes from 1 to as many as 100. Another reason for approaching miRNA mediated regulation of drug resistance is due to the established premise that β -III gene expression is indeed regulated at the level of miRNA (miR-200c) (178,181,186). MicroRNAs are evolutionarily conserved and since they exert pleiotropic effects (targeting several mRNAs), it was hypothesized that drug resistance mechanisms could be mapped to miRNA expression profiles, not restricted to β -III tubulin gene expression regulation. I therefore investigated miRNA expression profiles within representative resistant sub-lines. NGS of the small RNAome from the selected cell lines was undertaken using the Illumina platform. Small RNA isolated from WT SKBR-3 were also sequenced (n=2) to compare the profiles obtained from resistant cell lines. Hierarchical clustering analysis was performed to group the cell lines to reflect the sequential evolution of drug sensitivity to drug resistance and the miRNAs contributing to the distinction between the cells lines. It was seen that there are two distinct lineages from among the cell lines sequenced. The first contains the WT and ($IC_{50} \times 10^{-3}$)³ cell lines and these are more closely related to each other as expected from the clustering patterns, suggesting minimal evolutionary divergence due to drug selection (or cells showing weak resistance, if any from the WT cell line). Regardless, there has been a selection pressure and hence it is not

surprising that these cell lines were clearly distinct from one another. I preferred sequencing biological replicates for each cell line as opposed to technical replicates wherein same RNA is split from a single experiment to perform two sequencing reactions. Cell line models are prone to artifacts and as such, biological replicates were more meaningful to capture the variations due to evolutionary (selection) pressures. One of the $(IC_{50} \times 10^{-3})^2$ cells was more closely related to the WT cells than the second replicate. This suggests inter-population genetic variance accruing during the growth period that has also resulted in slight divergence between these samples (Figure 4-4).

The second distinct group contained $(IC_{50} \times 10^{-3})^4$, $(IC_{50} \times 10^{-3})^5$, and $(IC_{50} \times 10^{-3})^7$ cell lines. Genetic changes may have occurred in these cells to an extent that would influence the overall expression patterns. The profiles were very distinct from the WT and $(IC_{50} \times 10^{-3})^2$ cell lines. I observed that in the $(IC_{50} \times 10^{-3})^5$ and $(IC_{50} \times 10^{-3})^7$ cell lines, one of the replicates showed closer relationship to the cell line that preceded it in development or selection process as compared to the other replicate. Again, this suggested that there is inter-population genetic variation occurring during the process: from trypsinization of one population through seeding and growth to confluency in the replicates handled in independent experiments. Nonetheless, the separation of drug sensitive and resistant cell lines is unequivocal based on the miRNA expression based clustering.

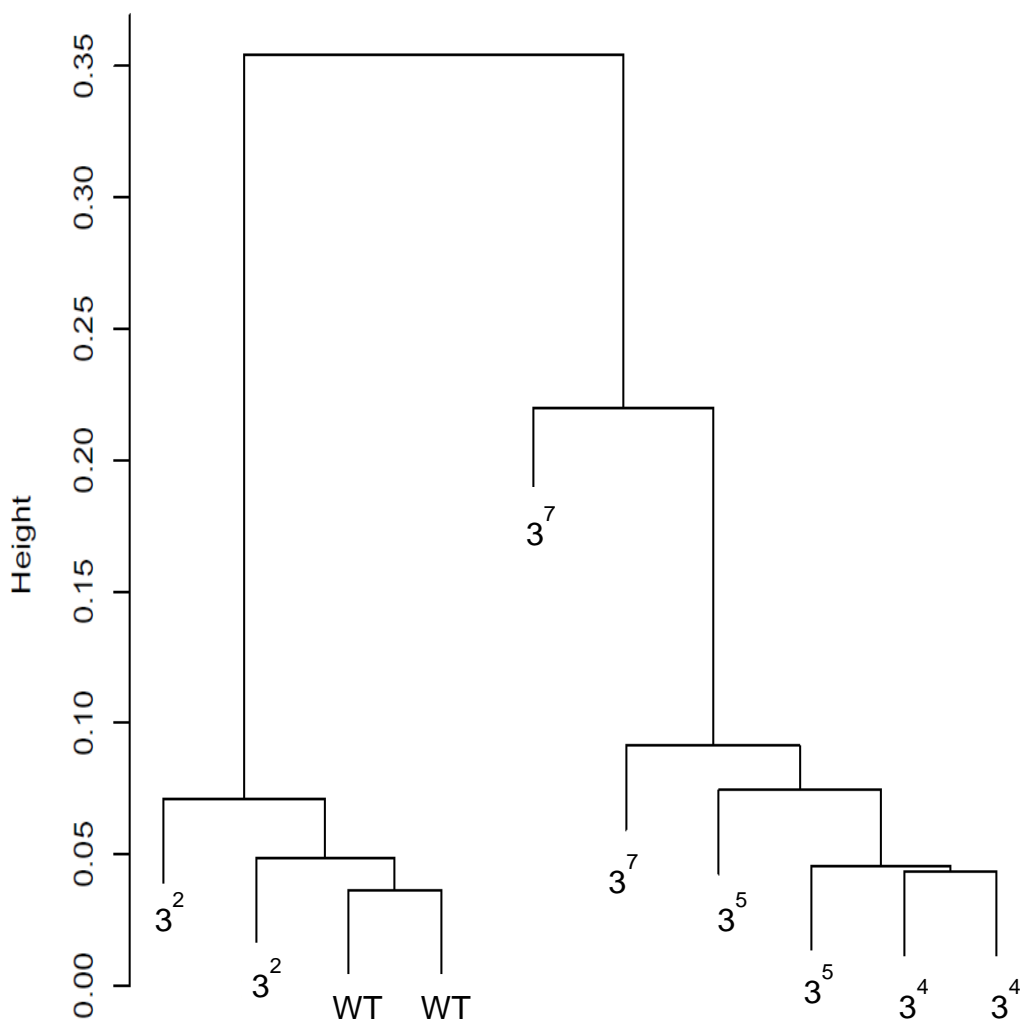


Figure 4-4. Hierarchical Clustering Analysis of SKBR-3 Resistant Sub-Lines

To show the miRNAs contributing to the phenotype classification based on drug sensitivities in various cell lines, I presented a summarized representative heat map with the relative expression of 100 miRNAs with the most variable expression within the panel of cells (Figure 4-5). The highest density and gradient of the blue colour in the panels reflect the

proportional increase in miRNA expression. The data represents the expression of both replicates (in adjacent lanes). Unmistakeably, there is a clear line of distinction separating the WT and $(IC_{50} \times 10^{-3})^2$ cell lines from the other three cell lines (Figure 4-5 arrow). The variable expression between the two groups of cells lines (sensitive vs. resistant) are clearly demarcated as four distinct blocks of miRNA expression patterns (Figure 4-5, shown in square bracket for each block on the right of the panel). The two upper blocks of miRNA represent down-regulation of expression within the more resistant cell lines. The two lower blocks of miRNA represent up-regulation of expression in the more resistant cell lines. This large number of variably expressed miRNA is a genetic feature separating the cell lines into the two distinct classes seen in Figure 4-4. Close inspection of the replicates, especially the more resistant ones found to the right of the vertical arrow, shows distinctions between the pairs. There is variability in miRNA expression among the pairs of replicates. The variability seemed to be greater the farther left you move along the heat map, which correlates with decreasing paclitaxel resistance among the cell lines. This evidence supported the evolutionary divergence seen among the cell lines in the hierarchical clustering analysis; possibly due to genetic instability found within the more resistant phenotypes as cells undergo multiple divisions.

4.6 Changes in miRNA-200c Expression within Resistant Sub-Lines

The regulatory mechanism contributing to the sudden appearance of β III tubulins remains to be elucidated. Previous reports have linked changes in expression of β III tubulin to a family of microRNAs, of which the major contributor is miR-200c (178-181). I wished to investigate this regulatory element as the mechanism in which β III was up-regulated in the panel of resistant SKBR-3 sub-lines.

The data showed resistance to paclitaxel was inversely proportional to levels of β III tubulin seen in western blot analyses. miR-200c was highly expressed in WT and $(IC_{50} \times 10^{-3})^2$ cell lines, close to 200 normalized counts in each cell line. High expression of miR-200c has been shown to contribute to the repression of the β III gene expression. Binding of miR-200c at the 3' UTR of the β III mRNA was shown as the mechanism for the translational inhibition (177-181), consistent with the observed absence of expression. The levels of miR-200c drop off drastically in $(IC_{50} \times 10^{-3})^4$ cell line to levels of near zero expression, resulting in expression of the β III tubulin gene and therefore its encoded protein as evidenced by the sudden appearance of this protein in drug resistant cell lines. I did not observe a stepwise or progressive loss of miR-200c; it was rather an acute down regulation of the gene encoding miR-200c. As a result, miR-200c expression remained near zero levels in the resistant cell lines. The mechanism by which the gene encoding miR-200c is down-regulated is unknown at this time (Figure 4-6).

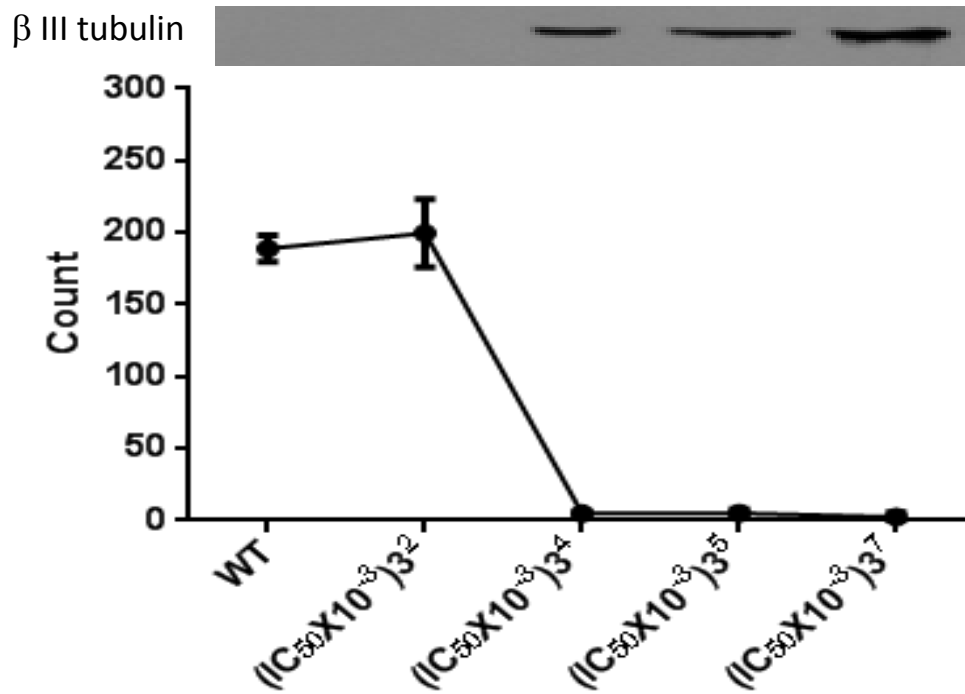


Figure 4-6. Changes in the Expression of miR-200c Shows Reciprocal Expression Patterns with β III Tubulin Protein

4.7 Changes in Expression Profile in Other microRNAs as Potential Contributors to Drug Resistance

To determine any additional mechanisms of resistance influencing IC₅₀ values observed in the resistant cell lines, expression profiles of other miRNAs were examined. Additional to miR-200c, 39 other miRNAs with variable expression were identified. Of these 39, 15 signatures were up-regulated and 24 were down-regulated (Table 4-2). Many of these miRNAs have been referenced in the literature as being deregulated in cancers. Although they have been identified as having differential expression in cancerous tissue compared to normal tissue, the functions of all 39 miRNAs are far from clear and further investigations are warranted (Figure 4-5). The exploratory analyses of differential miRNA

profiles and drug resistance support the initial premise that the resistance determinants are not restricted to a single gene regulation.

Table 4-2. Top 40 miRNA With Significantly Altered Expression (Normalized Counts)

Up Regulated	WT	(IC ₅₀ X10 ⁻³) ³ ²	(IC ₅₀ X10 ⁻³) ³ ⁴	(IC ₅₀ X10 ⁻³) ³ ⁵	(IC ₅₀ X10 ⁻³) ³ ⁷
"hsa-let-7c"	109	94	299	312	310
"hsa-miR-10a-5p"	8	10	610	538	174
"hsa-miR-10b-5p"	5	19	1702	1638	746
"hsa-miR-21-5p"	128	152	813	858	407
"hsa-miR-99a-5p"	31	37	231	248	252
"hsa-miR-143-3p"	4	37	16	228	320
"hsa-miR-199a-5p"	0	2	109	128	313
"hsa-miR-214-3p"	1	0	79	69	186
"hsa-miR-221-3p"	1	4	131	144	255
"hsa-miR-107"	17	10	48	58	52
"hsa-miR-125b-5p"	4	6	51	52	58
"hsa-miR-126-5p"	2	1	24	28	17
"hsa-miR-196a-5p"	4	4	21	25	28
"hsa-miR-218-5p"	0	0	36	37	32
"hsa-miR-320a"	20	16	43	43	80

Table 4-2 Cont.

Down Regulated	WT	$(IC_{50} \times 10^{-3})^3$	$(IC_{50} \times 10^{-3})^4$	$(IC_{50} \times 10^{-3})^5$	$(IC_{50} \times 10^{-3})^7$
"hsa-let-7e-5p"	307	289	67	86	38
"hsa-let-7f-5p"	945	830	43	57	46
"hsa-miR-148a-3p"	1667	1745	7	41	68
"hsa-let-7b-5p"	145	116	5	8	14
"hsa-miR-181a-5p"	195	176	2	10	32
"hsa-miR-186-5p"	111	123	52	53	37
"hsa-miR-200c-3p"	189	200	5	5	2
"hsa-miR-98-5p"	226	213	5	2	8
"hsa-let-7d-5p"	68	50	1	2	1
"hsa-let-7g-5p"	114	117	14	19	20
"hsa-let-7i-5p"	66	78	16	13	58
"hsa-miR-141-3p"	71	60	0	0	0
"hsa-miR-181a-3p"	43	26	0	0	1
"hsa-miR-181b-5p"	57	51	2	1	12
"hsa-miR-205-5p"	13	24	0	0	0
"hsa-miR-23a-3p"	45	28	14	22	9
"hsa-miR-27a-3p"	124	75	23	22	14
"hsa-miR-29c-3p"	61	48	15	10	2
"hsa-miR-30b-5p"	56	48	9	5	11
"hsa-miR-30d-5p"	77	61	5	13	14
"hsa-miR-335-3p"	23	19	0	0	0
"hsa-miR-335-5p"	36	21	0	0	1
"hsa-miR-33b-5p"	24	17	4	2	0
"hsa-miR-660-5p"	22	24	44	40	17
"hsa-miR-941"	55	68	8	5	11

5. Discussion and Conclusions

5.1 Amino Acids Implicated in Intermediate Binding are Not the Sole Determinants of Taxane Binding

Among women, breast cancer is the highest diagnosed cancer and second highest contributing to cancer related mortality. Progress made over the past several decades in both detection and treatment led to relatively favorable outcomes for those afflicted with this disease. However, intrinsic or developed mechanisms of resistance to treatment are a mounting clinical problem. One such problem related to taxane treatment is the much debated up regulation of β III tubulin expression. Even though up-regulation of β -III in cell line models resistant to taxanes and other drugs is fairly well established (with some exceptions(151)), such simplistic insights were inadequate to explain drug resistance in the studies utilizing clinical samples (conclusions reached from retrospective studies). To interrogate the residues relevant for intermediate binding site, four paclitaxel analogs were tested. These analogs were designed specifically to address the role of 275 and 278 residues (Figure 1-4). The conserved amino acid residues in β I and II (Ser 275), and β -III tubulin (Ala 275) and Ser 278 (β -tubulins I, II, and III) were targeted on the premise that in paclitaxel, the interacting moieties (Figure 1-3; C-7 and C-10 positions) are the critical determinants. Ala in β III tubulin was predicted not to result in favorable interaction even with the parent compound, paclitaxel (Figure 1-6) and hence the resistance to paclitaxel under conditions of β III

up regulation. In Tx-A and Tx-C, I expected even less of an interaction and very high IC₅₀ values but the experimental results suggest the opposite – i.e., that these compounds are equally effective as paclitaxel (Figure 1-6). On the contrary, the Tx-D and Tx-F were designed to promote higher interaction with Ser 278 in β I, II and III and I therefore expected IC₅₀ values approaching that of paclitaxel (Figure 1-6); again this simplistic notion was challenged. It was of interest to experimentally address these questions and gain insights on the role of the putative residues, 275 and 278, in the intermediate binding site (nano-pore) that supposedly navigates the drug molecule to the active pocket. Also of interest was to know if the designed drugs could be synthesized at all, and if these drugs would show cytotoxic activity as predicted.

In this study, extensive *in vitro* cell line work has been done to provide evidence to determine the effectiveness of each of the paclitaxel analogs. The data obtained shows an overall consistent trend. Paclitaxel was the most cytotoxic, with similar cytotoxicity found in the analog, Tx-A, indicated by a lack of statistically significant differences in IC₅₀ values between the two compounds, in a majority of cell lines tested. Data provided from experiments carried out at the University of Texas Health Science Centre San Antonio showed that there is a minor distinction between polymerization induced by paclitaxel and Tx-A both in total polymerized $\alpha\beta$ II and $\alpha\beta$ III and rate of polymerization (Figure A1-2). In majority of the cell lines tested, Tx-C was less cytotoxic than paclitaxel or

Tx-A (Tables 3-1, 3-2, 4-1). The data suggests that Tx-A did not behave as expected. Tx-C was predicted to show slight loss in cytotoxicity compared to paclitaxel, an observation supported from data from some of the tested cell lines (Figures 3-1 A and C; and 3-3). There is supportive evidence from the *in vitro* tubulin polymerization assays wherein Tx-C was marginally less effective than paclitaxel and Tx-A at promoting rate of and total polymerization (Figure A1-2). In the light of these observations, it is therefore difficult to support the premise that amino acid 275 mediates the suggested interactions with the analog, Tx-A. One drug was inconsistently behaving as predicted (Tx-C) while the other was behaving completely opposite from the original expectations (Tx-A). I have concluded that amino acid 275 is not involved in intermediate binding, as a singular amino acid. I suggest that predicting the involvement of a single amino acid interacting with a single side chain appears to be an over simplification. There are likely a number of amino acids within the proximity of 275 that contribute to the overall binding potential of the analogs. An alteration made to Tx-A (OH→H) did not contribute a strong enough change to elicit a significant drop in tubulin polymerization or cytotoxicity. Similarly, the change made to Tx-C (OH→F) may affect interaction with a number of amino acids. Additionally, the changes in cytotoxicity observed in Tx-C may be attributed to the differences in binding potential of this analog to the taxol active site. *In silico* docking analysis is yet to be attempted using

the compounds that were synthesized, which limits my ability to interpret these findings.

When I considered the results obtained from Tx-D and Tx-F, they too did not behave as predicted. Both of these drugs were significantly less effective than paclitaxel, opposite to what was predicted. In a majority of cases, Tx-F seemed to be slightly more cytotoxic; however there is little statistical evidence to support this claim. These drugs were predicted to be close, if not better at inducing tubulin polymerization and cell kill, compared to paclitaxel. The interaction of these two analogs with Ser 278 was thought to improve intermediate binding and facilitate quick movement of the drug to the active site. It is difficult based on the experiments *in vitro* or to comment on suggested interactions but the read-out in terms of cytotoxic activity suggested trends opposite to what was predicted. I considered several alternative interpretations to explain this (apparent) deviation from expectations.

(i) It is possible that these drugs behaved as predicted, and bound to Ser 278, but too strongly. Weak interactions between paclitaxel and this amino acid are the natural occurrence. The engineered changes may have resulted in stronger interactions that are unfavorable for dissociation from the intermediate binding site. Intermediate binding should be weak, exhibit higher dissociation to facilitate movement of the drug molecule to the final binding/catalytic location therefore resulting in less microtubule polymerization and cell cytotoxicity.

(ii) Even if there are favorable rates of dissociation, the side chain modifications on Tx-D and Tx-F may hinder binding to the taxol active site. As previously eluded to, *in silico* binding analysis of these drugs was not conducted at the paclitaxel binding site and it warrants further investigations. Side chain modifications at the C-10 position are bulky or due to the added length may present as a steric hindrance limiting interactions with the appropriate amino acids. Drug - ligand interactions are thought of as a model simulating an induced fit (lock and key); if the structure of the key is altered drastically, as in Tx-D and Tx-F, one would expect less than optimal binding or interactions and eventual poor catalysis at the active site.

(iii) And lastly, the binding of the analogs at the intermediate and final site do not occur since the size of the 1 pore of the B lattice may be too small for favorable movement into the intermediate binding site. With the addition of a side chain at the C-10 position designed to elongate this dimension by between 4 and 9 Å, the ability of these new compounds to enter the nano-pore may be hindered. By elongating this side chain, the number of possible conformations in which the analogs can enter the pore may be highly restrictive and therefore fewer drug molecules are gaining access to the intermediate binding site and also the active site.

One could invoke other possible interpretations for Tx-A, Tx-D, and Tx-F cytotoxic profiles in cell lines but the specific experiments performed during the course of current investigations only offer limited scope for

interpretations. Further modeling will need to be done to elucidate the binding action of each of these drugs.

5.2 The Role of β III Tubulin in Paclitaxel Analog Binding at Site 275 and 278

It was originally predicted that each of the novel analogs would be less effective in *in vitro* polymerization assays and in cell line cytotoxicity assays if β III tubulin were the predominant protein factor. It was also originally predicted that amino acid 275 being an Ala in β III tubulin, instead of Ser, would have implications on binding of these four analogs, particularly Tx-A and Tx-C, reducing their affinity for the intermediate binding site. Several cell lines were tested with paclitaxel analogs and I observed a near consistent pattern.

(i) In experiments carried out in the breast cancer cell lines, paclitaxel showed higher IC_{50} in MDA-MB-231 cells which also presented with an corresponding constitutive expression of β III tubulin. However, the presence of β III tubulin did not maintain similar influences on MDA-MB-231 cells treated with Tx-A and Tx-C. Finer interpretations for these observed IC_{50} values for paclitaxel and analogs, based on this MDA-MB-231 cell line in comparisons to other cell lines used cannot be made since different cell lines exhibited constitutive expression of β -III, and background origins of cell lines are also not constant.

(ii) Interesting observations were made on drug titration profiles for paclitaxel analogs in cell lines with \pm P-gp expression (Table 3-2). The

pairs of cell lines, MESSA and DX5, were originally used to determine if analogs are substrates for multidrug resistance. Each of these cell lines treated with paclitaxel in the presence and absence of verapamil showed no statistical difference in cytotoxicity (IC_{50} values) despite the fact that DX5 cells express P-gp (Figure 3-5A). Western blot analysis showed that MESSA cells express high levels of β III tubulin, so much so that the intrinsic resistance of each cell line was the same, each utilizing a different mechanism. This was not the case when I treated each of these cell lines with all four analogs. It seems that with the analogs, the resistance was much higher in DX5 cells than in MESSA cells. This indicates that expression of P-gp had a greater effect on resistance to the four analogs than the presence of β III, compared to paclitaxel. It should be noted that although DX5 cells expressed modest levels of P-gp, it was enough to contribute to greater resistance to the analogs as compared to the high levels of β III tubulin present within MESSA cells. The added verapamil is not the limiting factor since the resistance to drugs could be overcome in R7 cells with very high expression levels for P-gp.

(iii) Evidence provided by the polymerization experiments carried out at the University of Texas demonstrated that there is no difference in polymerization due to the presence of β III tubulin as compared to β II (Figure A1-1, 2). These findings are similar to that previously reported in the literature (187). The data showed that all five of the drugs, paclitaxel and analogs, did not differ in their ability to induce microtubule

polymerization of the immuno-affinity enriched β III tubulin fractions compared to β II protein enriched fractions. Considering the overwhelming *in vitro* and *in vivo* evidence that suggests that over expression of β III tubulin induces resistance to paclitaxel (154,156-159,188), this data is surprising. The results provided from San Antonio represent the simplest evidence of the role β III tubulin plays in resistance to the analogs. This type of data does not however represent what is occurring in a living system. Microtubules do not polymerize from a single pair of isotypes, suggesting that even *in vitro* polymerization assays carried out under these experimental conditions are to be viewed with caution.

5.3 P-gp as a Mechanism of Resistance to Paclitaxel and Analogs

P-gp over-expression is a suggested mechanism of resistance seen both *in vitro* as well as *in vivo* (138,189-193). Alterations made to moieties within the paclitaxel structure had little impact for Tx-A mediated effects whereas I noticed significant differences in IC_{50} values for Tx-D and Tx-F. Because these alterations did have an effect on cytotoxic potential of the analogs, I wished to determine if these alterations would also affect the ability of P-gp efflux pump to expel them from the cell. The data showed that indeed these analogs are substrates for P-gp (Table 3-2). This however is not surprising. P-gp does not function through co-ordination with a particular substrate or its 3 dimensional structure. This protein binds to a multitude of structurally unrelated substrates based on hydrophobicity and charge, with some preference to neutral and positively

charged structures (141,143,144). I presume that the alterations made did not alter these properties drastically. It is difficult to judge if the alterations made will influence in any way the substrate specificity. Data from MESSA/DX5 experiments suggest that these analogs showed differences in IC_{50} values between WT (MESSA) and P-gp (DX5) expressing cell lines; however the same two cell lines treated with paclitaxel showed very similar IC_{50} values (Figure 3-5A). Overall, compared to paclitaxel, the analogs were much more sensitive to the presence of P-gp, and therefore more susceptible to *MDR-1* mediated resistance.

However when I look at the data obtained for the K562/R7 cell lines, it was seen that the original observation is not maintained in these new cell lines. K562 cells treated with paclitaxel had an IC_{50} value of 6 ± 2 nM and R7 440 ± 26 nM which was ~ 83-fold increase in drug resistance. The drug with the next closest fold change is Tx-A, with a difference in IC_{50} values between K562 and R7 cells of approximately 29-fold. Each of the other drugs resulted in fold changes due to the presence of P-gp lower than that of Tx-A. This data suggested that paclitaxel is more specific for P-gp compared to the analogs (Table 3-2).

The DX5 cell line was originally developed through step-wise exposure of MESSA cells to increasing concentrations of doxorubicin (182). Similarly, R7 cells were also created through step wise passages of K562 cells with increasing concentrations of doxorubicin (183). This type of selective pressure will alter other mechanisms of resistance within the

cells, similar to the changes observed in the resistant sub-lines. These differences can be seen in the western blot analysis experiments of β tubulin isotypes within the cells. β II and III isotypes were lost in the DX5 cells compared to MESSA cells, while β IV expression was lost in R7 cells compared to K562 cells (Figure 3-4). P-gp is likely not the only mechanism by which DX5 and R7 cells resisted treatment with paclitaxel and analogs. Additionally, it can be assumed that the mechanisms employed by each of these resistant cells are not necessarily the same. Paclitaxel and doxorubicin mediated resistance mechanisms were shown to be distinct from global gene expression profiling experiments (194). Therefore, it is because of these reasons that I believe that resistance to paclitaxel and analogs are different in each pair of cell lines, and not due to differences in binding potential of the analogs to P-gp, caused by their side chain alterations.

Given the above findings and literature derived insights, I conclude that these drugs are substrates for multidrug resistance efflux pump P-gp. Since P-gp exhibits broad substrate specificities, I was unable to establish whether or not the analogs of paclitaxel showed differential specificity the efflux pump. I therefore conclude that subtle differences between paclitaxel and its analogs, if present, were not resolvable given the experimental design.

5.4 Verapamil as an Inhibitor to P-gp Mediated Drug Resistance

Verapamil, where indicated, was added at 5 $\mu\text{g/ml}$ in addition to paclitaxel or its analog to treated cells to determine if cytotoxicity in P-gp expressing DX5 and R7 cells could be decreased to a level in which their sensitivities were similar to those of their parental cell lines, MESSA and K562, respectively. The data shows that in MESSA/DX5 cell lines treated with verapamil or each of the analogs there was a decrease in IC_{50} values to about equal or less than that of MESSA cells not treated with verapamil, demonstrating the greater cytotoxicity of these compounds when used in combination with P-gp inhibitors. I also found that there was a significant decrease in the IC_{50} values of MESSA cells treated with the drugs and verapamil. This suggests that there were either favorable off-target interactions occurring or a possible synergistic effect through treatment with these two compounds and verapamil (Figure 3-5).

Similar to the MESSA/DX5 cells, the trend was also observed but to a lesser extent in K562/R7 cells. R7 cells treated with paclitaxel, Tx-A and Tx-C showed a significant decrease in IC_{50} values but not to levels of K562 cells treated without verapamil. This was likely due to the overwhelming expression of P-gp in R7 cells (Figure 3-4). The concentration of verapamil was not high enough to completely eliminate resistance due to P-gp expression. Tx-D and Tx-F in combination with verapamil treatment of R7 cells showed IC_{50} values lower than that of K562 cells treated without verapamil, again demonstrating potential off-

target interactions or increased IC_{50} values both these drugs demonstrated in combination treatments with verapamil (Figure 3-7).

One anomalous finding was that when MESSA cells were treated with paclitaxel, Tx-D or Tx-F, and K562 cells treated with Tx-A, Tx-C, Tx-D, Tx-F, each showed significant decreases in IC_{50} despite no expression of P-gp. The most significant drops in IC_{50} values in these cells lines were with Tx-D and Tx-F. There are two possible explanations for these results; the first being synergistic interaction, in which the combination of the two compounds (verapamil and analog) was more effective than treatment with a single analog. Previous reports in literature showed the synergistic activity of verapamil in combination with paclitaxel (185). However, since not all of the analogs or paclitaxel showed increase IC_{50} values in combination with verapamil, it may not be the only explanation for the observed results. Off-target interactions are likely occurring within these cells. Verapamil is a broad spectrum calcium channel blocker and has previously been shown to have a number of intercellular targets (195). Verapamil was likely inhibiting other functions of the cells. These cellular targets have been demonstrated within leukocytes and given the role verapamil plays as a pharmaceutical in diseases of the circulatory system, the effects were pronounced in K562 cells of leukocyte origin (196). And finally, since there were such large drops in IC_{50} values of sensitive cells treated with both Tx-D and Tx-F, this suggests that the structural changes made to these analogs made them strong targets for unknown

mechanisms of resistance within the cells in which verapamil is inhibiting (Figure 3-7).

5.5 Development of a Panel of SKBR-3 Paclitaxel Resistant Sub-Lines: Expression Patterns of β III Tubulin and Associated Resistance

In the interest of defining mechanisms of resistance to paclitaxel (a major chemotherapeutic treatment option for a variety of cancer types including breast, ovarian, prostate and bladder, among others), I developed a panel of resistant cell lines. The goal was to create a model that had a controlled and progressive development of drug resistance. Using these cells I wished to determine if resistance to paclitaxel could be explained in terms of β tubulin isotype expression profiles, and miRNA expression profiles in the resistant sub-lines. I successfully created eight cell lines through seven subsequent drug increases with a total drug resistance increase of ~9.2-fold (Table 4-1).

The method used resulted in changes to each drug's sensitivity, β III tubulin expression and miRNA expression, each of which were goals when setting out to create the panel of cell lines. Much of the emphasis in generating the cell lines with paclitaxel resistance was due to the overwhelming evidence from cell line models showing up-regulation of β III as a possible mechanism. If over-expression of β III were to be a predominant mechanism underlying resistance, role of particular amino acids in mediating this resistance was evaluated in the context of the proposed intermediate binding site. I am now fully aware of the diverse

mechanisms of drug resistance in that several genes/pathways are involved rather than a single entity (β tubulin or P-gp). I have therefore substantiated my study with a global expression profiles for miRNA using next generation sequencing technology platform.

I investigated altered expression of β tubulin isotype expression within the panel of cell lines as a function of increasing drug resistance, to provide mechanistic insight. Of the major isotypes investigated, only β III showed differential expression (Figure 4-2). Expression first appeared in $(IC_{50} \times 10^{-3})^{3^4}$ cells and was highly expressed in $(IC_{50} \times 10^{-3})^{3^7}$ cells. The sudden appearance of β III tubulin within the $(IC_{50} \times 10^{-3})^{3^4}$ cell line was correlated to an increase in IC_{50} values. There was an increase in IC_{50} values in $(IC_{50} \times 10^{-3})^{3^4}$ cells treated with each drug, paclitaxel and four analogs, compared to $(IC_{50} \times 10^{-3})^{3^2}$ cells. These results varied slightly when comparing the differences between WT and $(IC_{50} \times 10^{-3})^{3^4}$ cells, as Paclitaxel and Tx-A showed no statistical difference, but the remaining three analogs became less cytotoxic in the presence of β III tubulin. As β III tubulin expression continued to rise so did the IC_{50} values, suggesting that β III tubulin expression was correlated to increased drug resistance. It appears that heightened expression of β III tubulin plays a larger role in drug resistance in the model cell lines. Paclitaxel and Tx-A treated cells did not show sensitivity to the sudden appearance of β III unlike the other analogs. However, as β III expression increased and became highly expressed in $(IC_{50} \times 10^{-3})^{3^7}$, there was also an increased resistance to each

of the five compounds in the cell lines, compared to the $(IC_{50} \times 10^{-3})^2$ and WT SKBR-3 cell lines (Table 4-1). It is difficult to determine if expression of β III tubulin was the only mechanism at work within these cells to contribute to taxane resistance. Due to this uncertainty, I was interested in evaluating miRNA expression with the hope that further evidence would be provided as to how cells develop resistance to paclitaxel.

5.6 The Role of miRNA Expression in Mediating Resistance to Paclitaxel

NGS was performed on a representative panel of four cell lines from my resistant SKBR-3 sub-lines. Both WT and high passage cell controls were used to investigate changes in the miRNAome as drug resistance changed from one cell line to the next. A total of 484 miRNAs were detected from the sequencing of the cell lines, of which 40 miRNAs showed differential expression at statistically significant levels (Table 4-2). Of these 40 miRNAs, expression was up-regulated for 15 miRNAs while expression was down-regulated for 25 miRNAs. Each of these miRNAs identified coincides with at least one report in the literature, where their expression has been significantly up or down regulated. Many of the functions of these miRNAs are known while the functions of others still remain to be determined. Although each miRNA has been previously reported independently in the literature, here I have identified a novel grouping of miRNAs never before listed together as having been differentially regulated in a single cell line to mediate resistance. The

complex interplay of miRNAs to mediate resistance to taxanes is not clear and requires further investigations.

One such miRNA in which I was interested was the expression of miR-200c. Recent publications have shown that this miRNA is responsible for inhibiting translation of β III tubulin in tissue in which it should not be expressed. These reports indicate that miR-200c is lost in resistant cells which show heightened expression of β III tubulin protein (178,179,181,197). There is also evidence that in cells transfected with silencing agents such as mimics of miR-200c, β III tubulin expression is decreased and cells become sensitized to chemotherapeutic treatments (181). I wished to determine if this was the mechanism in which my sub-lines were up-regulating β III expression. In these cells, β III was absent in WT and $(IC_{50} \times 10^{-3})^2$ cells, but suddenly appeared in $(IC_{50} \times 10^{-3})^4$ cells and was expressed at the highest level in $(IC_{50} \times 10^{-3})^7$ cells. When I examined the results for miR-200c I observed that β -III and miR-200c showed reciprocal expression. MiR-200c was highly expressed in WT and $(IC_{50} \times 10^{-3})^2$ cells, but expression dropped off to levels of near zero in $(IC_{50} \times 10^{-3})^4$ cells and remained low. Expression profiles of miR-200c were exactly as predicted. At the first onset of resistance to paclitaxel (appearance of β III expression) the levels of miR-200c were completely down-regulated and remained low in all cells lines showing resistance, indicating a tight regulation of miR-200c. The pattern of regulation of miR-200c was that of a “molecular switch” which is on or off; I expected levels

of miR-200c to correlate with expression changes in β -III tubulin. The western blot analysis however showed that β III tubulin expression was even more highly expressed in the $(IC_{50} \times 10^{-3})3^7$ cell than in the two preceding ones despite the fact that miR-200c was completely down regulated at the same instance as the first appearance of β III tubulin. It may be possible that other mechanisms were operational judging from the differential expression of miRNAs (whereas I have monitored only β -tubulin isotypes) and additional experiments are needed to understand the “molecular switch”.

Thirty-nine additionally identified miRNAs potentially play a role in drug resistance; they likely also contributed to the observed morphological differences seen within the subset of cell lines from my panel used in these experiments. Some of the more notable changes, which were visually identified, were the decrease in cell size, spheroid cell shape, quicker progression to confluency in flasks and the loss of both contact inhibition and anchorage dependence. Many of these traits are indicative of cells undergoing an epithelial to mesenchymal transition (EMT). This transition is indicative of cells that are becoming more invasive and have metastatic potential, which can be elucidated by the presence of anchorage independence. Several of the miRNA such as miR-125b, - 21, - 141, and - 205 were either up or down-regulated (Table 4-2) and have previously been implicated in either promotion or inhibition of EMT, which may explain the change in cell size and shape as well as becoming

anchorage independent (198-203). Variability in cancer growth rates, migration and metastatic potential influenced by up-regulation of miRNAs such as miR – 143, - 218 (204-207) and down regulation of let – 7s, miR - 141, - 27a, - 30b, - 205 (198,203,208-213), all of which may contribute the development of quicker rates to confluency and loss of anchorage dependence seen within the cells. In addition to the regulatory mechanisms contributed by these miRNAs which can be visualized as traits of the resistant cell lines, they have also been implicated in apoptosis, angiogenesis, hypoxia and deregulation of metabolic pathways, all contributing factors to tumorigenesis and resistance within my resistant sub-lines (199,206,207,214-219).

Although many miRNAs identified have had their functions elucidated based on reports in the literature, I have also identified several miRNAs whose altered expression was opposite of those expressed in the literature. MiRNAs such as miR-181, - 98, -29c, and -27a, showed a decrease in expression within my cells but have been shown to be up-regulated in cancer within the literature (220-223). Also miR-125b and - 218 have been previously shown to be down regulated or deleted in breast cancer, but have increased expression in my drug resistant cell lines (205). Additionally, within the literature there are several miRNAs whose expression has been reported as both up and down regulated within different tissue types. MiR-335 has been shown to promote proliferation and migration in mesenchymal stem cells (224), but has also been shown

to positively regulate p53 and BRCA1 expression to lower rates of proliferation (218,219). MiR-30b has been shown to be suppressed in both bladder and lung cancer, but up-regulated in medulla blastoma tumors (211,212,225). Not surprisingly, the results that may appear in conflict with reports found within the literature may be ascribed to two or more distinct phenotypes, i.e., duality of miRNA functions in tumour development and potentially resistance to drug treatment. Several of them can be classified as both oncogenic as well as tumor suppressive. Imperfect homology between miRNAs and mRNA targets allows miRNAs to have many targets. It is because of this reason that I can only speculate the function of deregulation within the 40 miRNAs identified in this work. Deeper evaluation will be required to discover how each of these miRNAs are functioning within the cell lines utilized for profiling. When I consider all of the morphological and biochemical changes seen within the resistant sub-lines due to changes in miRNA expression, I can consider taxane drug resistance is mediated through diverse mechanisms working together to achieve the goal of continuous life.

5.7 Conclusion

At the outset, I agree with several investigators who showed an association of induction of β -III tubulin and appearance of drug resistance to paclitaxel. The studies outlined in this thesis using miRNA profiling also suggest as yet other unidentified mechanisms to explain the overall resistance to paclitaxel. MiRNA analysis provided an extensive view into

the genetic variation among the resistant cells. Altered regulation in miRNA influences processes such as; proliferation, apoptosis, angiogenesis, invasion and metastases, and the biochemical changes within the functional pathways influenced the observed changes in resistance as can be seen in my resistant SKBR-3 sub-lines. Based on this miRNA evidence and that from *in vitro* and cell line work pertaining to β III expression, it still remains unclear what the exact role is, and to what extent β III tubulin is playing as a mechanism of resistance or as a surrogate marker for a more intricate level of regulated genes. I did not observe β -III expression in DX5 and R7 cells, and yet the resistance appeared to be mediated entirely by the P-gp mechanism. I propose that perhaps β III tubulin is not the singular mechanism of resistance that was originally thought. This premise is well supported by others. In a global gene expression profiling of mRNAs in MCF-7 cells (sensitive and resistant lines for paclitaxel), the investigators identified P-gp regulation as a major mechanism but also differential expression from apoptotic and cell cycle regulation genes to also contribute to the P-gp mediated resistance (226). Another study described using ovarian cancer cell line model that P-gp is not the major mechanism of resistance to paclitaxel (194). Similarly, miR-135 was shown to contribute to paclitaxel resistance in tumor cells, both *in vitro* from cell line models and *in vivo* from mouse xenograft models (227).

Previous publications show that tubulin pools devoid of β III polymerize into microtubules at a much faster rate (154). However other work has shown that pools made up of entirely β III polymerize into microtubules just as well as those that are made up of entirely β II, similar to the data presented here (Figure A1-1,2). If β III tubulin alone forms microtubules at rates similar to that of β II, then perhaps the role it plays in resistance is only seen when it is a constituent of the overall microtubule structure, interacting with other isotypes, or with proteins involved in microtubule binding. This then suggests that β III tubulin mediated resistance potentially can encompass a number of additional variables. Since β III tubulin mediated resistance may be dependent on other factors within the cell that are interacting with β III to alter microtubule dynamics, differences among cell lines pertaining to these factors would contribute to differences seen in resistance. Therefore, western blot analysis of cells does not provide a complete picture of the entire β III mediated resistance mechanism used by each of the cell lines to be resistant to paclitaxel and the analogs. Other recent publications provide evidence that not only β III tubulin expression influence microtubule polymerization in cellular systems, but that it functions as a mechanism of resistance as a soluble heterodimer. β III tubulin containing heterodimers may provide protection to microtubules and mitochondria from free radicals species induced damage (228,229). Given the abundance of free radical species within cancerous systems, and the numerous reports implicating β III tubulin in

drug resistance, it is safe to include β III tubulin among the resistance mechanisms. Given the number of genetic and epigenetic changes that are likely occurring in resistant cell lines or in recurrent breast cancer, it is possible that β III tubulin does induce resistance, but to assume this as the only mechanisms is simplistic.

Initially, I was trying to implicate specific amino acid residues in the intermediate binding of taxanes, and how variations in those residues play a role in β III mediated taxane resistance. The evidence provided suggests that resistance is not a single mechanism at work preventing the cytotoxic potential of a drug. Through the extensive work using cell line cytotoxicity assays and the development of a model system showing changes in drug resistance, I have provided evidence of a multitude of mechanisms at work within the cell which eventually confer resistance to taxanes.

6. Future work

The data provided in this thesis is foundational work providing insight into the mechanisms of taxane drug resistance. I provided evidence that refuted the original hypothesis pertaining to two implicated amino acids involved in binding and their role in β III tubulin mediated resistance. I also developed a model system to assess the roles of mechanisms of resistances and showed that β III tubulin and a number of miRNAs are differentially expressed. However, the information gathered during this work seems to have only been the beginning, raising more questions in the process of answering the original ones I had set out to answer at the beginning of this work. Throughout this chapter I will identify several thought experiments that have been generated and the subsequent approaches that could be utilized to provide the answers.

6.1 Analog *In Silico* Binding Analysis and *In Vitro* Subcellular Localization Provides Insight into Actual Functions

Preliminary *in silico* docking analysis was performed using paclitaxel to identify the two amino acid involved in binding. Using these amino acids as a starting point the four analogs of paclitaxel were developed. More work is needed to provide evidence of the binding energies for each of these four analogs with the target protein, tubulin. This is very important and may shed some light on the *in vitro* experiments; the results that were for the most part, excluding Tx-C, were the exact opposite of what was originally hypothesized.

Mapping the subcellular localization of each of these drugs will provide the most information on sites of accumulation within the cell. Subcellular localization of taxane drugs can be determined using a technology previously used to show lateral movement of paclitaxel through microtubule pores to the active site (230). Fluorescence conjugates of paclitaxel are available through Life Technologies Corporation. Using this methodology it may be possible to make fluorescence conjugates of the paclitaxel analogs. These conjugates can be visualized for localization in the cell using fluorescent confocal microscopy (231,232). This method can be used to determine several factors influencing the analogs ability to induce apoptosis. Intracellular vs. extracellular localization, determine the ability of these analogs to gain access to the cell. Similarly, I can determine the localization of the analogs to P-gp within the plasma membrane of the cell, in which I can determine any potential differences in substrate specificity to this efflux pump in competitive binding assays. This assay can be used to determine any off-target interactions occurring at subcellular localization within a cell. In addition to cell line work, *in vitro* analysis can be done using fluorescent analogs, wherein the ability of each analog to gain access to the taxol binding site can be determined using polymerized microtubules and photo bleaching (230). Time lapse experiments can be conducted to determine how long it takes each of the drugs to gain access to the lumen compared to paclitaxel. The evidence provided from this experiment will directly answer my questions related to

Tx-D and Tx-F and whether they lose potency because of intermediate binding or taxol site binding.

Using all the data, future manipulations can be made in which improved cytotoxicity is achieved through novel design of taxane analogs.

6.2 β Tubulin Mutagenesis and Its Role in Taxane Drug Resistance

One of the original aims of this work was to perform polymerization assays using site specific mutant β tubulin. If successful in demonstrating the interactions of taxol analogs with the amino acid residues implicated in binding, mutation of these residues and demonstrating a diminished binding would have been the unambiguous way to support the hypothesis on the role of the amino acids in the intermediate binding site. Reports in the literature have shown the effects of point mutations within cell lines (233,234). However, I believe that other confounding factors within a cell may also be contributing to taxane resistance. By removing the other variables within the cells through the *in vitro* polymerization assays, I would implicate each mutation and/or a combination of mutations in taxane resistance. However, tubulin molecules cannot fold into a native conformation naturally and a full repertoire of chaperons and cofactors are needed to make the reconstitution of the polymerization assay proved to be a difficult undertaking. I nevertheless began with the baby steps and asked the question if recombinant tubulin expression in itself is a feasible option as this was never attempted before by any in this area of work. Generating a recombinant DNA construct with defined mutations in tubulin

genes in itself did not appear as a hindrance, but to anticipate the recombinant tubulin expressed in *E.coli* system to remain in solution or not and if the reconstituted proteins show activity (dimerization with a subunits) in the absence of cofactors or post translational modifications needed to be ascertained through experiments. To make the long story short, I did succeed in the expression of recombinant protein in bacterial system; bulk of the tubulin protein ended up in the inclusion bodies, as expected for the recombinant eukaryotic proteins. I managed to extract tubulin proteins from inclusion bodies (at least partially) and showed some progress in purification in Ni-affinity columns. Refolding of partially purified tubulin fractions were attempted. Reconstitution assays for tubulin polymerization were not successful due to spontaneous precipitation/agglutination of proteins in the assay even with single subunits of the heterodimer or in the absence of GTP.

The use of prokaryotic systems is limiting for eukaryotic tubulin expression, in that the proteins required for proper folding, heterodimer formation, and post translational modifications are not present in these systems. Recent reports in the literature provided evidence for eukaryotic expression of site directed mutants of β I tubulin proteins using cDNA transfection (234) in mammalian expression systems. Ultracentrifugation can be used to separate tubulin pools from cells lines (235-237). These tubulin pool fractions can be purified using Ni-NTA for His tagged recombinant proteins, where native conformations have not been lost.

Purification of recombinant tubulin from within a eukaryotic system would provide native protein that can then be used to investigate site specific mutagenesis of β tubulin and taxane resistance. This type of methodological optimization is a large undertaking and would possibly be the focus of an entire Master's thesis or a large portion of Ph.D thesis.

6.3 Quantitatively Determining Ratios of β Tubulin Isozyme Found within Resistant Cell Lines

Following the experiments in which I determined the cytotoxicity of paclitaxel analogs, I wished to determine the absolute expression of each β tubulin isozyme in the cell lines. By doing this I hoped to profile patterns of tubulin expression within each cell line to determine if these ratios were contributing to the unexpected cytotoxic results. Using these ratios, cytotoxicity curves could be adjusted for cell type specific differences to potentially offer a more consistent picture for each analog. Western blot analysis was used to determine differences in expression. Using consistently loaded protein, intensity of each signal provides a function of the amount each β tubulin isozyme to construct the ratios for each cell line. I did not take into account the vast differences in which each primary antibody would bind to their protein in my original assumptions. This resulted in different exposure times ranging from 5s to 1 hour, in which images for each isozyme could no longer be used to compare total expression within the cells for quantitatively determining the expression of each isozyme.

Q-RT-PCR is a method that can be used to determine the absolute levels of mRNA for each isotype (167). This method has the advantage over western blot of being able to detect the levels of each different isotype as well as the splice variants IIa/IIb and IVa/IVb, using the appropriate primers (145). Although determined transcript levels would provide a quantitative measure of differential β tubulin expression, mRNA levels are not always a direct indicator of protein expression. I am therefore interested in using proteomic technology to determine quantitative levels of β tubulin protein. Using stable isotope labeling and liquid chromatography-mass spectrometry analysis it may be possible to determine levels of β tubulin isotypes with a protein sample as a function of total protein (238-240) in WT and resistant cell lines I developed. Using this methodology may be ambitious as it is currently difficult to determine differences in splice variants and peptides with very similar sequences. Given the homology of β tubulin proteins, quantification of isotype mRNA may be as far as I can take this work (241).

6.4 Effects of β III Tubulin Expression on Drug Resistance in the Resistant SKBR-3 Sub-Lines

It would be of great interest to determine the extent of the role played by β III tubulin within each of the biological systems to reflect on taxane resistance. I successfully showed that β III tubulin is up-regulated in the $(IC_{50} \times 10^{-3})^{37}$ cells, which were ~ 9.2 -fold more resistant to paclitaxel than the parental SKBR-3 cells. Unfortunately, through miRNA analysis I

also demonstrated that there are many miRNAs which are differentially expressed potentially conferring resistance in addition to β III. Further analysis can be done which provides stronger indications of the role of β III tubulin. This can be achieved through two methods. First, $(IC_{50} \times 10^{-3})^{37}$ cells can have their β III tubulin expression knocked down, either through siRNA (242-245) or miRNA 200c mimics (181,186). By knocking out only β III, I can determine to what extent β III contributes to the 9.2-fold increase in resistance. Similarly, this can be done with MDA-MB-231 and MESSA cell lines to determine if differences in cytotoxicity to paclitaxel and analogs can be achieved when β III tubulin is not present.

Conversely, I can implicate β III tubulin expression in resistance within SKBR-3 cells without influences from other mechanisms of resistance, such as differential miRNA expression. This can be achieved by transfecting my cells with β III tubulin cDNA. As previously mentioned in section 6.2, cDNA transfection of both mutant and WT β tubulin is effective at over-expression of each isotype (234,246,247). Although this has been done previously to show the correlation between β III tubulin expression and resistance, as it pertains to this work, I will be able to show how over-expression of β III correlates to the 9.2-fold increase in drug resistance within my SKBR-3 cells. By both inhibiting and promoting the expression of β III tubulin within the cells and performing cytotoxicity experiments with the aim to compare these new cell kill potentials with the 9.2-fold increase

in drug resistance seen in the resistant cells, I can better understand the magnitude in which β III contributes to resistance.

6.5 Understanding the Roles of 40 Differentially Expressed miRNAs within the Resistant Cell Lines

NGS analysis indicated that my resistant cell lines exhibit differential expression of 40 miRNAs. I have referenced the literature for a majority of these miRNAs to better understand what their molecular targets are within the cells. A survey of the literature has indicated that many of these miRNAs have target mRNA in pathways involved in proliferation, apoptosis, angiogenesis, invasion and metastases. Reports on several of these miRNAs in the literature seem contradictory as well. It is suggested that there is a duality in function of miRNAs, meaning that several of them function as both tumor suppressors and oncogenes, perhaps depending on tumor conditions as well as tumor types. I wish to elucidate the biochemical function of each of the miRNAs identified in this study. To do this, gene ontology can be performed to classify the targets for each of the miRNAs to discover the cellular component, molecular functions and biological processes of each of the differentially expressed miRNA targets (mRNAs) within my system. *In silico* binding predictions can also be done to identify putative mRNA targets based on sequence homology for the miRNAs with no known targets or functions (248). These attempts will provide an initial perspective on the transcripts that these miRNAs are targeting within the cells. Additionally, knock in or out biochemical experiments can be conducted, *in vitro* work can provide

experimental evidence for *in silico* work, elucidating the function of each identified miRNA.

References

- (1) Hanahan D, Weinberg RA. The hallmarks of cancer. *Cell* 2000 Jan 7;100(1):57-70.
- (2) Hanahan D, Weinberg RA. Hallmarks of cancer: the next generation. *Cell* 2011 Mar 4;144(5):646-674.
- (3) Negrini S, Gorgoulis VG, Halazonetis TD. Genomic instability--an evolving hallmark of cancer. *Nat Rev Mol Cell Biol* 2010 Mar;11(3):220-228.
- (4) Kinzler KW, Vogelstein B. Cancer-susceptibility genes. Gatekeepers and caretakers. *Nature* 1997 Apr 24;386(6627):761, 763.
- (5) Lane DP. Cancer. p53, guardian of the genome. *Nature* 1992 Jul 2;358(6381):15-16.
- (6) Dvorak HF. Tumors: wounds that do not heal. Similarities between tumor stroma generation and wound healing. *N Engl J Med* 1986 Dec 25;315(26):1650-1659.
- (7) DeNardo DG, Andreu P, Coussens LM. Interactions between lymphocytes and myeloid cells regulate pro- versus anti-tumor immunity. *Cancer Metastasis Rev* 2010 Jun;29(2):309-316.
- (8) Grivennikov SI, Greten FR, Karin M. Immunity, inflammation, and cancer. *Cell* 2010 Mar 19;140(6):883-899.

- (9) Colotta F, Allavena P, Sica A, Garlanda C, Mantovani A. Cancer-related inflammation, the seventh hallmark of cancer: links to genetic instability. *Carcinogenesis* 2009 Jul;30(7):1073-1081.
- (10) Cheng N, Chytil A, Shyr Y, Joly A, Moses HL. Transforming growth factor-beta signaling-deficient fibroblasts enhance hepatocyte growth factor signaling in mammary carcinoma cells to promote scattering and invasion. *Mol Cancer Res* 2008 Oct;6(10):1521-1533.
- (11) Bhowmick NA, Neilson EG, Moses HL. Stromal fibroblasts in cancer initiation and progression. *Nature* 2004 Nov 18;432(7015):332-337.
- (12) Yuan TL, Cantley LC. PI3K pathway alterations in cancer: variations on a theme. *Oncogene* 2008 Sep 18;27(41):5497-5510.
- (13) O'Reilly KE, Rojo F, She QB, Solit D, Mills GB, Smith D, et al. mTOR inhibition induces upstream receptor tyrosine kinase signaling and activates Akt. *Cancer Res* 2006 Feb 1;66(3):1500-1508.
- (14) Lipinski MM, Jacks T. The retinoblastoma gene family in differentiation and development. *Oncogene* 1999 Dec 20;18(55):7873-7882.
- (15) Ghebranious N, Donehower LA. Mouse models in tumor suppression. *Oncogene* 1998 Dec 24;17(25):3385-3400.
- (16) Okada T, Lopez-Lago M, Giancotti FG. Merlin/NF-2 mediates contact inhibition of growth by suppressing recruitment of Rac to the plasma membrane. *J Cell Biol* 2005 Oct 24;171(2):361-371.

- (17) Bierie B, Moses HL. Tumour microenvironment: TGFbeta: the molecular Jekyll and Hyde of cancer. *Nat Rev Cancer* 2006 Jul;6(7):506-520.
- (18) Craik AC, Veldhoen RA, Czernick M, Buckland TW, Kyselytzia K, Ghosh S, et al. The BH3-only protein Bad confers breast cancer taxane sensitivity through a nonapoptotic mechanism. *Oncogene* 2010 Sep 30;29(39):5381-5391.
- (19) Adams JM, Cory S. Bcl-2-regulated apoptosis: mechanism and therapeutic potential. *Curr Opin Immunol* 2007 Oct;19(5):488-496.
- (20) Lowe SW, Cepero E, Evan G. Intrinsic tumour suppression. *Nature* 2004 Nov 18;432(7015):307-315.
- (21) Junttila MR, Evan GI. p53--a Jack of all trades but master of none. *Nat Rev Cancer* 2009 Nov;9(11):821-829.
- (22) White E, DiPaola RS. The double-edged sword of autophagy modulation in cancer. *Clin Cancer Res* 2009 Sep 1;15(17):5308-5316.
- (23) Apel A, Zentgraf H, Buchler MW, Herr I. Autophagy-A double-edged sword in oncology. *Int J Cancer* 2009 Sep 1;125(5):991-995.
- (24) Toussaint O, Remale J, Dierick JF, Pascal T, Fripiat C, Zdanov S, et al. From the Hayflick mosaic to the mosaics of ageing. Role of stress-induced premature senescence in human ageing. *Int J Biochem Cell Biol* 2002 Nov;34(11):1415-1429.
- (25) Shay JW, Wright WE. Hayflick, his limit, and cellular ageing. *Nat Rev Mol Cell Biol* 2000 Oct;1(1):72-76.

- (26) Wong KK, Chang S, Weiler SR, Ganesan S, Chaudhuri J, Zhu C, et al. Telomere dysfunction impairs DNA repair and enhances sensitivity to ionizing radiation. *Nat Genet* 2000 Sep;26(1):85-88.
- (27) Hansel DE, Meeker AK, Hicks J, De Marzo AM, Lillemoe KD, Schulick R, et al. Telomere length variation in biliary tract metaplasia, dysplasia, and carcinoma. *Mod Pathol* 2006 Jun;19(6):772-779.
- (28) Artandi SE, DePinho RA. Mice without telomerase: what can they teach us about human cancer? *Nat Med* 2000 Aug;6(8):852-855.
- (29) Masutomi K, Possemato R, Wong JM, Currier JL, Tothova Z, Manola JB, et al. The telomerase reverse transcriptase regulates chromatin state and DNA damage responses. *Proc Natl Acad Sci U S A* 2005 Jun 7;102(23):8222-8227.
- (30) Maida Y, Yasukawa M, Furuuchi M, Lassmann T, Possemato R, Okamoto N, et al. An RNA-dependent RNA polymerase formed by TERT and the RMRP RNA. *Nature* 2009 Sep 10;461(7261):230-235.
- (31) Bergers G, Benjamin LE. Tumorigenesis and the angiogenic switch. *Nat Rev Cancer* 2003 Jun;3(6):401-410.
- (32) Mac Gabhann F, Popel AS. Systems biology of vascular endothelial growth factors. *Microcirculation* 2008 Nov;15(8):715-738.
- (33) Carmeliet P. VEGF as a key mediator of angiogenesis in cancer. *Oncology* 2005;69 Suppl 3:4-10.

- (34) Zee YK, O'Connor JP, Parker GJ, Jackson A, Clamp AR, Taylor MB, et al. Imaging angiogenesis of genitourinary tumors. *Nat Rev Urol* 2010 Feb;7(2):69-82.
- (35) Turner HE, Harris AL, Melmed S, Wass JA. Angiogenesis in endocrine tumors. *Endocr Rev* 2003 Oct;24(5):600-632.
- (36) Cavallaro U, Christofori G. Cell adhesion and signalling by cadherins and Ig-CAMs in cancer. *Nat Rev Cancer* 2004 Feb;4(2):118-132.
- (37) Crnic I, Strittmatter K, Cavallaro U, Kopfstein L, Jussila L, Alitalo K, et al. Loss of neural cell adhesion molecule induces tumor metastasis by up-regulating lymphangiogenesis. *Cancer Res* 2004 Dec 1;64(23):8630-8638.
- (38) Micalizzi DS, Farabaugh SM, Ford HL. Epithelial-mesenchymal transition in cancer: parallels between normal development and tumor progression. *J Mammary Gland Biol Neoplasia* 2010 Jun;15(2):117-134.
- (39) Taube JH, Herschkowitz JI, Komurov K, Zhou AY, Gupta S, Yang J, et al. Core epithelial-to-mesenchymal transition interactome gene-expression signature is associated with claudin-low and metaplastic breast cancer subtypes. *Proc Natl Acad Sci U S A* 2010 Aug 31;107(35):15449-15454.
- (40) Wellner U, Schubert J, Burk UC, Schmalhofer O, Zhu F, Sonntag A, et al. The EMT-activator ZEB1 promotes tumorigenicity by repressing stemness-inhibiting microRNAs. *Nat Cell Biol* 2009 Dec;11(12):1487-1495.
- (41) Kalluri R, Zeisberg M. Fibroblasts in cancer. *Nat Rev Cancer* 2006 May;6(5):392-401.

- (42) Karnoub AE, Dash AB, Vo AP, Sullivan A, Brooks MW, Bell GW, et al. Mesenchymal stem cells within tumour stroma promote breast cancer metastasis. *Nature* 2007 Oct 4;449(7162):557-563.
- (43) Hugo H, Ackland ML, Blick T, Lawrence MG, Clements JA, Williams ED, et al. Epithelial--mesenchymal and mesenchymal--epithelial transitions in carcinoma progression. *J Cell Physiol* 2007 Nov;213(2):374-383.
- (44) Folkman J. Role of angiogenesis in tumor growth and metastasis. *Semin Oncol* 2002 Dec;29(6 Suppl 16):15-18.
- (45) Gupta GP, Minn AJ, Kang Y, Siegel PM, Serganova I, Cordon-Cardo C, et al. Identifying site-specific metastasis genes and functions. *Cold Spring Harb Symp Quant Biol* 2005;70:149-158.
- (46) Vajdic CM, van Leeuwen MT. Cancer incidence and risk factors after solid organ transplantation. *Int J Cancer* 2009 Oct 15;125(8):1747-1754.
- (47) Teng MW, Swann JB, Koebel CM, Schreiber RD, Smyth MJ. Immune-mediated dormancy: an equilibrium with cancer. *J Leukoc Biol* 2008 Oct;84(4):988-993.
- (48) Kim R, Emi M, Tanabe K. Cancer immunoediting from immune surveillance to immune escape. *Immunology* 2007 May;121(1):1-14.
- (49) Smyth MJ, Dunn GP, Schreiber RD. Cancer immunosurveillance and immunoediting: the roles of immunity in suppressing tumor development and shaping tumor immunogenicity. *Adv Immunol* 2006;90:1-50.

- (50) WARBURG O. On respiratory impairment in cancer cells. Science 1956 Aug 10;124(3215):269-270.
- (51) WARBURG O. On the origin of cancer cells. Science 1956 Feb 24;123(3191):309-314.
- (52) DeBerardinis RJ, Lum JJ, Hatzivassiliou G, Thompson CB. The biology of cancer: metabolic reprogramming fuels cell growth and proliferation. Cell Metab 2008 Jan;7(1):11-20.
- (53) POTTER VR. The biochemical approach to the cancer problem. Fed Proc 1958 Jul;17(2):691-697.
- (54) Vander Heiden MG, Cantley LC, Thompson CB. Understanding the Warburg effect: the metabolic requirements of cell proliferation. Science 2009 May 22;324(5930):1029-1033.
- (55) Colfry AJ,3rd. Miscellaneous syndromes and their management: occult breast cancer, breast cancer in pregnancy, male breast cancer, surgery in stage IV disease. Surg Clin North Am 2013 Apr;93(2):519-531.
- (56) Langlands FE, Horgan K, Dodwell DD, Smith L. Breast cancer subtypes: response to radiotherapy and potential radiosensitisation. Br J Radiol 2013 Mar;86(1023):20120601.
- (57) Mitchison T, Kirschner M. Dynamic instability of microtubule growth. Nature 1984 Nov 15-21;312(5991):237-242.

- (58) Saji S. Evolving Approaches to Metastatic Breast Cancer Patients Pre-treated with Anthracycline and Taxane. *BioDrugs* 2013 May 9.
- (59) Horio T, Hotani H. Visualization of the dynamic instability of individual microtubules by dark-field microscopy. *Nature* 1986 Jun 5-11;321(6070):605-607.
- (60) Tria Tirona M. Breast cancer screening update. *Am Fam Physician* 2013 Feb 15;87(4):274-278.
- (61) Fauzee NJ. Taxanes: promising anti-cancer drugs. *Asian Pac J Cancer Prev* 2011;12(4):837-851.
- (62) Parsyan A, Alqahtani A, Mesurolle B, Meterissian S. Impact of Preoperative Breast MRI on Surgical Decision Making and Clinical Outcomes: A Systematic Review. *World J Surg* 2013 May 10.
- (63) Jones T, Neboori H, Wu H, Yang Q, Haffty BG, Evans S, et al. Are Breast Cancer Subtypes Prognostic for Nodal Involvement and Associated with Clinicopathologic Features at Presentation in Early-Stage Breast Cancer? *Ann Surg Oncol* 2013 May 10.
- (64) Hernandez-Aya LF, Gonzalez-Angulo AM. Adjuvant systemic therapies in breast cancer. *Surg Clin North Am* 2013 Apr;93(2):473-491.
- (65) Chacon RD, Costanzo MV. Triple-negative breast cancer. *Breast Cancer Res* 2010;12 Suppl 2:S3.

(66) Sorlie T, Perou CM, Tibshirani R, Aas T, Geisler S, Johnsen H, et al. Gene expression patterns of breast carcinomas distinguish tumor subclasses with clinical implications. *Proc Natl Acad Sci U S A* 2001 Sep 11;98(19):10869-10874.

(67) Sorlie T, Tibshirani R, Parker J, Hastie T, Marron JS, Nobel A, et al. Repeated observation of breast tumor subtypes in independent gene expression data sets. *Proc Natl Acad Sci U S A* 2003 Jul 8;100(14):8418-8423.

(68) Dent R, Trudeau M, Pritchard KI, Hanna WM, Kahn HK, Sawka CA, et al. Triple-negative breast cancer: clinical features and patterns of recurrence. *Clin Cancer Res* 2007 Aug 1;13(15 Pt 1):4429-4434.

(69) Sotiriou C, Pusztai L. Gene-expression signatures in breast cancer. *N Engl J Med* 2009 Feb 19;360(8):790-800.

(70) Wang Y, Yin Q, Yu Q, Zhang J, Liu Z, Wang S, et al. A retrospective study of breast cancer subtypes: the risk of relapse and the relations with treatments. *Breast Cancer Res Treat* 2011 Nov;130(2):489-498.

(71) Kassam F, Enright K, Dent R, Dranitsaris G, Myers J, Flynn C, et al. Survival outcomes for patients with metastatic triple-negative breast cancer: implications for clinical practice and trial design. *Clin Breast Cancer* 2009 Feb;9(1):29-33.

(72) Farmer H, McCabe N, Lord CJ, Tutt AN, Johnson DA, Richardson TB, et al. Targeting the DNA repair defect in BRCA mutant cells as a therapeutic strategy. *Nature* 2005 Apr 14;434(7035):917-921.

(73) Bhattacharyya A, Ear US, Koller BH, Weichselbaum RR, Bishop DK. The breast cancer susceptibility gene BRCA1 is required for subnuclear assembly of

Rad51 and survival following treatment with the DNA cross-linking agent cisplatin. *J Biol Chem* 2000 Aug 4;275(31):23899-23903.

(74) Turner N, Tutt A, Ashworth A. Hallmarks of 'BRCAness' in sporadic cancers. *Nat Rev Cancer* 2004 Oct;4(10):814-819.

(75) Shah SP, Roth A, Goya R, Oloumi A, Ha G, Zhao Y, et al. The clonal and mutational evolution spectrum of primary triple-negative breast cancers. *Nature* 2012 Apr 4;486(7403):395-399.

(76) Curtis C, Shah SP, Chin SF, Turashvili G, Rueda OM, Dunning MJ, et al. The genomic and transcriptomic architecture of 2,000 breast tumours reveals novel subgroups. *Nature* 2012 Apr 18;486(7403):346-352.

(77) Bankfalvi A, Simon R, Brandt B, Burger H, Vollmer I, Dockhorn-Dworniczak B, et al. Comparative methodological analysis of erbB-2/HER-2 gene dosage, chromosomal copy number and protein overexpression in breast carcinoma tissues for diagnostic use. *Histopathology* 2000 Nov;37(5):411-419.

(78) Wolff AC, Hammond ME, Schwartz JN, Hagerty KL, Allred DC, Cote RJ, et al. American Society of Clinical Oncology/College of American Pathologists guideline recommendations for human epidermal growth factor receptor 2 testing in breast cancer. *Arch Pathol Lab Med* 2007;131(1):18-43.

(79) Romond EH, Perez EA, Bryant J, Suman VJ, Geyer CE, Jr, Davidson NE, et al. Trastuzumab plus adjuvant chemotherapy for operable HER2-positive breast cancer. *N Engl J Med* 2005 Oct 20;353(16):1673-1684.

(80) Perez EA, Romond EH, Suman VJ, Jeong JH, Davidson NE, Geyer CE, Jr, et al. Four-year follow-up of trastuzumab plus adjuvant chemotherapy for operable human epidermal growth factor receptor 2-positive breast cancer: joint analysis of data from NCCTG N9831 and NSABP B-31. *J Clin Oncol* 2011 Sep 1;29(25):3366-3373.

(81) Gianni L, Dafni U, Gelber RD, Azambuja E, Muehlbauer S, Goldhirsch A, et al. Treatment with trastuzumab for 1 year after adjuvant chemotherapy in patients with HER2-positive early breast cancer: a 4-year follow-up of a randomised controlled trial. *Lancet Oncol* 2011 Mar;12(3):236-244.

(82) Scholzen T, Gerdes J. The Ki-67 protein: from the known and the unknown. *J Cell Physiol* 2000 Mar;182(3):311-322.

(83) Kontzoglou K, Palla V, Karaolani G, Karaiskos I, Alexiou I, Pateras I, et al. Correlation between Ki67 and breast cancer prognosis. *Oncology* 2013;84(4):219-225.

(84) Cheang MC, Voduc D, Bajdik C, Leung S, McKinney S, Chia SK, et al. Basal-like breast cancer defined by five biomarkers has superior prognostic value than triple-negative phenotype. *Clin Cancer Res* 2008 Mar 1;14(5):1368-1376.

(85) Cheang MC, Chia SK, Voduc D, Gao D, Leung S, Snider J, et al. Ki67 index, HER2 status, and prognosis of patients with luminal B breast cancer. *J Natl Cancer Inst* 2009 May 20;101(10):736-750.

(86) Colleoni M, Cole BF, Viale G, Regan MM, Price KN, Maiorano E, et al. Classical cyclophosphamide, methotrexate, and fluorouracil chemotherapy is

more effective in triple-negative, node-negative breast cancer: results from two randomized trials of adjuvant chemoendocrine therapy for node-negative breast cancer. *J Clin Oncol* 2010 Jun 20;28(18):2966-2973.

(87) Guiu S, Michiels S, Andre F, Cortes J, Denkert C, Di Leo A, et al. Molecular subclasses of breast cancer: how do we define them? The IMPAKT 2012 Working Group Statement. *Ann Oncol* 2012 Dec;23(12):2997-3006.

(88) Hu Z, Fan C, Oh DS, Marron JS, He X, Qaqish BF, et al. The molecular portraits of breast tumors are conserved across microarray platforms. *BMC Genomics* 2006 Apr 27;7:96.

(89) Perou CM, Jeffrey SS, van de Rijn M, Rees CA, Eisen MB, Ross DT, et al. Distinctive gene expression patterns in human mammary epithelial cells and breast cancers. *Proc Natl Acad Sci U S A* 1999 Aug 3;96(16):9212-9217.

(90) Eroles P, Bosch A, Perez-Fidalgo JA, Lluch A. Molecular biology in breast cancer: intrinsic subtypes and signaling pathways. *Cancer Treat Rev* 2012 Oct;38(6):698-707.

(91) Verdier-Pinard P, Pasquier E, Xiao H, Burd B, Villard C, Lafitte D, et al. Tubulin proteomics: towards breaking the code. *Anal Biochem* 2009 Jan 15;384(2):197-206.

(92) Wade RH. On and around microtubules: an overview. *Mol Biotechnol* 2009 Oct;43(2):177-191.

(93) Gardner M., Zanic M., Howard J. Microtubule catastrophe and rescue *Current opinion in cell biology* 2013;25:14-22.

- (94) Campos SM, Dizon DS. Antimitotic inhibitors. *Hematol Oncol Clin North Am* 2012 Jun;26(3):607-28, viii-ix.
- (95) Nogales E, Whittaker M, Milligan RA, Downing KH. High-resolution model of the microtubule. *Cell* 1999 Jan 8;96(1):79-88.
- (96) Dutcher SK. The tubulin fraternity: alpha to eta. *Curr Opin Cell Biol* 2001 Feb;13(1):49-54.
- (97) Lopez-Fanarraga M, Avila J, Guasch A, Coll M, Zabala JC. Review: postchaperonin tubulin folding cofactors and their role in microtubule dynamics. *J Struct Biol* 2001 Aug;135(2):219-229.
- (98) Friesen DE, Barakat KH, Semenchenko V, Perez-Pineiro R, Fenske BW, Mane J, et al. Discovery of small molecule inhibitors that interact with gamma-tubulin. *Chem Biol Drug Des* 2012 May;79(5):639-652.
- (99) Keating TJ, Borisy GG. Immunostuctural evidence for the template mechanism of microtubule nucleation. *Nat Cell Biol* 2000 Jun;2(6):352-357.
- (100) Joshi HC, Palacios MJ, McNamara L, Cleveland DW. Gamma-tubulin is a centrosomal protein required for cell cycle-dependent microtubule nucleation. *Nature* 1992 Mar 5;356(6364):80-83.
- (101) Moritz M, Agard DA. Gamma-tubulin complexes and microtubule nucleation. *Curr Opin Struct Biol* 2001 Apr;11(2):174-181.
- (102) Wiese C, Zheng Y. A new function for the gamma-tubulin ring complex as a microtubule minus-end cap. *Nat Cell Biol* 2000 Jun;2(6):358-364.

- (103) Lewis SA, Tian G, Cowan NJ. The alpha- and beta-tubulin folding pathways. *Trends Cell Biol* 1997 Dec;7(12):479-484.
- (104) Tian G, Vainberg IE, Tap WD, Lewis SA, Cowan NJ. Specificity in chaperonin-mediated protein folding. *Nature* 1995 May 18;375(6528):250-253.
- (105) Tian G, Vainberg IE, Tap WD, Lewis SA, Cowan NJ. Quasi-native chaperonin-bound intermediates in facilitated protein folding. *J Biol Chem* 1995 Oct 13;270(41):23910-23913.
- (106) Nogales E, Wolf SG, Downing KH. Structure of the alpha beta tubulin dimer by electron crystallography. *Nature* 1998 Jan 8;391(6663):199-203.
- (107) Tian G, Lewis SA, Feierbach B, Stearns T, Rommelaere H, Ampe C, et al. Tubulin subunits exist in an activated conformational state generated and maintained by protein cofactors. *J Cell Biol* 1997 Aug 25;138(4):821-832.
- (108) Kortazar D, Fanarraga ML, Carranza G, Bellido J, Villegas JC, Avila J, et al. Role of cofactors B (TBCB) and E (TBCE) in tubulin heterodimer dissociation. *Exp Cell Res* 2007 Feb 1;313(3):425-436.
- (109) Jordan MA, Wilson L. Microtubules as a target for anticancer drugs. *Nat Rev Cancer* 2004 Apr;4(4):253-265.
- (110) Wall ME. Camptothecin and taxol: discovery to clinic. *Med Res Rev* 1998 Sep;18(5):299-314.

- (111) Arbuck SG, Christian MC, Fisherman JS, Cazenave LA, Sarosy G, Suffness M, et al. Clinical development of Taxol. J Natl Cancer Inst Monogr 1993;(15)(15):11-24.
- (112) Wall ME, Wani MC, Fullas F, Oswald JB, Brown DM, Santisuk T, et al. Plant antitumor agents. 31. The calycopterones, a new class of biflavonoids with novel cytotoxicity in a diverse panel of human tumor cell lines. J Med Chem 1994 May 13;37(10):1465-1470.
- (113) McGuire WP, Rowinsky EK, Rosenshein NB, Grumbine FC, Ettinger DS, Armstrong DK, et al. Taxol: a unique antineoplastic agent with significant activity in advanced ovarian epithelial neoplasms. Ann Intern Med 1989 Aug 15;111(4):273-279.
- (114) Yared JA, Tkaczuk KH. Update on taxane development: new analogs and new formulations. Drug Des Devel Ther 2012;6:371-384.
- (115) Clarke SJ, Rivory LP. Clinical pharmacokinetics of docetaxel. Clin Pharmacokinet 1999 Feb;36(2):99-114.
- (116) Derry WB, Wilson L, Jordan MA. Substoichiometric binding of taxol suppresses microtubule dynamics. Biochemistry 1995 Feb 21;34(7):2203-2211.
- (117) Rao S, He L, Chakravarty S, Ojima I, Orr GA, Horwitz SB. Characterization of the Taxol binding site on the microtubule. Identification of Arg(282) in beta-tubulin as the site of photoincorporation of a 7-benzophenone analogue of Taxol. J Biol Chem 1999 Dec 31;274(53):37990-37994.

- (118) Snyder JP, Nettles JH, Cornett B, Downing KH, Nogales E. The binding conformation of Taxol in beta-tubulin: a model based on electron crystallographic density. *Proc Natl Acad Sci U S A* 2001 Apr 24;98(9):5312-5316.
- (119) Prussia AJ, Yang Y, Geballe MT, Snyder JP. Cyclostreptin and microtubules: is a low-affinity binding site required? *Chembiochem* 2010 Jan 4;11(1):101-109.
- (120) Buey RM, Calvo E, Barasoain I, Pineda O, Edler MC, Matesanz R, et al. Cyclostreptin binds covalently to microtubule pores and luminal taxoid binding sites. *Nat Chem Biol* 2007 Feb;3(2):117-125.
- (121) Jordan MA, Toso RJ, Thrower D, Wilson L. Mechanism of mitotic block and inhibition of cell proliferation by taxol at low concentrations. *Proc Natl Acad Sci U S A* 1993 Oct 15;90(20):9552-9556.
- (122) Jordan MA, Wendell K, Gardiner S, Derry WB, Copp H, Wilson L. Mitotic block induced in HeLa cells by low concentrations of paclitaxel (Taxol) results in abnormal mitotic exit and apoptotic cell death. *Cancer Res* 1996 Feb 15;56(4):816-825.
- (123) Noguchi S. Predictive factors for response to docetaxel in human breast cancers. *Cancer Sci* 2006 Sep;97(9):813-820.
- (124) Brown J, Shvartsman HS, Deavers MT, Burke TW, Munsell MF, Gershenson DM. The activity of taxanes in the treatment of sex cord-stromal ovarian tumors. *J Clin Oncol* 2004 Sep 1;22(17):3517-3523.

- (125) Bartel DP. MicroRNAs: genomics, biogenesis, mechanism, and function. *Cell* 2004 Jan 23;116(2):281-297.
- (126) Reinhart BJ, Weinstein EG, Rhoades MW, Bartel B, Bartel DP. MicroRNAs in plants. *Genes Dev* 2002 Jul 1;16(13):1616-1626.
- (127) Ying SY, Chang DC, Lin SL. The microRNA (miRNA): overview of the RNA genes that modulate gene function. *Mol Biotechnol* 2008 Mar;38(3):257-268.
- (128) Lee Y, Ahn C, Han J, Choi H, Kim J, Yim J, et al. The nuclear RNase III Drosha initiates microRNA processing. *Nature* 2003 Sep 25;425(6956):415-419.
- (129) Eulalio A, Huntzinger E, Nishihara T, Rehwinkel J, Fauser M, Izaurralde E. Deadenylation is a widespread effect of miRNA regulation. *RNA* 2009 Jan;15(1):21-32.
- (130) Wu L, Fan J, Belasco JG. MicroRNAs direct rapid deadenylation of mRNA. *Proc Natl Acad Sci U S A* 2006 Mar 14;103(11):4034-4039.
- (131) Liu H. MicroRNAs in breast cancer initiation and progression. *Cell Mol Life Sci* 2012 Nov;69(21):3587-3599.
- (132) Ambros V, Lee RC. Identification of microRNAs and other tiny noncoding RNAs by cDNA cloning. *Methods Mol Biol* 2004;265:131-158.
- (133) Iorio MV, Casalini P, Piovan C, Di Leva G, Merlo A, Triulzi T, et al. microRNA-205 regulates HER3 in human breast cancer. *Cancer Res* 2009 Mar 15;69(6):2195-2200.

- (134) Calin GA, Croce CM. MicroRNA signatures in human cancers. *Nat Rev Cancer* 2006 Nov;6(11):857-866.
- (135) Shi L, Cheng Z, Zhang J, Li R, Zhao P, Fu Z, et al. Hsa-Mir-181a and Hsa-Mir-181b Function as Tumor Suppressors in Human Glioma Cells. *Brain Res* 2008 Oct 21;1236:185-193.
- (136) Volinia S, Calin GA, Liu CG, Ambs S, Cimmino A, Petrocca F, et al. A microRNA expression signature of human solid tumors defines cancer gene targets. *Proc Natl Acad Sci U S A* 2006 Feb 14;103(7):2257-2261.
- (137) Iorio MV, Ferracin M, Liu CG, Veronese A, Spizzo R, Sabbioni S, et al. MicroRNA gene expression deregulation in human breast cancer. *Cancer Res* 2005 Aug 15;65(16):7065-7070.
- (138) Gottesman MM, Fojo T, Bates SE. Multidrug resistance in cancer: role of ATP-dependent transporters. *Nat Rev Cancer* 2002 Jan;2(1):48-58.
- (139) Murray S, Briasoulis E, Linardou H, Bafaloukos D, Papadimitriou C. Taxane resistance in breast cancer: mechanisms, predictive biomarkers and circumvention strategies. *Cancer Treat Rev* 2012 Nov;38(7):890-903.
- (140) Huisman MT, Chhatta AA, van Tellingen O, Beijnen JH, Schinkel AH. MRP2 (ABCC2) transports taxanes and confers paclitaxel resistance and both processes are stimulated by probenecid. *Int J Cancer* 2005 Sep 20;116(5):824-829.
- (141) Mechetner E, Kyshtoobayeva A, Zonis S, Kim H, Stroup R, Garcia R, et al. Levels of multidrug resistance (MDR1) P-glycoprotein expression by human

breast cancer correlate with in vitro resistance to taxol and doxorubicin. Clin Cancer Res 1998 Feb;4(2):389-398.

(142) Trock BJ, Leonessa F, Clarke R. Multidrug resistance in breast cancer: a meta-analysis of MDR1/gp170 expression and its possible functional significance. J Natl Cancer Inst 1997 Jul 2;89(13):917-931.

(143) Ro J, Sahin A, Ro JY, Fritsche H, Hortobagyi G, Blick M. Immunohistochemical analysis of P-glycoprotein expression correlated with chemotherapy resistance in locally advanced breast cancer. Hum Pathol 1990 Aug;21(8):787-791.

(144) Verrelle P, Meissonnier F, Fonck Y, Feillel V, Dionet C, Kwiatkowski F, et al. Clinical relevance of immunohistochemical detection of multidrug resistance P-glycoprotein in breast carcinoma. J Natl Cancer Inst 1991 Jan 16;83(2):111-116.

(145) Leandro-Garcia LJ, Leskela S, Landa I, Montero-Conde C, Lopez-Jimenez E, Leton R, et al. Tumoral and tissue-specific expression of the major human beta-tubulin isotypes. Cytoskeleton (Hoboken) 2010 Apr;67(4):214-223.

(146) Kavallaris M, Kuo DY, Burkhart CA, Regl DL, Norris MD, Haber M, et al. Taxol-resistant epithelial ovarian tumors are associated with altered expression of specific beta-tubulin isotypes. J Clin Invest 1997 Sep 1;100(5):1282-1293.

(147) Shalli K, Brown I, Heys SD, Schofield AC. Alterations of beta-tubulin isotypes in breast cancer cells resistant to docetaxel. FASEB J 2005 Aug;19(10):1299-1301.

- (148) Ohishi Y, Oda Y, Basaki Y, Kobayashi H, Wake N, Kuwano M, et al. Expression of beta-tubulin isotypes in human primary ovarian carcinoma. *Gynecol Oncol* 2007 Jun;105(3):586-592.
- (149) Lobert S, Jefferson B, Morris K. Regulation of beta-tubulin isotypes by micro-RNA 100 in MCF7 breast cancer cells. *Cytoskeleton (Hoboken)* 2011 Jun;68(6):355-362.
- (150) Haber M, Burkhart CA, Regl DL, Madafiglio J, Norris MD, Horwitz SB. Altered expression of M beta 2, the class II beta-tubulin isotype, in a murine J774.2 cell line with a high level of taxol resistance. *J Biol Chem* 1995 Dec 29;270(52):31269-31275.
- (151) Aoki D, Oda Y, Hattori S, Taguchi K, Ohishi Y, Basaki Y, et al. Overexpression of class III beta-tubulin predicts good response to taxane-based chemotherapy in ovarian clear cell adenocarcinoma. *Clin Cancer Res* 2009 Feb 15;15(4):1473-1480.
- (152) Derry WB, Wilson L, Khan IA, Luduena RF, Jordan MA. Taxol differentially modulates the dynamics of microtubules assembled from unfractionated and purified beta-tubulin isotypes. *Biochemistry* 1997 Mar 25;36(12):3554-3562.
- (153) Panda D, Miller HP, Banerjee A, Luduena RF, Wilson L. Microtubule dynamics in vitro are regulated by the tubulin isotype composition. *Proc Natl Acad Sci U S A* 1994 Nov 22;91(24):11358-11362.
- (154) Lu Q, Luduena RF. Removal of beta III isotype enhances taxol induced microtubule assembly. *Cell Struct Funct* 1993 Jun;18(3):173-182.

- (155) Kamath K, Wilson L, Cabral F, Jordan MA. BetaIII-tubulin induces paclitaxel resistance in association with reduced effects on microtubule dynamic instability. *J Biol Chem* 2005 Apr 1;280(13):12902-12907.
- (156) Stengel C, Newman SP, Leese MP, Potter BV, Reed MJ, Purohit A. Class III beta-tubulin expression and in vitro resistance to microtubule targeting agents. *Br J Cancer* 2010 Jan 19;102(2):316-324.
- (157) De Donato M., Mariani M., Petrella L., Martinelli L., Zannoni G.F., Vellone V., et al. Class III beta-Tubulin and the Cytoskeletal Gateway for Drug Resistance in Ovarian Cancer. *Journal of cellular physiology* 2011;227:1034.
- (158) Carrara L, Guzzo F, Roque DM, Bellone S, Emiliano C, Sartori E, et al. Differential in vitro sensitivity to patupilone versus paclitaxel in uterine and ovarian carcinosarcoma cell lines is linked to tubulin-beta-III expression. *Gynecol Oncol* 2012 Apr;125(1):231-236.
- (159) Mariani M, Zannoni GF, Sioletic S, Sieber S, Martino C, Martinelli E, et al. Gender influences the class III and V beta-tubulin ability to predict poor outcome in colorectal cancer. *Clin Cancer Res* 2012 May 15;18(10):2964-2975.
- (160) Karki R, Mariani M, Andreoli M, He S, Scambia G, Shahabi S, et al. betaIII-Tubulin: biomarker of taxane resistance or drug target? *Expert Opin Ther Targets* 2013 Apr;17(4):461-472.
- (161) Seve P, Reiman T, Isaac S, Trillet-Lenoir V, Lafanechere L, Sawyer M, et al. Protein abundance of class III beta-tubulin but not Delta2-alpha-tubulin or tau

is related to paclitaxel response in carcinomas of unknown primary site.

Anticancer Res 2008 Mar-Apr;28(2B):1161-1167.

(162) Azuma K, Sasada T, Kawahara A, Takamori S, Hattori S, Ikeda J, et al.

Expression of ERCC1 and class III beta-tubulin in non-small cell lung cancer patients treated with carboplatin and paclitaxel. Lung Cancer 2009

Jun;64(3):326-333.

(163) Hara T, Ushio K, Nishiwaki M, Kouno J, Araki H, Hikichi Y, et al. A mutation

in beta-tubulin and a sustained dependence on androgen receptor signalling in a newly established docetaxel-resistant prostate cancer cell line. Cell Biol Int 2010

Jan 25;34(2):177-184.

(164) Hasegawa S, Miyoshi Y, Egawa C, Ishitobi M, Tamaki Y, Monden M, et al.

Mutational analysis of the class I beta-tubulin gene in human breast cancer. Int J Cancer 2002 Sep 1;101(1):46-51.

(165) Yoshida N, Takada T, Yamamura Y, Adachi I, Suzuki H, Kawakami J.

Inhibitory effects of terpenoids on multidrug resistance-associated protein 2- and breast cancer resistance protein-mediated transport. Drug Metab Dispos 2008

Jul;36(7):1206-1211.

(166) Lee AJ, Endesfelder D, Rowan AJ, Walther A, Birkbak NJ, Futreal PA, et

al. Chromosomal instability confers intrinsic multidrug resistance. Cancer Res 2011 Mar 1;71(5):1858-1870.

(167) Giannakakou P, Sackett DL, Kang YK, Zhan Z, Buters JT, Fojo T, et al.

Paclitaxel-resistant human ovarian cancer cells have mutant beta-tubulins that

exhibit impaired paclitaxel-driven polymerization. *J Biol Chem* 1997 Jul 4;272(27):17118-17125.

(168) Wiesen KM, Xia S, Yang CP, Horwitz SB. Wild-type class I beta-tubulin sensitizes Taxol-resistant breast adenocarcinoma cells harboring a beta-tubulin mutation. *Cancer Lett* 2007 Nov 18;257(2):227-235.

(169) Verrills NM, Flemming CL, Liu M, Ivery MT, Cobon GS, Norris MD, et al. Microtubule alterations and mutations induced by desoxyepothilone B: implications for drug-target interactions. *Chem Biol* 2003 Jul;10(7):597-607.

(170) Giannakakou P, Gussio R, Nogales E, Downing KH, Zaharevitz D, Bollbuck B, et al. A common pharmacophore for epothilone and taxanes: molecular basis for drug resistance conferred by tubulin mutations in human cancer cells. *Proc Natl Acad Sci U S A* 2000 Mar 14;97(6):2904-2909.

(171) Diaz JF, Barasoain I, Andreu JM. Fast kinetics of Taxol binding to microtubules. Effects of solution variables and microtubule-associated proteins. *J Biol Chem* 2003 Mar 7;278(10):8407-8419.

(172) Freedman H, Huzil JT, Luchko T, Luduena RF, Tuszynski JA. Identification and characterization of an intermediate taxol binding site within microtubule nanopores and a mechanism for tubulin isotype binding selectivity. *J Chem Inf Model* 2009 Feb;49(2):424-436.

(173) Kenicer J, Lambros M, Sabine V, Reis-Filho J, Bartlett J. An Investigation into a Panel of Isogenic Taxane Resistant Breast Cancer Cell Lines Using

Transcriptomic and Genomic Methods. CANCER RESEARCH

2009;69(24):581S-582S.

(174) Guo B, Villeneuve DJ, Hembruff SL, Kirwan AF, Blais DE, Bonin M, et al. Cross-resistance studies of isogenic drug-resistant breast tumor cell lines support recent clinical evidence suggesting that sensitivity to paclitaxel may be strongly compromised by prior doxorubicin exposure. *Breast Cancer Res Treat* 2004 May;85(1):31-51.

(175) Fauzee NJ, Wang YL, Dong Z, Li QG, Wang T, Mandarry MT, et al. Novel hydrophilic docetaxel (CQMU-0519) analogue inhibits proliferation and induces apoptosis in human A549 lung, SKVO3 ovarian and MCF7 breast carcinoma cell lines. *Cell Prolif* 2012 Aug;45(4):352-364.

(176) LOWRY OH, ROSEBROUGH NJ, FARR AL, RANDALL RJ. Protein measurement with the Folin phenol reagent. *J Biol Chem* 1951 Nov;193(1):265-275.

(177) Howe EN, Cochrane DR, Cittelly DM, Richer JK. miR-200c targets a NF-kappaB up-regulated TrkB/NTF3 autocrine signaling loop to enhance anoikis sensitivity in triple negative breast cancer. *PLoS One* 2012;7(11):e49987.

(178) Howe EN, Cochrane DR, Richer JK. The miR-200 and miR-221/222 microRNA families: opposing effects on epithelial identity. *J Mammary Gland Biol Neoplasia* 2012 Mar;17(1):65-77.

(179) Leskela S, Leandro-Garcia LJ, Mendiola M, Barriuso J, Inglada-Perez L, Munoz I, et al. The miR-200 family controls beta-tubulin III expression and is

associated with paclitaxel-based treatment response and progression-free survival in ovarian cancer patients. *Endocr Relat Cancer* 2010 Dec 21;18(1):85-95.

(180) Cochrane DR, Howe EN, Spoelstra NS, Richer JK. Loss of miR-200c: A Marker of Aggressiveness and Chemoresistance in Female Reproductive Cancers. *J Oncol* 2010;2010:821717.

(181) Cochrane DR, Spoelstra NS, Howe EN, Nordeen SK, Richer JK. MicroRNA-200c mitigates invasiveness and restores sensitivity to microtubule-targeting chemotherapeutic agents. *Mol Cancer Ther* 2009 May;8(5):1055-1066.

(182) Harker WG, Sikic BI. Multidrug (pleiotropic) resistance in doxorubicin-selected variants of the human sarcoma cell line MES-SA. *Cancer Res* 1985 Sep;45(9):4091-4096.

(183) Delmer A, Marie JP, Thevenin D, Cadiou M, Viguie F, Zittoun R. Multivariate analysis of prognostic factors in acute myeloid leukemia: value of clonogenic leukemic cell properties. *J Clin Oncol* 1989 Jun;7(6):738-746.

(184) Weber GF. Molecular mechanisms of metastasis. *Cancer Lett* 2008 Nov 8;270(2):181-190.

(185) Wang F, Zhang D, Zhang Q, Chen Y, Zheng D, Hao L, et al. Synergistic effect of folate-mediated targeting and verapamil-mediated P-gp inhibition with paclitaxel -polymer micelles to overcome multi-drug resistance. *Biomaterials* 2011 Dec;32(35):9444-9456.

(186) Cittelly DM, Dimitrova I, Howe EN, Cochrane DR, Jean A, Spoelstra NS, et al. Restoration of miR-200c to ovarian cancer reduces tumor burden and increases sensitivity to paclitaxel. *Mol Cancer Ther* 2012 Dec;11(12):2556-2565.

(187) Ranganathan S, McCauley RA, Dexter DW, Hudes GR. Modulation of endogenous beta-tubulin isotype expression as a result of human beta(III)cDNA transfection into prostate carcinoma cells. *Br J Cancer* 2001 Sep 1;85(5):735-740.

(188) Kamath K, Wilson L, Cabral F, Jordan MA. BetaIII-tubulin induces paclitaxel resistance in association with reduced effects on microtubule dynamic instability. *J Biol Chem* 2005 Apr 1;280(13):12902-12907.

(189) Gyorffy B, Surowiak P, Kiesslich O, Denkert C, Schafer R, Dietel M, et al. Gene expression profiling of 30 cancer cell lines predicts resistance towards 11 anticancer drugs at clinically achieved concentrations. *Int J Cancer* 2006 Apr 1;118(7):1699-1712.

(190) Marcelletti JF, Multani PS, Lancet JE, Baer MR, Sikic BI. Leukemic blast and natural killer cell P-glycoprotein function and inhibition in a clinical trial of zosuquidar infusion in acute myeloid leukemia. *Leuk Res* 2009 Jun;33(6):769-774.

(191) Ambudkar SV, Kimchi-Sarfaty C, Sauna ZE, Gottesman MM. P-glycoprotein: from genomics to mechanism. *Oncogene* 2003 Oct 20;22(47):7468-7485.

- (192) Campos L, Guyotat D, Archimbaud E, Calmard-Oriol P, Tsuruo T, Troncy J, et al. Clinical significance of multidrug resistance P-glycoprotein expression on acute nonlymphoblastic leukemia cells at diagnosis. *Blood* 1992 Jan 15;79(2):473-476.
- (193) Mahadevan D, List AF. Targeting the multidrug resistance-1 transporter in AML: molecular regulation and therapeutic strategies. *Blood* 2004 Oct 1;104(7):1940-1951.
- (194) Lamendola DE, Duan Z, Yusuf RZ, Seiden MV. Molecular description of evolving paclitaxel resistance in the SKOV-3 human ovarian carcinoma cell line. *Cancer Res* 2003 May 1;63(9):2200-2205.
- (195) Elferink JG, Deierkauf M. The effect of verapamil and other calcium antagonists on chemotaxis of polymorphonuclear leukocytes. *Biochem Pharmacol* 1984 Jan 1;33(1):35-39.
- (196) Srinivasan V, Sivaramakrishnan H, Karthikeyan B. Detection, isolation and characterization of principal synthetic route indicative impurities in verapamil hydrochloride. *Sci Pharm* 2011 Sep;79(3):555-568.
- (197) Sorrentino A, Liu CG, Addario A, Peschle C, Scambia G, Ferlini C. Role of microRNAs in drug-resistant ovarian cancer cells. *Gynecol Oncol* 2008 Dec;111(3):478-486.
- (198) Sun YM, Lin KY, Chen YQ. Diverse functions of miR-125 family in different cell contexts. *J Hematol Oncol* 2013 Jan 15;6:6-8722-6-6.

(199) Zhu X, Li H, Long L, Hui L, Chen H, Wang X, et al. miR-126 enhances the sensitivity of non-small cell lung cancer cells to anticancer agents by targeting vascular endothelial growth factor A. *Acta Biochim Biophys Sin (Shanghai)* 2012 Jun;44(6):519-526.

(200) Schaefer A, Jung M, Mollenkopf HJ, Wagner I, Stephan C, Jentzmik F, et al. Diagnostic and prognostic implications of microRNA profiling in prostate carcinoma. *Int J Cancer* 2010 Mar 1;126(5):1166-1176.

(201) Gregory PA, Bert AG, Paterson EL, Barry SC, Tsykin A, Farshid G, et al. The miR-200 family and miR-205 regulate epithelial to mesenchymal transition by targeting ZEB1 and SIP1. *Nat Cell Biol* 2008 May;10(5):593-601.

(202) Lebanony D, Benjamin H, Gilad S, Ezagouri M, Dov A, Ashkenazi K, et al. Diagnostic assay based on hsa-miR-205 expression distinguishes squamous from nonsquamous non-small-cell lung carcinoma. *J Clin Oncol* 2009 Apr 20;27(12):2030-2037.

(203) Selth LA, Townley S, Gillis JL, Ochnik AM, Murti K, Macfarlane RJ, et al. Discovery of circulating microRNAs associated with human prostate cancer using a mouse model of disease. *Int J Cancer* 2012 Aug 1;131(3):652-661.

(204) Yamagata T, Yoshizawa J, Ohashi S, Yanaga K, Ohki T. Expression patterns of microRNAs are altered in hypoxic human neuroblastoma cells. *Pediatr Surg Int* 2010 Dec;26(12):1179-1184.

(205) Leite KR, Sousa-Canavez JM, Reis ST, Tomiyama AH, Camara-Lopes LH, Sanudo A, et al. Change in expression of miR-let7c, miR-100, and miR-218 from

high grade localized prostate cancer to metastasis. *Urol Oncol* 2011 May-Jun;29(3):265-269.

(206) Tie J, Pan Y, Zhao L, Wu K, Liu J, Sun S, et al. MiR-218 inhibits invasion and metastasis of gastric cancer by targeting the Robo1 receptor. *PLoS Genet* 2010 Mar 12;6(3):e1000879.

(207) Alajez NM, Lenarduzzi M, Ito E, Hui AB, Shi W, Bruce J, et al. MiR-218 suppresses nasopharyngeal cancer progression through downregulation of survivin and the SLIT2-ROBO1 pathway. *Cancer Res* 2011 Mar 15;71(6):2381-2391.

(208) Jiang Y, Qin Z, Hu Z, Guan X, Wang Y, He Y, et al. Genetic variation in a hsa-let-7 binding site in RAD52 is associated with breast cancer susceptibility. *Carcinogenesis* 2013 Mar;34(3):689-693.

(209) Zhang M, Jin M, Yu Y, Zhang S, Wu Y, Liu H, et al. Associations of miRNA polymorphisms and female physiological characteristics with breast cancer risk in Chinese population. *Eur J Cancer Care (Engl)* 2012 Mar;21(2):274-280.

(210) Ichikawa T, Sato F, Terasawa K, Tsuchiya S, Toi M, Tsujimoto G, et al. Trastuzumab produces therapeutic actions by upregulating miR-26a and miR-30b in breast cancer cells. *PLoS One* 2012;7(2):e31422.

(211) Wszolek MF, Rieger-Christ KM, Kenney PA, Gould JJ, Silva Neto B, Lavoie AK, et al. A MicroRNA expression profile defining the invasive bladder tumor phenotype. *Urol Oncol* 2011 Nov-Dec;29(6):794-801.e1.

(212) Gao W, Shen H, Liu L, Xu J, Xu J, Shu Y. MiR-21 overexpression in human primary squamous cell lung carcinoma is associated with poor patient prognosis. *J Cancer Res Clin Oncol* 2011 Apr;137(4):557-566.

(213) Caswell PT, Chan M, Lindsay AJ, McCaffrey MW, Boettiger D, Norman JC. Rab-coupling protein coordinates recycling of alpha5beta1 integrin and EGFR1 to promote cell migration in 3D microenvironments. *J Cell Biol* 2008 Oct 6;183(1):143-155.

(214) Chen R, Alvero AB, Silasi DA, Kelly MG, Fest S, Visintin I, et al. Regulation of IKKbeta by miR-199a affects NF-kappaB activity in ovarian cancer cells. *Oncogene* 2008 Aug 7;27(34):4712-4723.

(215) Dolt KS, Mishra MK, Karar J, Baig MA, Ahmed Z, Pasha MA. cDNA cloning, gene organization and variant specific expression of HIF-1 alpha in high altitude yak (*Bos grunniens*). *Gene* 2007 Jan 15;386(1-2):73-80.

(216) Zhao A, Zeng Q, Xie X, Zhou J, Yue W, Li Y, et al. MicroRNA-125b induces cancer cell apoptosis through suppression of Bcl-2 expression. *J Genet Genomics* 2012 Jan;39(1):29-35.

(217) Zeng CW, Zhang XJ, Lin KY, Ye H, Feng SY, Zhang H, et al. Camptothecin induces apoptosis in cancer cells via microRNA-125b-mediated mitochondrial pathways. *Mol Pharmacol* 2012 Apr;81(4):578-586.

(218) Scarola M, Schoeftner S, Schneider C, Benetti R. miR-335 directly targets Rb1 (pRb/p105) in a proximal connection to p53-dependent stress response. *Cancer Res* 2010 Sep 1;70(17):6925-6933.

(219) Heyn H, Engelmann M, Schreek S, Ahrens P, Lehmann U, Kreipe H, et al. MicroRNA miR-335 is crucial for the BRCA1 regulatory cascade in breast cancer development. *Int J Cancer* 2011 Dec 15;129(12):2797-2806.

(220) Mutalib NSA, Yoke-Kqueen C, Rahman SA, Sidik SM, Singh A, Learn-Han L. Differential microRNA expression and identification of putative miRNA targets and pathways in head and neck cancers. *International Journal of Molecular Medicine* 2011;28:327.

(221) Yan LX, Huang XF, Shao Q, Huang MY, Deng L, Wu QL, et al. MicroRNA miR-21 overexpression in human breast cancer is associated with advanced clinical stage, lymph node metastasis and patient poor prognosis. *RNA* 2008 Nov;14(11):2348-2360.

(222) Sun Q, Gu H, Zeng Y, Xia Y, Wang Y, Jing Y, et al. Hsa-mir-27a genetic variant contributes to gastric cancer susceptibility through affecting miR-27a and target gene expression. *Cancer Sci* 2010 Oct;101(10):2241-2247.

(223) Calin GA, Croce CM. MicroRNA signatures in human cancers. *Nat Rev Cancer* 2006 Nov;6(11):857-866.

(224) Tome M, Lopez-Romero P, Albo C, Sepulveda JC, Fernandez-Gutierrez B, Dopazo A, et al. miR-335 orchestrates cell proliferation, migration and differentiation in human mesenchymal stem cells. *Cell Death Differ* 2011 Jun;18(6):985-995.

- (225) Lu Y, Ryan SL, Elliott DJ, Bignell GR, Futreal PA, Ellison DW, et al. Amplification and overexpression of Hsa-miR-30b, Hsa-miR-30d and KHDRBS3 at 8q24.22-q24.23 in medulloblastoma. PLoS One 2009 Jul 7;4(7):e6159.
- (226) Kars MD, Iseri OD, Gunduz U. A microarray based expression profiling of paclitaxel and vincristine resistant MCF-7 cells. Eur J Pharmacol 2011 Apr 25;657(1-3):4-9.
- (227) Holleman A, Chung I, Olsen RR, Kwak B, Mizokami A, Saijo N, et al. miR-135a contributes to paclitaxel resistance in tumor cells both in vitro and in vivo. Oncogene 2011 Oct 27;30(43):4386-4398.
- (228) Luduena RF. A hypothesis on the origin and evolution of tubulin. Int Rev Cell Mol Biol 2013;302:41-185.
- (229) Maldonado EN, Patnaik J, Mullins MR, Lemasters JJ. Free tubulin modulates mitochondrial membrane potential in cancer cells. Cancer Res 2010 Dec 15;70(24):10192-10201.
- (230) Ross JL, Fygenson DK. Mobility of taxol in microtubule bundles. Biophys J 2003 Jun;84(6):3959-3967.
- (231) Choi H, Kin S, Song J, Son J, Son J, Hong S, et al. Localization of Paclitaxel in Suspension Culture of *Taxus chinensis*. Journal of Microbiology and Biotechnology 2001;11(3):458.
- (232) Naill MC, Roberts SC. Flow cytometric identification of Paclitaxel-accumulating subpopulations. Biotechnol Prog 2005 May-Jun;21(3):978-983.

- (233) Yin S, Bhattacharya R, Cabral F. Human mutations that confer paclitaxel resistance. *Mol Cancer Ther* 2010 Feb;9(2):327-335.
- (234) Yin S, Zeng C, Hari M, Cabral F. Random mutagenesis of beta-tubulin defines a set of dispersed mutations that confer paclitaxel resistance. *Pharm Res* 2012 Nov;29(11):2994-3006.
- (235) Thrower D, Jordan MA, Wilson L. Quantitation of cellular tubulin in microtubules and tubulin pools by a competitive ELISA. *J Immunol Methods* 1991 Jan 24;136(1):45-51.
- (236) Hamel E, Lin CM. Separation of active tubulin and microtubule-associated proteins by ultracentrifugation and isolation of a component causing the formation of microtubule bundles. *Biochemistry* 1984 Aug 28;23(18):4173-4184.
- (237) Pipeleers DG, Pipeleers-Marichal MA, Sherline P, Kipnis DM. A sensitive method for measuring polymerized and depolymerized forms of tubulin in tissues. *J Cell Biol* 1977 Aug;74(2):341-350.
- (238) Ong SE, Mann M. Mass spectrometry-based proteomics turns quantitative. *Nat Chem Biol* 2005 Oct;1(5):252-262.
- (239) Bantscheff M, Schirle M, Sweetman G, Rick J, Kuster B. Quantitative mass spectrometry in proteomics: a critical review. *Anal Bioanal Chem* 2007 Oct;389(4):1017-1031.
- (240) Lengqvist J, Sandberg A. Stable isotope labeling methods in protein profiling. *Methods Mol Biol* 2013;1023:21-51.

- (241) Forshed J. Protein Quantification by Peptide Quality Control (PQPQ) of Shotgun Proteomics Data. *Methods Mol Biol* 2013;1023:149-158.
- (242) Mhaidat NM, Thorne RF, de Bock CE, Zhang XD, Hersey P. Melanoma cell sensitivity to Docetaxel-induced apoptosis is determined by class III beta-tubulin levels. *FEBS Lett* 2008 Jan 23;582(2):267-272.
- (243) Gan PP, Pasquier E, Kavallaris M. Class III beta-tubulin mediates sensitivity to chemotherapeutic drugs in non small cell lung cancer. *Cancer Res* 2007 Oct 1;67(19):9356-9363.
- (244) Gan PP, McCarroll JA, Byrne FL, Garner J, Kavallaris M. Specific beta-tubulin isotypes can functionally enhance or diminish epothilone B sensitivity in non-small cell lung cancer cells. *PLoS One* 2011;6(6):e21717.
- (245) Risinger AL, Jackson EM, Polin LA, Helms GL, LeBoeuf DA, Joe PA, et al. The taccalonolides: microtubule stabilizers that circumvent clinically relevant taxane resistance mechanisms. *Cancer Res* 2008 Nov 1;68(21):8881-8888.
- (246) Blade K, Menick DR, Cabral F. Overexpression of class I, II or IVb beta-tubulin isotypes in CHO cells is insufficient to confer resistance to paclitaxel. *J Cell Sci* 1999 Jul;112 (Pt 13)(Pt 13):2213-2221.
- (247) Narvi E, Jaakkola K, Winsel S, Oetken-Lindholm C, Halonen P, Kallio L, et al. Altered TUBB3 expression contributes to the epothilone response of mitotic cells. *Br J Cancer* 2013 Jan 15;108(1):82-90.

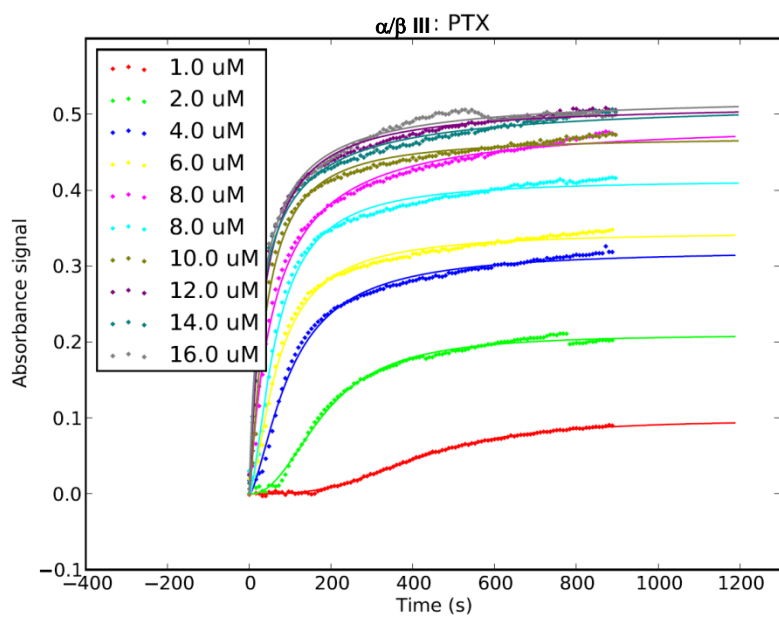
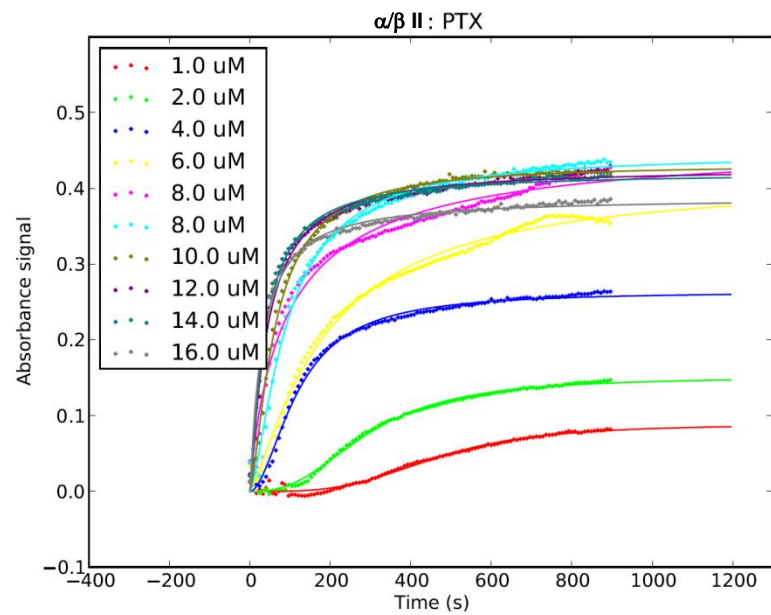
(248) Chaudhuri K, Chatterjee R. MicroRNA detection and target prediction: integration of computational and experimental approaches. *DNA Cell Biol* 2007 May;26(5):321-337.

1. Appendix I

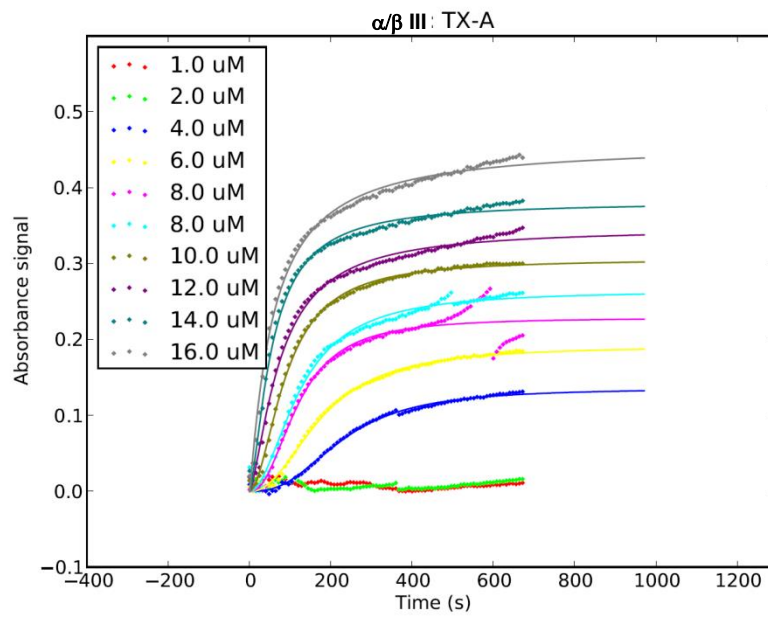
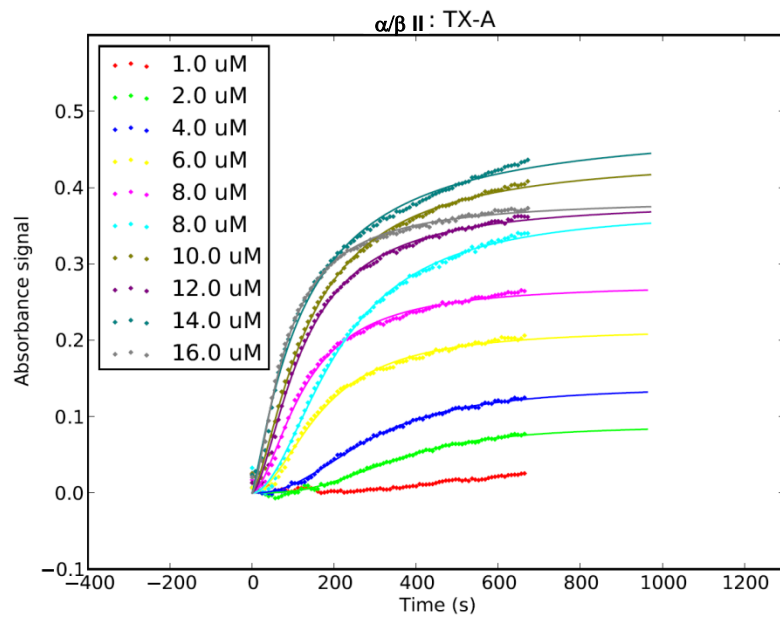
1.1 *In Vitro* Tubulin Polymerization using Paclitaxel and Synthesized Analogs

Preliminary experimental work was performed in the laboratory of Dr. Richard Luduena, University of Texas Health Science Centre, using the paclitaxel analogs. These experiments used affinity purified $\alpha\beta$ II and $\alpha\beta$ III bovine brain tubulin isotypes. They were performed to assess the polymerization potential, and isotype specificity of each analog compared to paclitaxel, across a range of drug concentrations (Figure A1-1). Each experiment was carried out using 1.4mg/ml isotypically pure bovine brain tubulin in tubulin buffer (0.1M MES-Na, 1mM EGTA, 0.1mM EDTA, 0.5Mm $MgCl_2$, 1mM GTP, pH6.4). Turbidity was measured at 37°C 350nm every 8 sec. Further analysis was performed by Philip Winter in the Tuszynski lab to highlight the parameters of maximum assembly and critical point as a function of paclitaxel and analog concentration (Figure A1-2). Maximum assembly represents the highest level of absorbance reached, which represents total polymerization. Critical point represents the time in which absorbance readings are no longer exponential, representing the point at which exponential microtubules growth is attenuated, and is representative of overall polymerization rate under each drug and drug concentration.

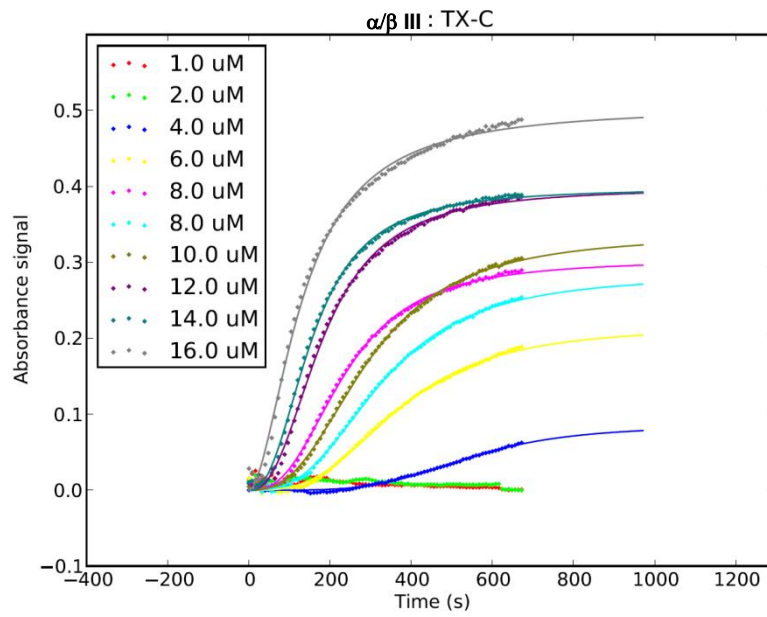
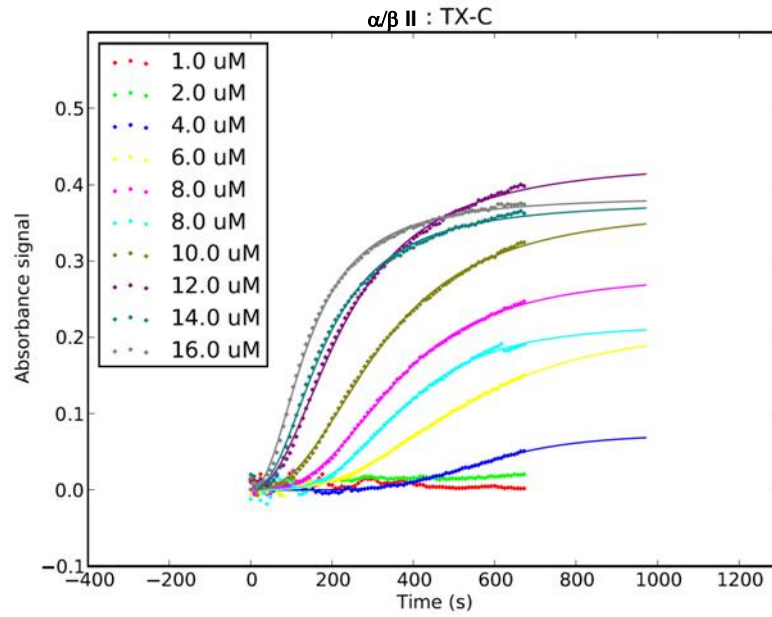
A)



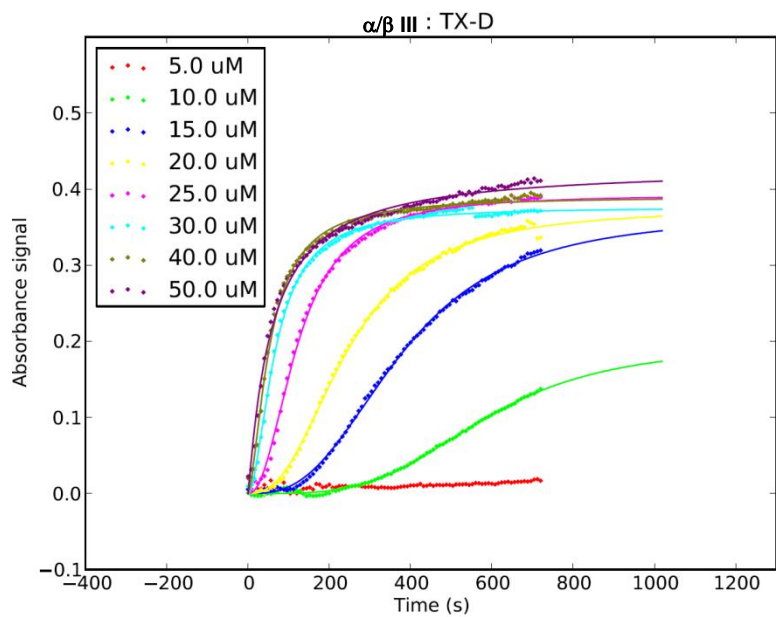
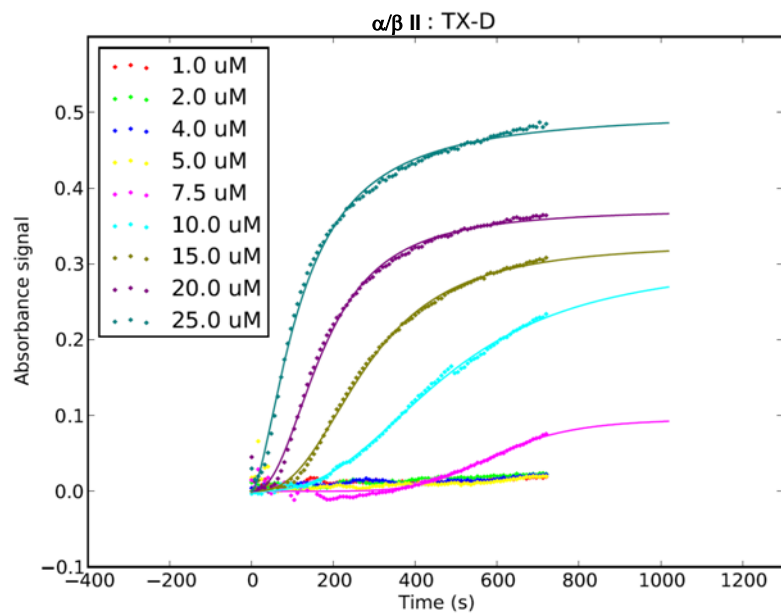
B)



C)



D)



E)

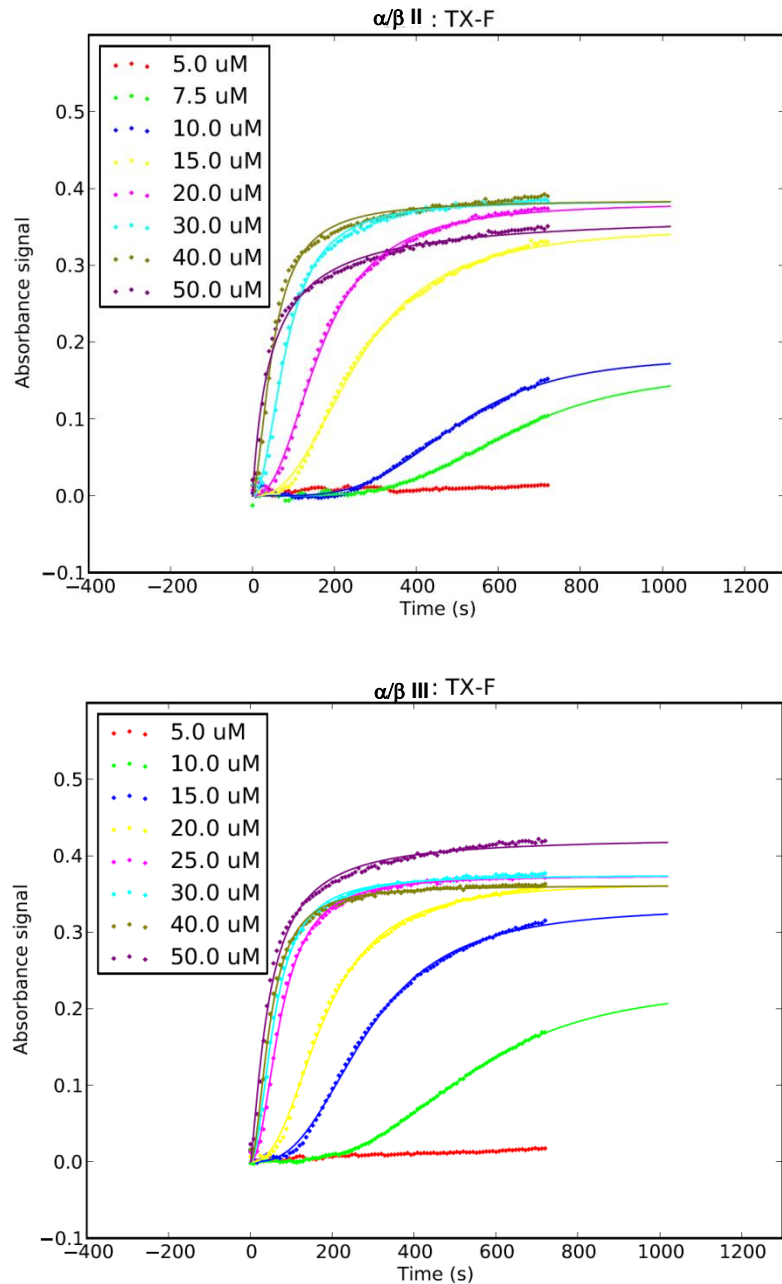


Figure A1-1. Dose Dependent Polymerization of Purified Bovin Brain Tubulin, Facilitated by Paclitaxel and Analogs

Isotypically pure bovin brain tubulin was used to assess polymerization of paclitaxel and analogs. 1.4 mg/ml of either α/β II or α/β III tubulin was polymerized at 37°C and rate and degree of polymerization was determined by measuring turbidity every 8 sec at 350nm using a spectrophotometer.

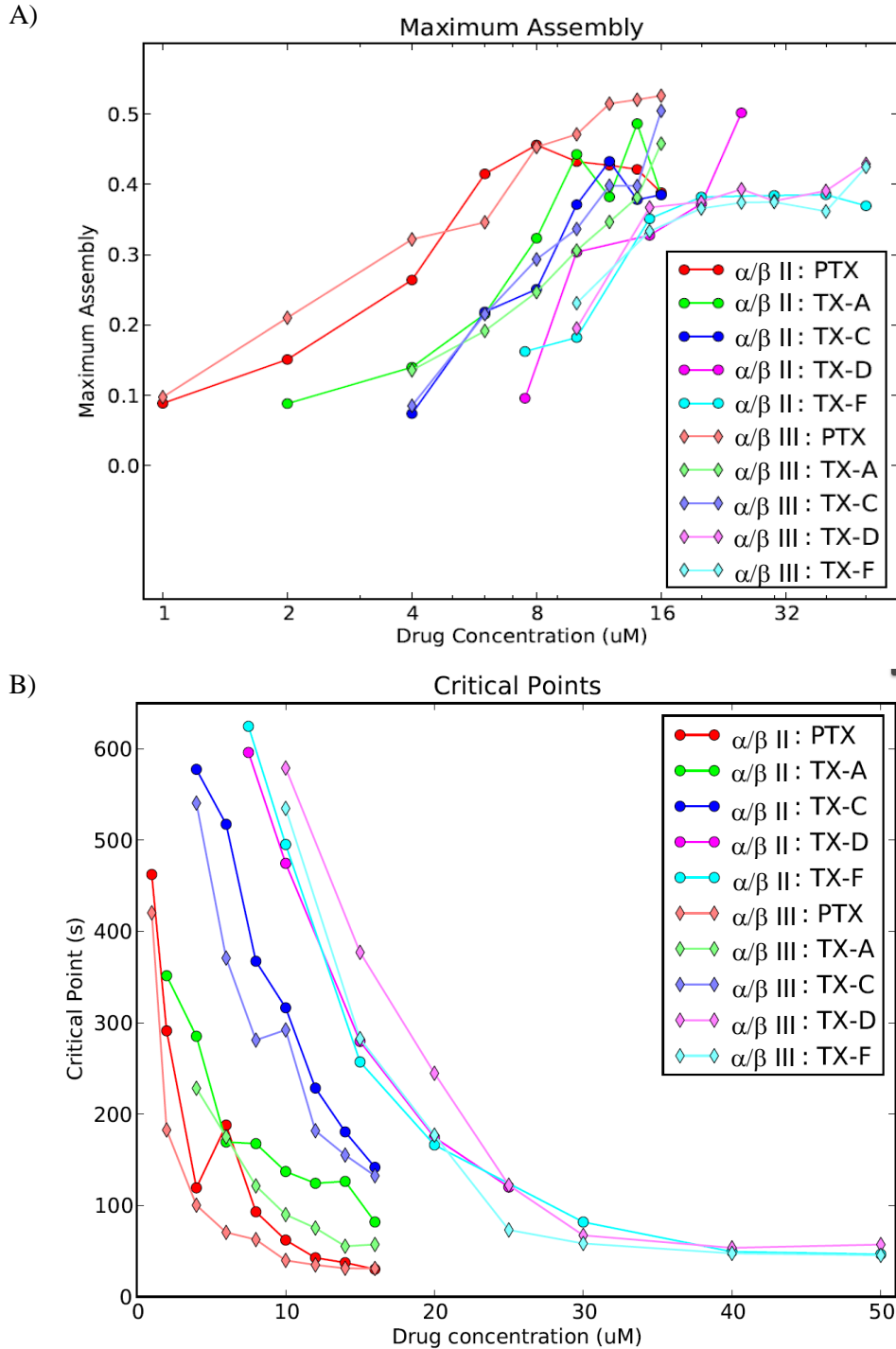


Figure A1-2. Assessing the Dynamics of Polymerizing Microtubules in the Presence of Paclitaxel and Analogs

(A) Maximum assembly is the highest absorbance reading achieved at each concentration, indicative of maximum polymerization of the tubulin heterodimers. (B) Critical point represents the time taken for microtubule growth to reach a plateau following its exponential growth phase.

2. Appendix II

2.1 Recombinant Tubulin Purification and Polymerization

Tubulin polymerization assays are effective means by which to test the ability of a microtubule binding agents to induce polymerization or depolymerization of microtubules. Beyond the desire to test the ability of the paclitaxel analogs on their ability to induce microtubule polymerization, I also wish to determine the effects of single or multiple point mutations within the β tubulin structure and the effects on the ability of paclitaxel and novel derivatives to induce polymerization. Provided with recombinant 6 x His tagged wild type α and β , as well as mutant β tubulin expressed in BL312 *E. coli* cells, purified protein was intended to be used in the same manner that bovine and porcine brain tubulin is used for polymerization assays. Partial purification of these tubulin proteins was carried out successfully using Ni-NTA affinity chromatography (Figure A2-1). The first successfully purified tubulins were WT α and β , with final total protein concentrations of 2.54 mg/ml and 4.9 mg/ml respectively. The purified product of each protein did have slight contaminations resulting in lower than detected tubulin protein concentrations used for polymerization.

Polymerization was carried out under a number of experimental conditions to determine if the purified recombinant tubulin could successfully polymerize into microtubules. The experimental conditions have demonstrated little specificity for polymerization with and without the

drug, indicating non-specific effects. Control experiments were carried out to determine if polymerization of microtubules is truly occurring or if it is just an aggregation of the tubulin protein present in the well that is changing the optical density of the assay media. Experiments using WT β tubulin alone, β tubulin without GTP present (a requirement for polymerization), α tubulin alone, and mutant V316I β tubulin alone with and without Colchicine, a known depolymerizing agent were carried out. Each of these experimental conditions resulted in detectable level of changes to optical density. β tubulin in the presence of paclitaxel had the fast exponential growth phase, greater than that of one replicate of α/β tubulin without paclitaxel and a rate similar to that of α/β with paclitaxel and one replicate without. β tubulin without GTP also had a significant change in optical density. α tubulin in the presence of paclitaxel had low change in optical density and V316I had the lowest change, with no effect due to the presence or absence of colchicine (Figure A2-2). Experimental conditions mimicking these but using purified bovine or porcine brain tubulin have not led to these non-specific effects (A2-1). Aggregate formation is likely occurring, resulting in the observed changes in optical density, not only in the control experiments but is also likely occurring in the experiments containing both purified α and β tubulin.

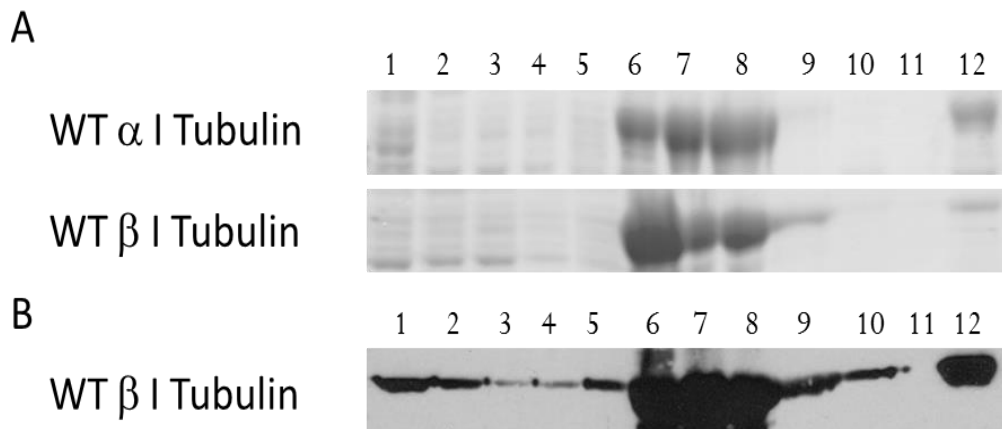


Figure A2-1. Representative SDS PAGE and Western Blot Analysis of the Fractions Collected from the Purification of Wild Type Recombinant Tubulin

25 μ g of each fraction was loaded onto a 10% polyacrylamide gel. (A) Stained with Coomassie blue; (B) Western blot carried out using human β I primary antibody (ab11312). Identical fractions were loaded on to gels for both panels, A and B: Fractions analyzed from the affinity purification column are as follows: (1)-Post Lysis, (2)-Inclusion Body Wash I, (3)-Inclusion Body Wash II, (4)-Inclusion Body Wash III, (5)-Inclusion Body Wash IV, (6)-Pre Binding, (7)-Post Binding, (8)-Denaturing Binding Wash I, (9)-Denaturing Wash I, (10)-Native Wash I, (11)-Native Wash IV, (12)-Enriched Final Protein. The major protein bands shown in fractions 6-8 and 12 correspond to a molecular weight of 51 KDa.

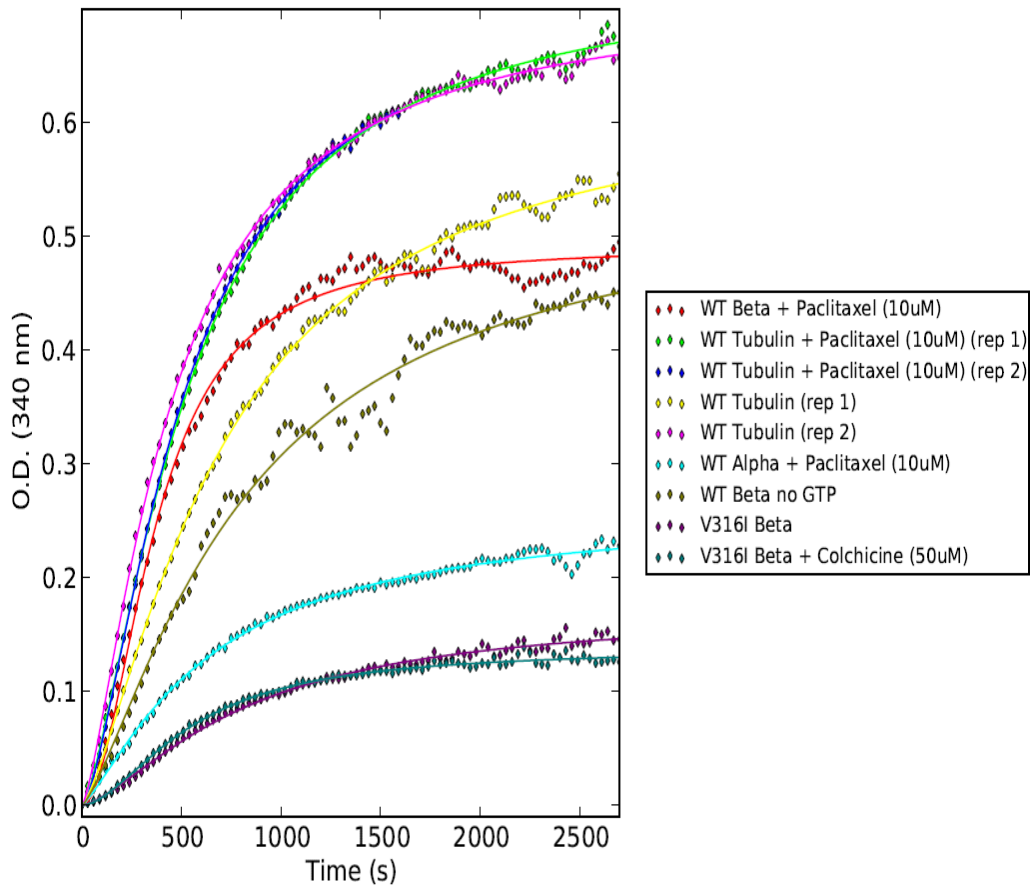


Figure A2-2. Recombinant Tubulin Polymerization Assay

Wild type α , β and V316I mutant β tubulins were used for experiments. Experiments performed were in half the volume of each 96 well plate at 37°C for 45min under a variety of tubulin compositions, \pm GTP and drug concentrations. Readings were taken every 30 s at 340nm.